DENITRICATION AND N_2O PRODUCTION IN CANADIAN LAKES: EFFECTS OF NUTRIENT RATIOS ACTING THROUGH PRIMARY PRODUCER SELECTION

By

Joseph James Bautista

Bachelor of Science Applied Chemistry and Biology,

Ryerson University, 2002

A thesis presented to

Ryerson University

in partial fulfillment of the requirements for the degree of

Master of Science

in the program of

Molecular Science

Toronto, Ontario, Canada, 2009

Author's Declaration

I hereby declare that I am the sole author of this thesis.

I authorize Ryerson University to lend this thesis to other institutions or individuals for the purpose of scholarly research.

I further authorize Ryerson University to reproduce this thesis by photocopying or by other means, in total or in part, at the request of other institutions or individuals for the purpose of scholarly research.

Author's Declaration

I hereby declare that I am the sole author of this thesis.

I authorize Ryerson University to lend this thesis to other institutions or individuals for the purpose of scholarly research.

Jo

I further authorize Ryerson University to reproduce this thesis by photocopying or by other means, in total or in part, at the request of other institutions or individuals for the purpose of scholarly research.

DENITRICATION AND N_2O PRODUCTION IN CANADIAN LAKES: EFFECTS OF NUTRIENT RATIOS ACTING THROUGH PRIMARY PRODUCER SELECTION

By

Joseph James Bautista

Bachelor of Science Applied Chemistry and Biology,

Ryerson University, 2002

A thesis presented to

Ryerson University

in partial fulfillment of the requirements for the degree of

Master of Science

in the program of

Molecular Science

Toronto, Ontario, Canada, 2009

Ryerson University requires the signature of all persons using or photocopying this thesis. Please sign below, and give address and date.

ABSTRACT

DENITRICATION AND N_2O PRODUCTION IN CANADIAN LAKES: EFFECTS OF NUTRIENT RATIOS ACTING THROUGH PRIMARY PRODUCER SELECTION

Joseph Bautista
Master of Science
Molecular Science
January, 2009
Ryerson University

Anthropogenic nutrient loading to aquatic systems may increase atmospheric release of nitrous oxide (N_2O) greenhouse gas by enhancing denitrification and/or nitrification. High Si:N loading may favour diatom abundance, whereas low N:P loading may favour cyanobacteria dominance. Systems with diatom or green algal dominance may have greater export of organic matter to sediments, whereas systems dominated by cyanobacteria may have organic matter recycled within the water column due to differences in cell density and sinking. With increased export of organic matter to sediments, denitrification and N_2O production may be stimulated. In laboratory bench-scale microcosms, nitrous oxide production was affected by Si:N loading ratios as predicted, although N:P loading did not affect N_2O production in the manner predicted. However, the predicted effects of nutrient loading ratio on microphyte community composition were not supported by microscopy. Field mesocosm experiments indicated no significant relationship between N_2O production and nutrient loading ratios.

ACKNOWLEDGEMENTS

My research was funded by NSERC Operating Grants to Dr. Andrew Laursen and Ryerson University`s Department of Chemistry and Biology. I would like to extend my thanks to my committee: Dr. Andrew Laursen, Dr. McCarthy, and Dr. Vadim Bostan for their support and access to their research facilities. Technical lab assistance was greatly appreciated from Juliet Ajambo-Doherty, Monisa Nandi, Teresa Young and Scott Robertson for the technical lab support. Dr. Roxane Maranger and her graduate students from Université de *Montréal* contributed to a large portion of the membrane inlet mass spectrometer analysis. I would like to thank my family, my parents, Celso and Lolita Bautista, for their love, financial support throughout the years and access to their yard for my mesocosm experiment. My brother, Brian Bautista, was a great help in mesocosm sample collection. And thanks to all my friends and labmates for their emotional support.

My heartfelt thanks to Dr. Andrew Laursen who has supported and found confidence in me during this research experience. His assistance in experimental design and data analysis was monumental to my microcosm and mesocosm setup. With great patience, Dr. Andrew Laursen has given me a greater appreciation of the biogeochemistry sciences. With great warmth, I would like to thank Dr. Lynda McCarthy for her encouragement and support throughout my academic career, comfort in the fact that her office door is always open. And special thanks to Teresa Young, you have always been there.

Save the Great Lakes!

TABLE OF CONTENTS

LIST OF TABLES

LIST OF FIGURES

LIST OF APPENDICES

LIST OF ABREATIONS

ANAMMOX	Anaerobic Ammonia Oxidation
ANOVA	Analysis of Variance
AOB	Ammonia-Oxidizing Bacteria
Ar	Argon
Co	Cobalt
Cu	Copper
DANAK	Danish Accreditation Scheme
DHI	Danish Hydraulic Institute
DIN	Dissolved Inorganic Nitrogen
DIP	Dissolved Inorganic Phosphate
DOC	Dissolved Organic Carbon
DRNA	Dissolved Reduction of Nitrate into Ammonia
Fe	Iron
GC-ECD	Gas Chromatography with Electron Capture Detector
H_2S	Sulfide
HPLC	High Performance Liquid Chromatography
MANOVA	Multivariate Analysis of Variance
MIMS	Membrane Inlet Mass Spectrometry

N_2	Dinitrogen Gas
N_2O	Nitrous Oxide
NO_2^-	Nitrite
NO_3^-	Nitrate
N	Nitrogen
NH_2OH	Hydroxylamine
NH_3	Ammonia
NH_4^+	Ammonium
NO	Nitric Oxide
NOB	Nitrite-oxidizing Bacteria
NOx	Nitrogen Oxides (NO_3^- & NO_2^-)
P	Phosphorus
PC	Personal Computer
O_2	Oxygen Gas
ON	Ontario
ODS	Ozone Depleting Substances
S	Sulphur
BSi	Biogenic SiO_2
Si	Silicon
SiO_2	Silica

TOC	**Total Organic Carbon**
TOM	**Total Organic Matter**
UTCC	**University of Toronto Culture Collection of Algae and Cyanobacteria**
UV-Vis	**Ultra Violet – Visible Spectrometer**

1. INTRODUCTION

Worldwide biogeochemical nitrogen cycling in aquatic environments is characterized as the maintenance of small scale nitrogen conversions over global sediment fields. Open to atmospheric and terrestrial nitrogen pools, the N-cycle in aquatic systems is dynamic as N-deposition and agricultural run-off affect loading and sediment nitrogen-processing rates. Sinks in the N-cycle, principally denitrification, may create a nitrogen deficit situation allowing nitrogen to become an important limiting nutrient in some aquatic ecosystems (Howarth & Marino, 2006). Human activities in watersheds may increase loading of other nutrients (e.g. phosphorus, silica, potassium) to aquatic systems. The nature of the activity may influence the nutrient loading ratios to aquatic systems. In response to changes in nutrient ratios, the primary producer community composition may change as low N:P, for example, may favour cyanobacteria (Bulgakov & Levich, 1999) while high N:Si favours diatoms (Anderson, 2000). Shifts in community composition could impact denitrification in the sediment layer if organic carbon becomes redistributed and recycled near the sediment layer (due to algal growth, e.g. diatoms, or sinking algae) as opposed to organic carbon being recycled in the water column. If more organic matter is deposited on the sediment, organic matter remineralization in sediments will increase while remineralization in the water column will decrease. In turn, this should increase benthic nitrification of mineralized N, and denitrification coupled to nitrification. It may also increase the production of N_2O as a by-product of nitrogen cycling processes (nitrification and denitrification). Nitrous oxide is an important greenhouse gas and nitrogen cycling in aquatic systems has potential to contribute significantly to global climate change. Enhancement of nitrous oxide production due to shifts in nutrient loading

ratios could be an important outcome of human activities in watersheds that has not been considered previously. This study will develop an understanding of Si:N and P:N loading effects on seasonal microbial community diversity and their contribution to deposition and accumulation of sediment organic matter, remineralization of organic matter, and the production of N_2O and N_2, representing the permanent N removal from an aquatic system. Analysis of the conditions for nitrous oxide production becomes the main focus in this research for future applied greenhouse gas management (Aelion & Shaw, 2000).

1.1 Nitrogen Cycling

Nitrogen (N) is an important component in fertilizers to increase crop yield and a constituent of fossil fuels, released during combustion as nitrogen oxides (NOx). The ability of nitrogen to exist in many different oxidation states makes it a reactive element. Many microorganisms exploit the reactivity of nitrogen as an electron donor or acceptor in their metabolism, and microorganisms are responsible for most N transformations in the global nitrogen cycle within the biosphere. These key transformations include nitrogen fixation, ammonia assimilation, assimilatory nitrate reduction, and ammonification, nitrification, and denitrification (Figure 1-1). Under N-limiting conditions, nitrogen fixation transforms atmospheric nitrogen (i.e. N_2) into biologically available nitrogen (i.e. NH_3, NH_4^+) via enzyme-catalyzed reduction. As a result, nitrogen may be incorporated into biomass. The reciprocal process where NH_3 and NH_4^+ are generated through the breakdown of organic nitrogen (N-remineralization) is known as ammonification. An alternative NH_3/NH_4^+ fate, nitrification, results from the oxidation of these compounds into NO_2^- and NO_3^-. Nitrification is an aerobic process. Denitrification

transforms nitrate through several reduction steps into a final gaseous product of N_2O (partial reduction) or N_2 (complete reduction). Denitrification is a process in which the oxidized nitrogen form is used as a terminal electron acceptor when oxygen is absent or present at very low concentrations.

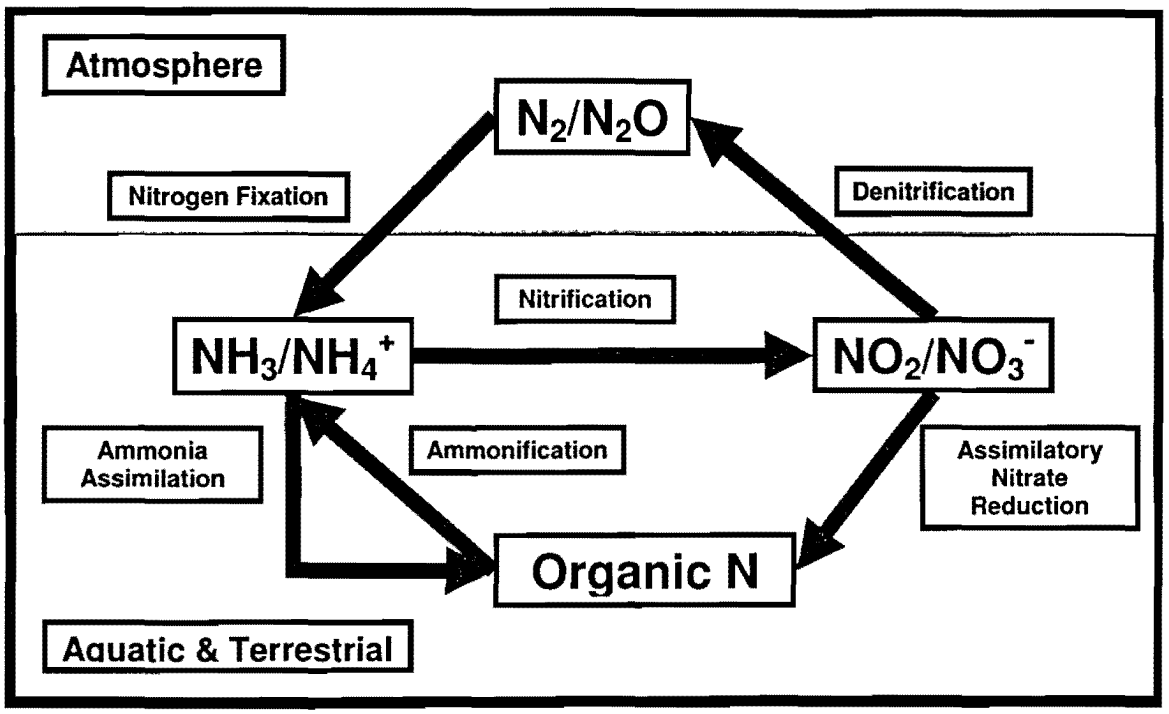

Figure 1-1. Conceptual model of microbially-mediated nitrogen transformations in aquatic systems

1.1.1 Atmospheric Nitrogen Cycle Overview

Global nitrogen is predominantly N_2, constituting 78% of the atmospheric gases, where N_2O makes up 99% of the remaining atmospheric N-compounds. Nitrous oxide accounts for about 0.0003% of the total atmospheric gases (Machefert, *et. al.*, 2002) or 318 ppb (global average) in 2004 (Hall *et. al.*, 2007). The remaining environmental N-gases include nitrogen oxides, and ammonia. Dinitrogen gas is derived from a complete nitrate reduction by microbial denitrification. Partial denitrification contributes nitrous oxide and nitrogen oxides to the troposphere which contains 0.6 Tg N as reactive nitrogen oxides (i.e. NOx, peroxyacetyl nitrate, and HNO_3) (Logan, 1985). The majority of nitrogen oxides (NOx) within this region react photochemically with oxidants (i.e. HO_2, RO_2, and OH) to form HNO_3 within 1 to 30 days. The ability of HNO_3 to exist as an aerosol or cloud moisture (liquid state at 47.6 torr and 20°C) allows this compound to be a persistent pollutant. Anthropogenic acid deposition results from sulphur and nitrogen oxide mixing with precipitation. Nitrogen oxides play a larger role in acid rain formation since they increase at a greater rate than sulphur oxides due to natural and industrial activities (Logan, 1985).

The largest ammonia contributor is supplied by ammonification and volatilization from animal excreta (Freney *et. al.*, 1983). As a result nitrate salt (i.e. NH_4NO_3) is produced, when nitric acid reacts with ammonia base:

$$NH_3(g) + HNO_3(g \text{ or } aq) \rightarrow NH_4NO_3 \text{ (s or aq)}$$

The majority of ammonia gas (NH_3) is cycled back to the biosphere in precipitation, or dry deposition. In transitional gas conditions, these reactants would be involved in cloud condensation or neutralizing acidic aerosols (Lawson, 1988).

1.1.2 Soil Nitrogen Cycle Overview

In terrestrial systems nitrogen is frequently a limiting nutrient because most organisms cannot use elemental atmospheric nitrogen and mineralized nitrogen is lost to the atmosphere by denitrification. Atmospheric nitrogen is incorporated into the soil by means of nitrogen fixation, including biological nitrogen fixation and abiotic (e.g. lightning) fixation. In natural soils, atmospheric nitrogen fixation and denitrification are roughly in balance. However, human activities can unbalance these processes, increasing N input relative to denitrification. Anthropogenic nitrogen fixation may be accomplished by the Haber-Bosch process to produce fertilizer (Howard & Rees, 1996) for agricultural application. Fossil fuel and biomass combustion release NOx indirectly which may be returned to soils in wet and dry deposition, and biological agricultural practises (e.g nitrogen soil recovery from clover and soybean field planting) can increase biological nitrogen fixation (Galloway *et. al.*, 1995; Smil, 1997). Leguminous plant roots are a main participant in the latter process by integrating atmospheric nitrogen into soil matrices via symbiotic *Rhizaobium* bacteria. These anaerobic diazotrophic (nitrogen-fixing) microbes commonly utilize nitrogenase enzyme as an integral part of this process. Nitrogenase consists of a Mo-Fe complex that binds nitrogen gas to the enzyme where it undergoes electron reduction in the Fe site (Igarashi & Seefeldt, 2003; Masukawa *et. al.*, 2007; Rees & Howard, 2000). The resultant free ion NH_3/NH_4^+ forms are unstable in aerobic conditions and will immediately be incorporated in organism biomass (Delwiche, 1981).

Along with nitrogen fixation, reduced nitrogen is also supplied to the system by dead organic soil matter through ammonification via heterotrophic bacteria. Nitrate is the most prevalent free ionic nitrogen form in oxic soil because 1) ammonium is assimilated

preferentially and 2) nitrifiers rapidly convert available ammonium (i.e. that not assimilated) to nitrate. Although nitrate may be incorporated in microbial soil biomass, it may also be involved in the denitrification process where it serves as a terminal electron acceptor to produce NOx intermediate products (Delwiche, 1981). These NOx products may be cycled back into soils by microbes, lighting and forest fires (Galloway *et. al.*, 1995). Human activities (e.g. fertilization, combustion of fossil fuels, and cultivation of legumes) combine to increase N loading to soils (Galloway *et. al.*, 1995; Vitousek *et. al.*, 1997). When denitrification fails to increase in proportion, excess nitrogen may be exported from soils to ground water and surface water, increasing N loading to these environments (Galloway *et. al.*, 1995).

1.1.3 Aquatic Nitrogen Cycle Overview

While nitrogen fixation is likely a dominant source of aquatic nitrogen in pelagic ocean waters, terrestrial run-off and anthropogenic additions are the most important inputs of bioavailable N in freshwater and near-shore marine systems (Moore *et. al.*, 2009). Nitrogen input through anthropogenic means and nitrogen fixation to a minor extent is offset (wholly or in part) by the permanent removal of nitrogen to the atmosphere by denitrification. When inorganic nitrogen is introduced into the aquatic environment, it cycles in the water column as a dissolved mineral form of N or becomes assimilated by primary producers. The biomass of primary producers (algae and cyanobacteria) may be recycled within the water column, however some portion will sink to the sediments and be recycled there. N-pools in the sediment include: organic N, porewater ammonium from remineralization of organic matter, pore water nitrate, and dissolved nitrogen gases

(Blackburn & Henriksen, 1983). These N-pools are constantly manipulated by microbially facilitated processes: remineralization, ammonification, ammonia assimilation, assimilatory nitrate reduction, dissolved reduction of nitrate into ammonia (DRNA), nitrification and denitrification.

1.2 Overview of Specific Nitrogen Cycling Processes

1.2.1 Remineralization of Nitrogen

Remineralization is the regeneration of inorganic nitrogen when organic nitrogen is metabolized, typically remineralization involves the production of ammonium through deamination or degradation of urea. This process is a by-product of both aerobic and anaerobic metabolism and is mediated by a wide variety of heterotrophic microorganisms (e.g. algae, fungi, bacteria) in sediments. The transport of nutrients from the sediment to the water column is an internal loading of nitrogen as it is distinguished from the external loading of terrestrially-derived nitrogen into an aquatic system. Internal loading may be an important source of ammonium from remineralization (ammonification) to the water column. Deep open waters like Lake Michigan favours this internal recycling where 95% of nutrient loading is internal, with nutrients recycled from the sediment to the water column (Brooks & Edgington, 1994). Nitrogen may continuously cycle between the sediment and water column, until it is permanently lost to the atmosphere through nitrification/denitrification processes (Présing *et. al.*, 2001). Remineralization may also occur by means of N-rich metabolite excretions from zooplankton and fish, and release of contents during cell lysis due to parasitism. The remineralization rate from the sediment

to the water column is defined by primary production, the deposition rate of the primary production and sediment resuspension (Farías, 2003).

Ecological Significance of Remineralization

The importance of remineralization is to regenerate inorganic nitrogen making it available to phytoplankton. This internal loading of nitrogen can be the major source of nitrogen that would support primary pelagic production during late summer and fall (Farías, 2003). With an upwelling of nutrients into the water column, the pelagic microbial community becomes more diverse with increasing competition than their benthic counterparts (McCarthy *et. al.*, 2007). McCarthy, *et. al.* (2007) suggest that

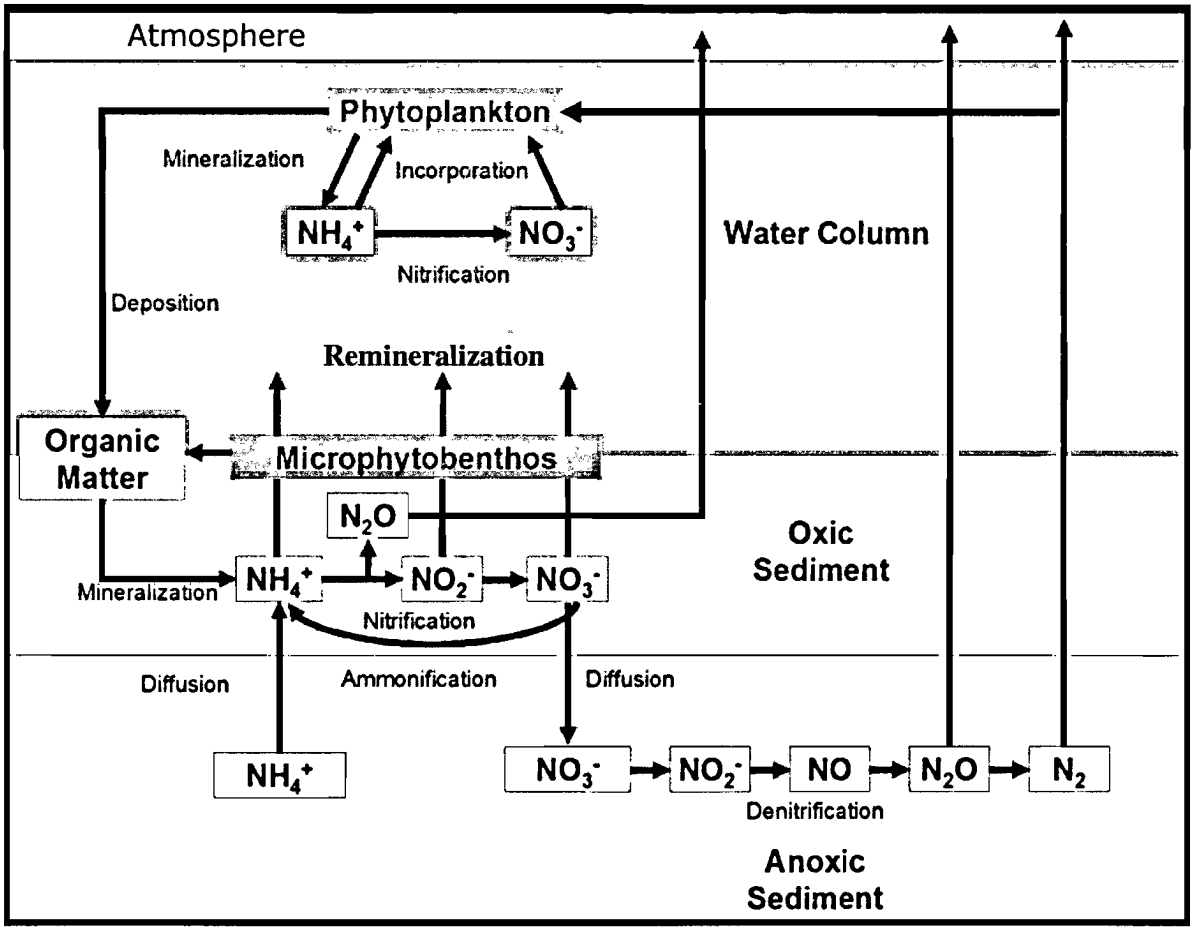

Figure 1- 1. Conceptual model of Sediment Denitrification

phytoplankton (i.e. cyanobacteria) can be nitrogen limited even when there is abundant nitrate if ammonium concentrations are low. During summer when phytoplankton biomass is at its highest, the N-compounds are incorporated as follows: ammonium > urea > nitrate (Présing *et. al.*, 2001). Therefore, the supply of remineralized nitrogen may determine microbial community dominance and influence the trophic status of the lake system as shown in the conceptual diagram (Figure 1-2) illustrating aquatic N-cycling.

Although the sediment region would become the source of recycled dissolved inorganic nitrogen (i.e. nitrate and ammonium) delivered to the overlying water, the benthic region (e.g. Northwestern Atlantic ridges) may be an N-sink as nitrate flux into the sediment may exceed ammonium efflux during the summer (Laursen & Seitzinger, 2002). Principally, all microorganisms involved in organic degradation participate in ammonification. During ammonification, organic nitrogen compounds (e.g. urea, amino acids) become hydrolyzed and deaminated to form carbon dioxide, ammonia, and ammonium under oxidizing conditions. For every molecule of urea oxidized, two molecules of ammonia are produced. Amines are produced under anaerobic ammonification. Heterotrophic bacteria facilitate this assimilation of nitrogen into the ammonifying organism. This incorporation of ammonium is utilized for metabolic purposes where the excess is distributed into the surrounding sediment for local uptake by primary producers and bacteria or use as an energy substrate by nitrifiers (Farías, 2003).

Factors Influencing Remineralization

This remineralization process is largely determined by the amount of available and reactive organic matter (derived from benthic primary production and deposition), sediment redox properties (oxic conditions vs. anoxic conditions), bioturbation and nutrient accumulation and burial rate (Farías, 2003).

Internal loading of remineralized nitrogen from sediments to the water column may be facilitated by diffusion or turbulent mixing and resuspension of sediments. Resuspension may increase remineralization by exposing buried metabolites for reoxidation and transferring substrate particles to the oxic layer (Aller, 1994). Sediment disturbances by benthic organisms (e.g. *Tubifex tubifex*) may also occur frequently during summer to increase nutrient exchange between sediment and water and stimulate remineralization (Scott *et. al.*, 2008). Warm temperatures in the summer (e.g. Great Lakes) may increase remineralization effects, with nutrient flux from sediments increasing with lake temperature and mixing (Klump *et. al.*, 2009).

1.2.2 Nitrification

Nitrification is mediated by chemolithotrophic bacteria: ammonia-oxidizing bacteria (AOB) and nitrite-oxidizing bacteria (NOB). AOB belong to the *Proteobacteria* group where they are further characterized into subclasses of Beta (i.e. *Nitrosospira* and *Nitrosonomas*) mainly inhibiting freshwater and Gamma (i.e. *Nitrosococcus*) mainly inhibiting marine environments, and NOB of the Alpha *Proteobacteria* subclass (i.e. *Nitrobacter*) and *Nitrospira* genera are most widely studied in aquatic systems (Fortunato

et. al., 2009). In lake environments, nitrification is initially facilitated by *Nitrosomonas* to produce nitrite from the oxidation of ammonium:

$$NH_4^+ + 11/2O_2 \rightarrow NO^{-2} + H_2O + 2H^+, \qquad \Delta G = -290 \text{ kJ/mol}$$

and then by *Nitrobacter* to oxidize the resultant nitrite into nitrate (Risgaard-Petersen, 2003):

$$NO_2^- + 1/2O_2 \rightarrow NO_3^-, \qquad \Delta G = -82 \text{ kJ/mol}$$

Generally, ammonium oxidation will proceed at a higher rate than nitrite oxidation. This is for reasons that ammonium oxidizers have higher half-saturation constants for substrate uptake and tolerance of lower oxygen concentrations before inhibition, and a greater substrate affinity than nitrite oxidizers (Miranda *et. al.*, 2008). This process occurs in the water column and in the oxic sediment layer. The sediment consists of two layers, the oxic and anoxic layers, where nitrification and denitrification occur respectively (Liikanen *et. al.*, 2002). Organic nitrogen is known to stimulate nitrification by supplying ammonium through remineralization (Meyer *et. al.*, 2001).

Ecological Significance of Nitrification

While nitrifying chemoautotrophs assist in nitrate production, nitrification also becomes an important pathway for carbon fixation, especially during dark cycles and deep water bodies. Both *Nitrosomonas* and *Nitrobacter* mainly assimilate carbon dioxide through the RuBisCo of the citric acid cycle where the latter synthesizes polyhydroxybutyrate to decrease the inhibitory effects of organic matter (Poughon *et. al.*, 2001). Carbon fixation via nitrification may account for a significant fraction of total fixed carbon. In coastal marine sediments, nitrification accounted for as much as 50% of total carbon fixation

(calculated from Laursen & Seitzinger, 2002). Nitrifiers may also compete with methane oxidizers for oxygen, which could suppress either methane or ammonium oxidation depending on the organic carbon available (Henriksen & Kemp, 1988). Elevated ammonium conditions, such as in Seine Estuary, France, created conditions of up to 60% total oxygen consumed by nitrification (Andersson *et. al.*, 2006). Even in coastal marine sediments with relatively low ammonium, nitrification may account for as much as 10% of oxygen consumption (calculated from Laursen & Seitzinger, 2002).

Nitrification functions to remove ammonium, a by-product of metabolism that could otherwise accumulate to toxic levels, by converting it into nitrate. Further, oxic sediment nitrification supplies nitrate and nitrite which can be used by primary producers in the water column (Passell, *et. al*, 2007) or sediments, or which can diffuse into anoxic sediments and be permanently removed through denitrification. However, highly labile carbon favours use of oxygen in respiration in freshwater environments, and methanotrophs have a greater affinity to oxygen and may reproduce 10-fold faster than nitrifiers (Megmw & Knowles, 1987). Nitrification is also ecologically significant as nitrous oxide, a potent greenhouse gas, may be formed as a nitrification intermediate (Bouwman *et. al.*, 1995).

Factors Influencing Nitrification

Nitrification optimally operates under conditions of substantial exchangeable NH_4^+ pool, low temperature, a moderately alkaline pH (8.0 - 8.5), low light, and relatively moderate dissolved oxygen content (Skadsen, 2002; Zhou, 2007). Sensitive to water temperature, nitrifier biodiversity changes and nitrification rates increase with a temperature rise from

4°C to 24°C (Miranda *et. al.*, 2008). As a self limiting system, nitrification lowers surrounding pH levels during nitrite production. However, photosynthesis may raise pH permitting nitrification to proceed without becoming self-limiting, thus producing a fairly narrow pH range in which nitrifiers function. As pH becomes greater than ~8.5, the availability of ammonium decreases (as NH_4^+ deprotonates, forming ammonia gas) (Skadsen, 2002). Therefore, algal blooms producing pH greater than 9 may hinder nitrifier processes (Lundholm *et. al.*, 2004). High alkaline conditions during summer algal blooms may promote phosphorus release from the sediment and accumulate toxic NH_3 which may further inhibit nitrifier activity (Focht & Verstraete, 1977; Vrede *et. al.*, 2009). The relationship with benthic photosynthesis is thus complex. Moderate levels of photosynthesis produce moderately alkaline conditions and provide labile organic matter for mineralization. Although these factors enhance nitrification, high rates of photosynthesis increase ammonium competition and create more extreme alkaline conditions which are detrimental to nitrifiers.

Organic rich sediment containing easily assimilable carbon may provide sediment heterotrophs a competitive advantage over nitrifiers. As a result, nitrate may be produced with low yield (Krishnan & Bharathi, 2009). The presence of organic carbon may diminish the rate and yield of nitrate production by diverting nitrogen from the nitrifiers to the heterotrophs. This depends on the C:N ratio and the quality of the organic compounds. High C:N and higher levels of labile organic carbon inhibits nitrification by decreasing nitrite oxidizing bacteria, whereas low C:N and high refractory organic carbon content enhances nitrification (Xia *et. al.*, 2008).

Microbial photosynthesis and respiration processes may also alter pH conditions as well as oxygen content, and inorganic carbon and nitrogen pools (Garnier & Billen, 2007). Nitrification may be conducted as this aerobic process by itself or its efficiency could be improved with the coupling of reducing agents by chemolithoautotrophic bacteria (Poughon *et. al.*, 2001). De Beer (2002) demonstrated that despite the inhibition effects of daylight, nitrification rate was proportional to the oxygen produced during photosynthesis. However, an excess may reduce nitrification due to oxygen limitation as oxygen is consumed in the remineralization process (Joye & Hollibaugh, 1995).

Competition of active binding sites may limit nitrifying rates with the exposure of seasonal precipitation. The precipitation of $CaCO_3$ is characteristic of hard water lakes in early summer (e.g. Lake Michigan, Lake Ontario), where Mg^{+2} and Mn^{+2} compete with Ca^{+2} for CO_3^- binding sites essentially enhancing carbon precipitation (i.e. $MgCOv_3$ and $MnCO_3$). Since nitrification is driven by chemolithotrophs, inorganic carbon becomes less available to support this nitrifying process (Farías, 2003; Hodell & Schelske, 1998; Jahnke & Jahnke, 2000). Similarly in the presence of iron (essential in N-fixation processes as it is a co-enzyme in the nitrogenase complex), the ferrous and ferric iron form prevalent in low pH environments may decrease nitrification as they strongly complex with organic matter to lower the supply of ammonium through organic matter remineralization (Baeseman *et. al.*, 2006; Routh *et. al.*, 2008). In addition, H_2S irreversibly inhibits nitrification (Joye & Hollibaugh, 1995). Mainly in marine environments, the associated free sulphide intermediates (i.e. H_2S and S^{2-}) from dissimlatory sulphate reduction will inhibit both nitrification and denitrification. Sulfide inhibition of nitrification is particularly important in marine systems where sulphate

reduction can contribute up to 20-40% organic matter reduction (Blackburn & Blackburn, 1993; Heggie *et. al.*, 2008; Hulth *et. al.*, 1999; Joye & Hollibaugh, 1995). Iron oxide may potentially decrease sulphide inhibition by binding to HS^- to form FeS. These metal bound sulphides (e.g. FeS) are an abundant component in freshwater sediments (Holmer & Storkholm, 2001).

Seasonal factors influence plume sedimentation, sediment resuspension, and horizontal advection to increase sediment deposition (Filstrup *et. al.*, 2009). Potentially spring nitrification rates may perform optimally as inhibiting labile carbon in sediment is low and turbulent mixing results in low light penetration (Filstrup *et. al.*, 2009; Ward *et. al.*, 1982). Possible seasonal transition in dissolved inorganic nitrogen composition from ammonium (spring) to nitrate (summer) may occur (Sugimoto *et. al.*, 2008). Summer nitrification may experience competition with heterotrophs as their populations increase with periphyton layer. Although ammonium pools are relatively high due to summer ammonification, nitrification becomes restricted to the diminished oxic layer until lake freezing (Kemp *et. al.*, 1990). During winter nitrate may be at its highest despite cold temperatures inhibiting nitrification as denitrification is also inhibited by low average winter lake temperatures (Filstrup *et. al.*, 2009).

1.2.3 Denitrification

The denitrifying process is the reduction of nitrate through several intermediate N-species, ultimately to dinitrogen gas, although the term can also be applied to the reduction of any

one intermediate to N_2, or to a second intermediate (Tesoriero, *et. al*, 2000). The overall process can be represented as:

$$2NO_3^- + 12\ H^+ + 10e^- \rightarrow N_2 + 6H_2O \text{ (non-specific } e^- \text{ donor)}$$

Denitrifying bacteria are ubiquitous, and are phylogenetically diverse with bacterial groups: *Bacillus, Enterobacter, Micrococcus, Pseudomonas, Spirillum,* and other anerobes containing some or all of the suite of enzymes to catalyze steps in the denitrifying pathway (Zhou, 2007). While denitrification is generally considered a bacterial process, the ability to denitrify has been reported in some archaea and eukaryotes (fungi) as well (Zumft, 1997). Most denitrifiers are facultative anaerobic heterotrophs that utilize denitrification as an alternative respiratory system and are able to grow equally well or better in oxygen. Conversely, the oxidation of inorganic carbon may be a different energy source for autotrophic denitrifiers that are not as widespread. Intermediate steps between the reduction of nitrate to dinitrogen gas form nitrite, nitric oxide, and nitrous oxide in order of sequence. By-products of this respiratory pathway are formed as well and are released as bicarbonate and sulphate ions, and carbon dioxide (Rivett *et. al.*, 2008).

1.2.3.1 Nitrate Sources for Denitrification

Coupling of Nitrification and Denitrification

With ample nutrient supply, stable bacterial community and minimal sediment bioturbation, the coupling of nitrification with denitrification is made possible (Lorenzen *et. al.*, 1998). Under high organic sediment load via the mineralization process, ammonium is made available for nitrification. Respiring bacteria readily consume

oxygen to metabolize organic carbon. At the periphyton surface where oxygen is plentiful (either by diffusion or photosynthetic production), nitrate becomes a dominant form of inorganic nitrogen. However, the nitrifiers must also compete with autotrophs for ammonium, and this competition can reduce nitrogen loss by denitrification when bacterial respiration out competes nitrifiers for available ammonium (Risgaard-Petersen, 2003). On the other hand, coupled nitrification/denitrification may be supported by photoautotrophs during photosynthesis as the depth of nitrification increases with greater sediment oxygen penetration (Rysgaard, *et. al*, 1994).

In the case of active sediment bioturbation, resuspension and/or benthic primary production under low NO_3^- and NH_4^+ concentrations during summer, nitrification in the sediment oxic layer will become evenly distributed allowing for the nitrification/denitrification coupling to become less efficient. This potentially may provide a greater opportunity for nitrate to be incorporated into primary production instead of denitrification (Rysgaard *et. al.*, 1995). However, bioturbation by various invertebrates either produced no effect or increased denitrification by providing additional oxygen surface area to improve nitrification (Howe *et. al.*, 2004; Karlson, 2007; Svensson *et. al.*, 2001). A greater oxygen depth penetration decreases the likelihood of nitrate loss to the water column, by delivering nitrate directly to the denitrification layer. However, this same oxic layer may act as a barrier to prevent the uptake of nitrate from the water column, even under high nitrate concentrations, as nitrifiers may become inhibited by an oxygen excess. Under O_2 concentrations greater than 200 μM, nitrifiers may retreat to the lower oxic region above the anoxic/oxic boundary (Jensen, *et. al*, 1994). Essentially, nitrification is the limiting factor for this coupling to exist. Thus, any

conditions where ammonium and oxygen supply cease it would consequently stop nitrification and subsequently denitrification under conditions of little water column nitrate diffusive supply (Blackburn *et. al.*, 1994).

Diffusion from the Water Column

In addition to coupled nitrification-denitrification, denitrifiers may receive nitrate by direct diffusion from the water column. Nitrate is soluble in water, possibly traveling great distances under less stagnant waters (i.e. rivers, streambeds) and is delivered to the anoxic layer depending on periphyton constituents (Duff *et. al.*, 2008; Mermillod-Blondin *et. al.*, 2008; Rust *et. al.*, 2000). Microphytobenthos particularly prokaryotes, may significantly affect this diffusion of nitrate as well as ammonia from porewater by means of assimilatory uptake (Seitzinger & Nixon, 1985). Nitrate uptake by assimilation may out compete denitrification for available nitrate when photoautrophic production is high. Despite these interferences, nitrate diffusion is dependent on both the oxic zone depth and the nitrate concentration within the water column, as implied by Fick's laws of diffusion (Lavery *et. al.*, 2001).

Denitrification supported by direct diffusion is restricted to the thickness of the oxic zone that controls the nitrate diffusional supply. Diffused nitrate is dependent on oxygen sediment depth penetration. The nitrate gradient profile becomes less steep with a longer diffusional path created by this sediment oxygen penetration on the sediment-water interface and associating bacterial nitrifying interactions (Risgaard-Petersen *et. al.*, 1994). Under these oxic conditions, nitrate diffusive flux may approximate net denitrification and will be lower than the gross denitrification rate where some coupled

nitrification-denitrification occurs. Nitrate diffusive flux would approximate gross denitrification rates without coupled nitrification, where denitrification is supported solely by external nitrate (Groffman *et. al.*, 2006). Nitrate diffusion may slow above nitrate concentrations greater than 4 mg L^{-1} that would support N-accumulation along the sediment-water interface and decreased nitrate concentration gradient within the sediment (James *et. al.*, 2008). These high nitrate situations are a result of saturated enzymes in denitrifier bacteria which may also result in low substrate efficiency and velocity.

1.2.3.2 Ecological Significance of Denitrification

Nitrogen losses in freshwater through denitrification have been estimated to account for between 1% and 36% of the total N-loading, also removing as much as 40-50% of inorganic nitrogen loading in estuaries (Seitzinger, 1988). In some cases, lakes were estimated to retain more than 50% of their N-inputs where a maximum 87% of N-inputs were removed (Alexander *et. al.*, 2002). It was estimated that global lake N-removal to be 19.7 Tg N yr^{-1} from watersheds, about 4 times the N-removal quantity than in estuaries (~5 Tg N yr^{-1}) (Seitzinger *et. al.*, 2006). Small lakes (size < 50 km^2) may remove 9.3 Tg N $year^{-1}$ which is almost half of the total global lake N-input (13.0 Tg N $year^{-1}$), a greater quantity than the large lake N-removal quantity of 3.7 Tg N $year^{-1}$. These global estimates may be attributed to these smaller lakes generally having a greater surface area (2.6 x 10^6 km^2) in comparison to large lakes (1.2 x 10^6 km^2). Such values were suggested to be underestimated, leading to a more significant effect of small lakes removing nitrogen via denitrification especially for countries with high lake densities (e.g. Canada) (Harrison *et. al.*, 2008).

Nitrogen availability in open lake bodies and especially in estuarine environments are based on denitrification because there are very few aquatic organisms (i.e. cyanobacteria) that can utilize N_2 as a nitrogen source (Risgaard-Petersen, 2003). Marine systems are generally nitrogen limited, and most of their eutrophication problems including hypoxic and anoxic dead zones and formation of harmful algal blooms can be attributed to nitrogen pollution (National Academy of Science, 2000). Denitrification becomes important to these systems as it is the major processes, besides anaerobic ammonia oxidation (ANAMMOX) that can ameliorate these impacts by permanently removing nitrogen (Conley *et. al.*, 2009).

Denitrification is also ecologically significant as some toxic (NO_2^-) and environmentally destructive (N_2O) intermediates are formed. Nitrite accumulation is typically negligible and nitrite is often not measurable in aquatic systems. Nitrous oxide production resulting from denitrification in aquatic systems, however, does contribute significantly to the atmospheric pool. As described above, this can contribute to radiative forcing and, potentially, to stratospheric ozone depletion.

1.2.3.3 Influential Environmental Factors of Denitrification

Organic Carbon

Globally, lakes are accumulating organic carbon at an estimated rate of ~42 Tg C yr^{-1}, where large lakes contribute to about 15% (6-7 Tg C yr^{-1}) (Filstrup *et. al.*, 2009). An increase in organic matter loading to sediments could stimulate remineralization and nitrification/denitrification (Wetzel, 1983). Jordan, *et. al.* (2009) stated that ammonia deposits from invertebrates may not contribute to enhanced denitrification rates if not

associated with an increase in labile carbon, as the lack of organic carbon for heterotrophic denitrifiers to accept electrons may hinder denitrification (Rivett *et. al.*, 2008). Improved NH_4^+ fluxes and anoxia resulting in the sediment release of phosphorus from oxidized iron may be an effect of both a large organic deposit and reduced denitrification (Eyre & Ferguson, 2002; Lavery & McComb, 1991; Owens & Stewart, 1983).

Heterotrophic denitrification mainly depends on bioavailable dissolved organic carbon (DOC) within the immediate vicinity of the porewater and groundwater rather than the total carbon content of the region (Rivett *et. al.*, 2008). This process is able to convert 0.93 mg N L^{-1} nitrate from 1 mg L^{-1} carbon based on the stoichiometry (Jacinthe *et. al.*, 2003; Jørgensen *et. al.*, 2004):

$$5CH_2O + 4NO_3^- \rightarrow 2N_2 + 4HCO_3^- + CO_2 + 3H_2O$$

Primarily controlled by mineralization, DOC may vary in concentration according to pH, temperature, oxidant concentrations, sorption affinities to mineral surfaces and DOC chemical composition (Hartog *et. al.*, 2004).

Local Redox Potential

Denitrification may only be permitted to react with a relatively small quantity of dissolved oxygen or nitrate (Hartog *et. al.*, 2004). Apart from the redox properties of the periphyton layer, rates of denitrification/nitrification may depend on the thickness of the periphyton layer (upper organic layer of sediment). This periphyton layer may also prevent water column carbon and dissolved inorganic nutrients from penetrating into deeper sediment regions by acting as a physical biomass barrier (Woodruff *et. al.*, 1999).

Nutrient impermeable sediment barriers, such as a thick periphyton layer, define nitrification as the major supplier of nitrate substrate to the denitrification process in some instances (Jordan *et. al.*, 2009).

Traditionally denitrification rates are measured in the sediment, however, Ishida, *et. al.* (2008) have shown that the periphyton layer were also capable of denitrification. Microbial metabolic activity consumes oxygen within periphyton, creating a solute gradient that would permit an anoxic layer deep in the periphyton where denitrification (simultaneously inhibiting nitrification) can occur, limiting nitrate diffusion into sediment and denitrification in sediment (Ishida *et. al.*, 2008; Krause-Jensen *et. al.*, 1999). The metabolic photoautotrophic activity may be dependent on the periphyton assemblages which are characteristic of their substrate and nutrient environment. Nitrifiers may benefit from this periphyton layer as algae and cyanobacteria within this biofilm supply labile carbon by the release of extracellular organic compounds and algal decomposition (Ishida *et. al.*, 2008).

Dissolved Oxygen

Denitrification requires low oxygen concentrations ($O_2 < 1 - 2$ mg/L) in order to proceed (DeSimone & Howes, 1998). Oxygen saturation regulates the genes that encode the enzymes required for denitrification, where gene expression is inhibited by high oxygen concentrations ($O_2 > 1$ μM) (Canfield *et. al.*, 2005; Curie *et. al.*, 2009; Seitzinger, 1988). Therefore, it is essential for denitrification to operate near the oxic/anoxic interface in sediments and biofilms. Sediment oxygen penetration depths and bottom water nitrate concentrations may vary independently within estuaries (Revsbech *et. al.*, 1980).

Balance between periphyton production and respiration, as well as sediment porosity and chemical oxygen demand will determine oxygen depth penetration. As previously stated, sediment oxygen penetration decreases with oxygen consumption (Duff *et. al.*, 2008). Oxygen penetration may increase with photosynthesis activity during daylight, where produced oxygen may reduce immediate surface denitrification rates by as much as 70%. As a result, water column nitrate may penetrate deeper into the anoxic sediment strata without stimulating denitrification (Blackburn & Henriksen, 1983).

Electron Acceptors and Donors

Under anoxic conditions, obligate anaerobes become dominant and utilize available electron acceptors according to their free energy (Korom, 1992):

NO_3^-: ΔG=-72.3 Kj/electron > Mn^{4+}:ΔG= -50.3Kj/electron > Fe^{3+}: ΔG= 4.6Kj/electron > SO_4^{-2}: ΔG= 21.4 Kj/electron

Based on relative abundance in freshwater systems and energy yield, nitrate is typically the most favoured alternate electron acceptor once oxygen is depleted. Once nitrate supplies have been exhausted, the oxidation of organic matter may proceed with other electron acceptors, typically in the sequence Mn^{4+}, Fe^{3+}, SO_4^{-2} and then fermentation (Froelich *et. al.*, 1979).

The reduction of nitrate by Fe^{+2} ions may be conducted as either biotic or abiotic processes, or even both. *Gallionella ferruginea* bacteria are known to facilitate the biotic nitrate reduction. Generally found near the anoxic/oxic boundary since it requires a small

quantity of oxygen, *G. ferruginea* reduce nitrate into nitrite under conditions of abundant ferrous iron (Korom, 1992). The abiotic formation of nitrite from the oxidation of Fe^{+2} may continue as long as there is available organic carbon which Fe^{+3} can oxidize in order to regenerate Fe^{2+} (Davidson *et. al.*, 2003). Under organic poor surroundings, denitrification may continue as Fe^{+3} terminally accepts electrons and precipitates into oxyhydroxide or oxide mineral (Korom, 1992). Metal catalysis (e.g. Cu^{+2}) may play a role in promoting these reduction reactions (Ottley *et. al.*, 1997).

Temperature and pH

Nitrate and oxygen limit denitrification with temperature as a minor influence on a global scale (Silvennoinen *et. al.*, 2008), although correlation between temperature and denitrification may be weak in some studies (Silvennoinen *et. al.*, 2008). Denitrification may operate at temperatures ranging from 2 to 50 °C, where optimum temperatures lie between 25 and 35°C (Brady & Weil, 2002). It could be assumed as the temperature increases, oxygen consumption increases while oxygen solubility decreases, subsequently facilitating other electron acceptors to continue the carbon degradation process (Harrison *et. al.*, 2008; Liikanen *et. al.*, 2002). Although climate could affect N loading by changing the runoff balance and evapotranspiration, denitrification is subject to more significant immediate effects (e.g. nutrient runoff) (Harrison *et. al.*, 2008).

Although optimal pH levels for denitrification are site specific, heterotrophic denitrifiers may prefer a pH range between 5.5 and 8.0 (Rust *et. al.*, 2000). Acidic environments (around 3.5 pH), such as industrial mining work areas, were shown to have a relatively low nitrate consumption and low pH would seem to inhibit denitrification

(Baeseman *et. al.*, 2006). Dissimilatory ferric iron reduction may also inhibit denitrification as these pathways compete for electrons under low pH conditions (Rust *et. al.*, 2000). Nitrite may be reactive under these pH conditions, particularly with ferric iron and light, existing as nitrous acid (protonated form) which was demonstrated to inhibit nitrate reduction at low concentrations of 0.04 mg L^{-1} HNO_2-N (Abeling & Seyfried, 1992). Under alkaline conditions (pH > 8), denitrification may be stimulated by the production of nitrate from ammonium or nitrite by the oxidation of ferrous iron (Fanning, 2000). Nitrate reduction by iron is pH dependent as ferric oxide or oxyhydroxide precipitation are formed from Fe^{+3} under neutral or alkaline conditions, hence denying iron access in denitrification (Ottley *et. al.*, 1997).

Seasonality

Denitrification rates become relatively low during spring/fall seasons ensuring that sediment nitrogen maintains high concentration nitrate gradients. Although spring denitrification rates may be relatively small, these rates may could be at least twice as great as those in winter due to improved daylight water penetration from relatively low microphytobenthos and high mineralization (Heggie *et. al.*, 2008). Both spring and fall seasons were reported to have the lowest seasonal ammonium and NOx concentrations in the water column.

According to the relatively high summer microbial efficiency and velocity from well-mixed lake conditions, high net ammonium release and low NOx uptake may lead to greater organic matter decomposition, enhanced ammonium release, and improved anoxic conditions for denitrification (Risgaard-Petersen, 2003). However, Spooner &

Maher (2009) reported that denitrification efficiencies may be at their lowest from receiving bay sediment of a dairy farm. Denitrification may also become less efficient under reducing conditions (i.e. low electron acceptors) where DRNA is favoured. Simultaneously, maximum benthic microbial consumption of surrounding oxygen may lower oxygen sediment penetration, limiting nitrification and coupled denitrification (Filstrup *et. al.*, 2009). Low microbial activity during the winter may contribute to low denitrification and accumulation of nitrate in the water column. As water begins to warm in the spring, water column nitrate is the dominant source of nitrate supporting denitrification (Risgaard-Petersen, 2003).

1.2.4 DRNA

Dissimlatory reduction of nitrate to ammonium (DRNA) functions in the anoxic sediment layer to produce ammonia from available nitrate pools. Denitrification competes with DRNA for nitrate as their nitrogen source, however, denitrification is generally dominant in freshwater environments (Scott *et. al.*, 2008). The reduction of ammonia is orchestrated by obligatory anaerobic heterotrophic bacteria which produce their energy from electron transport phosphorylation in the initial reduction step (i.e. NO_3^- reduction to NO_2^-) (Strohm *et. al.*, 2007; Tiedje, 1988). Conditions of high surrounding organic matter for electron donation in the presence of limited nitrate contributes to optimum NO_3^- reduction, and subsequent optimum phosphorylation (Tiedje, 1988; Tiedje *et. al.*, 1983). The later reduction of nitrite to ammonia serves as a co-enzyme oxidation station to re-energize the electron transport chain and to detoxify harmful nitrite. As previously stated, nitrification may act as an ammonia sink, converting ammonia back to nitrate and

may potentially be stimulated by DRNA (Burgin & Hamilton, 2007). An increased periphyton layer low in nitrates is also known to contribute to DRNA competition for ammonia (Harrison *et. al.*, 2008; Liikanen *et. al.*, 2002). By strictly observing the free energy produced between denitrification and DRNA (Tiedje, 1988):

Denitrification

$2NO_3^- + 2H^+ + 5H_2 \rightarrow N_2 + 6\ H_2O$, $\Delta G° = -1{,}120.5$ kJ per reaction

DRNA

$NO_3^- + 2\ H^+ + 4H_2 \rightarrow NH_4^+ + 3\ H_2O$, $\Delta G° = -599.6$ kJ per reaction

According to the greater free energy produced, denitrification may be the favoured reaction. However, Tiedje, (1988) demonstrated that denitrification had a lower free energy yield with respect to the net redox reaction of DRNA. This energy difference is attributed to DRNA having a greater electron transfer efficiency (8 electrons transferred per mole of nitrate in comparison to 5 electron transferred per nitrate mole) found in denitrification's electron transport chain. These findings corresponded with the greater amount of cells produced with DRNA when compared to the denitrification process (Strohm *et. al.*, 2007). DRNA activity also will increase with increased sediment mineralization (Harrison *et. al.*, 2008; Liikanen *et. al.*, 2002). Increased saline conditions may favour DRNA over denitrification but become less significant in lake environments due to the inhibition nature of sulphic compounds (abundant in marine conditions) on nitrification and denitrification (Sabumon, 2009).

1.3 Nitrous Oxide Production in Aquatic Systems

1.3.1 Nitrous oxide Production by Nitrification

In nitrification, production of nitrous oxide is initiated by the oxidation of ammonia to nitrate that may produce unstable intermediates (e.g. hydroxylamine, NH_2OH) that are likely bind to enzyme complexes and contribute to production of NO and N_2O specifically under low oxygen (De Bie *et. al.*, 2002; Jørgensen *et. al.*, 1984; Kester *et. al.*, 1997). The redox potential of this ammonia oxidation is -248 ± 25 mV when nitrate is produced in the presence of organic carbon (Sabumon, 2009). Facilitated by the enzyme ammonia mono oxygenase in proteobacterial ammonia oxidizers (i.e. genera: *Nitrosomonas, Nitrosococcus, Nitrosopspira, Nitrosovibrio* and *Nitrosolobus*) (Laanbroek *et. al.*, 1994), ammonia is initially oxidized to hydroxylamine in either oxic or anoxic environments (Schmidt *et. al.*, 2003):

Aerobic

$NH_3 + O_2 + 2H^+ + 2e^- \rightarrow NH_2OH + H_2O$; $\Delta G° = -120$ kJ/M

Anaerobic

$NH_3 + N_2O_4 + 2H^+ + 2e^- \rightarrow NH_2OH + 2NO + H_2O$; $\Delta G° = -140$ kJ/M

The anaerobic production of hydroxylamine produces greater free energy as the N_2O_4 dimer was more productive than the anammox nitrite and nitrate electron acceptors (Bodelier *et. al.*, 1996). The enzyme hydroxylamine oxidoreductase further oxidizes hydroxylamine into nitrite, where nitrite is oxidized into nitrate by nitrite oxidizers (Fernández *et. al.*, 2008). Under low oxygen and high NH_4^+ content, nitrous oxide is produced from the incomplete nitrification process (Goreau *et. al.*, 1980):

$$NH_4^+ \rightarrow NH_2OH \rightarrow N_2O$$

Nitrification is the primary source of nitrous oxide produced in the water column. In sediments, however, while nitrous oxide may be produced by nitrification, denitrification is the major contributor (Silvennoinen *et. al.*, 2008; Sutka *et. al.*, 2006).

1.3.2 Nitrous oxide Production by Denitrification

Summer periods in mesotrophic and eutrophic lakes can see the establishment of anoxic to hypoxic conditions in the hypolimnion (e.g. 5 to 30 μM O_2) suitable for nitrous oxide accumulation from denitrification (Twining *et. al.*, 2007; Yoh *et. al.*, 1983). Nitrous oxide production via denitrification occurs in the oxic/anoxic sediment boundary under conditions of high copper complexation by organic ligands (i.e. bioavailable copper complexed to carbonate in alkaline lake water/seawater) and reduced sulphur species (Mengis *et. al.*, 1997). Copper nitrite reductase enzyme requires copper to immediately reduce nitrite toxic effects by converting it to nitrous oxide (Granger & Ward, 2003). Ideal N_2O production conditions would involve a reducible bioavailable copper form in low concentrations due to its metal toxicity. Lake humic organic matter, and thiol ligands produced by surface eukaryotic and prokaryotic organisms prevent copper toxicity and are also other sources of competitive copper complexation (Twining *et. al.*, 2007).

A similar siderophore compound may be generated by methane-oxidizing bacteria in the presence of limited copper (Kim *et. al.*, 2004). Although copper sediment may be variable within different sediment sites, copper remains a trace metal in lakes since it readily undergoes chemical complexation, precipitation, and adsorption from the water column into the sediment. Other metal complexation options for nitrous oxide reductase could be iron which is the closest chemical substitute and may experience similar metal

conservation strategies within the phytoplankton community under metal limitation (Twining *et. al.*, 2007).

1.3.3 Global significance of Nitrous Oxide Production in Lakes

In the last century, nitrous oxide production from anthropogenic sources has been estimated to contribute about one third of the global total for N_2O production (Khalil & Rasmussen, 1992; Seitzinger *et. al.*, 2000). Freshwater systems contribute less than 20% of the total annual global N_2O emissions (Khalil & Rasmussen, 1992; Seitzinger *et. al.*, 2000; Wang *et. al.*, 2009). Oxygen deficient regions contribute to benthic nitrous oxide saturation within freshwater lakes, specifically mesotrophic and eutrophic lakes (Svensson, 1998; Wang *et. al.*, 2009; Yoh *et. al.*, 1983). The hypolimnetic region in oxic lakes and marine environments during summer stratification is also a source of saturated N_2O, where nitrous oxide (relatively inert) diffuses from the sediment into the water column (Mengis *et. al.*, 1996). Periods of transient oxygen change further emphasizes N_2O accumulation (Naqvi *et. al.*, 2000). Of the dinitrogen gas produced during denitrification, N_2O was reported to be in a range of 0.1 - 0.5% of the atmospheric N-total. Dong (2006) recorded a 3.3% N_2O:N_2 ratio where eutrophic conditions may create values as high as 6% (Dong *et. al.*, 2006; Seitzinger & Kroeze, 1998). Therefore, an estimated 19.7 Tg N $year^{-1}$ (lakes and reservoirs) of global N removed by denitrification could produce 197 to 985 Gg of N per year according to Seitzinger (1998).

1.3.4 Nitrous Oxide as a Greenhouse Gas

In a recent of ozone depleting substances (ODS), it was shown that N_2O emissions were the single most significant ODS and are expected to remain the largest throughout the 21st century (Ravishankara *et. al.*, 2009). Nitrous oxide is 310 times and 15 times more efficient greenhouse gas than carbon dioxide and methane, respectively, on a per molecule basis (Liikanen *et. al.*, 2002). It is estimated that N_2O concentrations are increasing by 0.25% per year by anthropogenic means (Twining *et. al.*, 2007), and N_2O has become the third most important greenhouse behind CO_2 and CH_4 (Meyer *et. al.*, 2008). Global N_2O emissions from rivers, estuaries, and continental shelves are calculated to be 4.9 (1.3-13.0) Tg N in 2050, of which two-thirds are from rivers (Seitzinger & Kroeze, 1998). As an anthropogenic based greenhouse gas, nitrous oxide saturation is associated with applied ammonium. De Wilde and de Bie (2000) reported an average N_2O saturation value of 0.14% (1 mol N_2O per 700 mol NH_4^+) and ranges of 0.04 – 0.42% N_2O saturation (1:1 molar ratio, N_2O:NH_4^+) were recorded in the Scheldt Estuary (De Wilde & De Bie, 2000). Lake Taihu N_2O saturation values were found to be from 70% to 1597%, where the late summer season and most eutrophic locations produced the greatest saturation values. In comparison to nitrous oxide saturation in rivers, flowing systems may be N_2O saturated at values from 631% to as high as 2708% (Wang *et. al.*, 2009).

1.4 Influence of Nutrient Cycling on Denitrification

1.4.1 Phosphorus Biogeochemical Cycle

Phosphorus (P) is the tenth most abundant element in the world. Within the pelagic region, P can exist in both inorganic and organic forms. It is prelevant in the PO_4^{-3} form either as a free orthophosphate (Pi) or combined with organic compounds. Rarely, are P-products found as phosphine gas (PH_3), or phosphide (-3) aquatic environments (Morton *et. al.*, 2005; Nriagu & Moore, 1984).

Phosphorus loading may become variable seasonally and annually from climatic variation, and can be reflected in phytoplankton biomass and community composition (Quigg *et. al.*, 2003; Van Donka *et. al.*, 2008). Some phosphorus may not participate in phosphorus cycling as it enters the system associated with detrital material, poor lability and high C:P or C:N ratios (Klump *et. al.*, 2009). Considering that fundamental role of P in cell function and cell structure (e.g. phospholipids in membranes and energy currency) and information storage (e.g. nucleic acids), phosphorus becomes readily taken up as biomass and has a relatively low existence in open water as an ionic free form (deDuve, 1991).

Phosphorus is regulated under the photosynthesis production regime (Karl, 2007) and commonly associated with other elemental cycles (e.g. C, O, S) and other trace elements (e.g. Fe, Zn, Co) (DeLong & Karl, 2005). Naturally, phosphorus is globally distributed by the combined forces of continental weathering and fluvial discharge, and is continually buried and layered within the sediment floor. Within the last the few centuries, anthropogenic P additions through riverine, sewage loading, and atmospheric deposition had resulted in organic P accumulations into the coastal zones and P-output into the

pelagic environment. Photosynthesis is the base of the aquatic foodweb, supplies reduced organic carbon to all heterotrophic organisms (e.g. bacteria to whales). Deep sediment receives pelagic P through means of gravitational influence of organic particulates, the active migration of zooplankton and fish and the downward movement of dissolved organic matter. This dissolved organic matter is degraded by benthic microbes and Pi is allowed to cycle back to the surface via diffusion and convection (internal loading) to support further primary production. This regeneration of P is termed "the biologicial pump" (Karl, 2007).

Considering that phosphorus is required for the growth and development of all organisms, the N:P ratio underlies the growth potential and structure of phytoplankton communites (Vrede *et. al.*, 2009). Most of P cycling is conducted by prokaryote (i.e. bacteria and archaea) metabolic activities (Bratbak, 1987) since their relatively higher surface area/volume ratio are more efficient at uptaking PO_4. These phosphates are central to transmission and energy production through the hydrolysis of the adenosine triphosphate (ATP) molecule (deDuve, 1991). Alfred Redfield recognized that the relative ratios of inorganic N and P concentrations in the marine pelagic environment reflected the particulate matter whose biomass was dominated by phytoplankton. The classic Redfield ratio C:N:P ratio of 106:16:1 (Redfield, 1934) implies a relationship among C, N, and P, and suggests that limits on biomass production may be inferred by the ratio of available nutrients (Redfield, 1958). Further, it can be implied that an excess of inorganic N (N:P > 16) represents biomass degradation. Conversely, an excess of inorganic P (N:P < 16) implies the removal of N through denitrification. Dissolved inorganic phosphorus may be increased with increasing anaerobic decomposition rates.

Recent studies have suggested that increased nitrogen fixation may lead towards P limitiation in freshwater ecosystems (Bergström *et. al.*, 2005; Bergström & Jansson, 2006; Vrede *et. al.*, 2009). Mesocosm studies have showed that with increased P loading there was a significant resultant particulate N content (Vrede *et. al.*, 2009). The relevance here is that this particulate N can be recycled either in the water column with little of the N passing through the denitrification pathway, or it can settle and be recycled in the sediments with a significant portion passing through the denitrification pathway. N fixation was positively related to total phosphate concentrations, and presumably P loading (Granhall & Lundgren, 1971; Levine & Schindler, 1999; Tõnno & Nõges, 2003).

. This suggests that increased particulate N linked to P loading is often in the form of cyanobacterial biomass, with N fixation permitting full exploitation of available P. When N is not limiting, P loading may increase biomass of other autotrophs as well as cyanobacteria. However, N:P loading would appear to be an important predictor of cyanobacterial growth relative to growth of other autotrophs (Smith, 1985).

Lake water column mixing with increased summer temperatures will enhance microbial-mediated P release from sediments and internal loading. During winter periods phosphours may accumulate in the sediment due its sorption onto iron oxides. Eutrophic lakes particularly may have high internal P loading which may favour cyanobacteria as excess N is lost to denitrification (Vrede *et. al.*, 2009), to be replaced by N-fixing cyanobacteria. A recently published 37-year whole-system study demonstrated that a nutrient management strategy which reduced nitrogen loading without reducing phosphorus loading could not control eutrophication, rather it shifted community composition to cyanobacterial dominance (Schindler *et. al.*, 2008).

In a Canadian context, governmental actions (e.g. banning phosphates in detergents and government grants for improved sewage systems) of the Canada Water Bill 1970s were implemented to decrease phosphorus loading (i.e. municipal sewage plants and argricultural runoff) into lake ecosystems (McGucken, 2000). However, Lake Erie experienced a rise in total phosphorus from 1990 to 1997 and generally decreased its rate in 1999 and 2000 (Dolan & McGunagle, 2005). In the early 1980s, zebra mussels were introduced to Lake Erie in which a large quantity of organic matter was removed from the water column to the sediment. This situation could enhance denitrification by moving organic N remineralization from the water column to the sediments, thereby decreasing N:P in the water column and favouring cyanobacteria (Bykova *et. al.*, 2006). During summer in lake Erie, nutrients associated with organic matter settle from the epilimnion to the hypolimnion causing the decrease of total phosphorus that ranged 0.012 ug L^{-1} yr^{-1} to 0.57 ug L^{-1} yr^{-1} (Rockwell *et. al.*, 2005).

Relevant to this thesis, nutrient management plans which specifically target N, trophic changes that enhance deposition of organic matter and denitrification, and physical/biological factors that enhance P release from sediment all have potential to change N:P loading ratios (external and internal considered), in a way that favors cyanobacterial growth. As will be discussed below, changes in primary producer community could affect delivery of organic matter to sediments through differences in buoyancy. This could affect where organic nitrogen is recycled (water column versus sediments), which consequently affects nitrogen processing.

1.4.2 Silica Biogeochemical Cycle

Silica exists in the environment as SiO_2 as part of macrocrystalline formations (quartz, rock crystal, amethyst, etc.), microcrystalline formations (flint, chert, jasper, etc.) and is a large component of sand and sandstone (Hem, 1985). Silicates (silicon combination with other elements) make up feldspar, hornblende, mica, asbestos and other clay minerals. Silica is also found in granite, basalt and shale. Silica is present in rock at 7-80% on average, and 50-80% in soil. The common silica aqueous forms are H_4SiO_4 and $H_3SiO_4^-$. High dissolved Si may be around 40-60 uM relative to low dissolved inorganic nitrogen (DIN) (NOx + 1.9uM NH_4^+) and dissolved inorganic phosphate (DIP) concentrations. During organic matter diagensis in sediments, flux of $Si(OH)_4$ to the water column relative to carbon mineralized has a mean ratio of 0.6 Si:1C, with a range between 0.30 to 0.86 in marine systems (Jahnke & Jahnke, 2000). Biologically, Si is essential in animal dietary needs and a nonessential nutrient for plants. Dissolved Si is essential for diatoms to construct frustules and Si can be a limiting nutrient for diatom growth. Dissolved Si can be used as a unique tracer for diatomaceous organic matter, flux of dissolved Si and inorganic nitrogen following organic matter diagenesis may be correlated since diatoms require SiO_2 to form new frustules and to divide (Guillard & Kilham, 1977; Heggie *et. al.*, 2008). A Si:N flux of ~1:1 is an indicator of diatom predominance in organic carbon (Brzezinski, 1985; Heggie *et. al.*, 2008).

Dissolved Si availability will influence diatom abundance and its distribution. Changes in Si:N and Si:P, particularly decreases in eutrophied environments associated with increased N and P loading, have resulted in phytoplankton community and food web changes (Fransz & Verhagen, 1985; Ragueneau *et. al.*, 1994). For example, the Black sea

experienced a shift from diatoms to other non-sliceous phytoplankton mid-1960s during dam construction , as the Mediterranean was formerly P limited (1960s to 1970s) before becoming Si limited in the late 1970s (Ludwig *et. al.*, 2009). Silica limitation may be a likely scenario in the Sargasso Sea water column as biogenic SiO_2 (BSi), associated with diatoms populations, have slower reminerlazation rates than particulate organic carbon and particulate organic nitrogen. Baek, *et. al.* (2009) demonstrated that diatoms may deal with these nutrient limitations (N and P) by constricting diatom growth, shifting the community to lower chlorophyll production and smaller cells that would better exploit the limited N and P as it was turned over during rain events.

Sinks for Si in aquatic systems are at a minimum except for burial as it does not participate in organic matter respiration as electron donor or acceptor. Silica sinks may be brought about by local hydrologic management, eutrophication and sinking of organic matter to sediment, and sediment biodeposition by invasive species (e.g. zebra mussels) (Ragueneau *et. al.*, 2005). River dam construction (e.g. Nile River and Mississippi River) showed decreased dissolved Si concentration on the flowing side, whereas, the river build up on the opposing dam side collects Si load via diatom debris (Rabalais *et. al.*, 2000; Turner & Rabalais, 1994). Similar effects noted in Ludwig (2009) for the Mediterranean becoming Si limited, so be sure to see that paper. The resultant reservoirs increase lake residence times that assist to retain this Si.

Eutrophic conditions are characterized as an increase in aquatic primary production, typically caused by increased N and/or P loading, limiting silica (Schelske *et. al.*, 1986; Schelske, 1988; Schelske *et. al.*, 2006). Although restricted SiO_2 may result in diatom decline, Schelske (2006) supported that immediate P loading may by pass this

nutrient effect and favour diatom growth under high N:P nutrients. Along with increased diatom growth, enriched N:P may improve diatom silica utilization (Schelske *et. al.*, 1986). Diatom sedimentation increases allowing for the improved store of sediment (BSi) and possible nutrient burial, subsequently leading to the reduction of water column BSi. Closely linked to the carbon cycle, global silica cycles are controlled via their biogenic silica form through diatom vectors. About 95% of diatom BSi is assumed to be recycled annually within the Great Lakes, where they are evenly distributed to 40% of the lake basin (Schelske, 1985; Schelske *et. al.*, 2006; Thomas, 1981). Detrital matter dissolution could significantly reduce BSi dissolution rate in the sediment. For example, BSi accumulation in Lake Superior increases annually at 10 mg g^{-1} when annual silica utilization in the water column is 0.21 mg SiO_2 L^{-1} (3.5 µmol L^{-1}). Since 95% of the silica is recycled, BSi accumulation would result in only a small net change in water-mass silica concentration 0.01 mg SiO_2 L^{-1} (0.17 µmol L^{-1}) (Schelske *et. al.*, 2006). This is relevant within coastal zones where anthropogenic induced eutrophication are relatively high, and within lakes of long residence time.

Research driven by changes in diatom production and its influence on biogeochemical silica cycles have been conducted in the Great Lakes. Shifts in Si:N and Si:P (decreases) have resulted from increased N and P loading within these lakes, and from constructed obstacles (e.g. damming projects) that have retained Si in reservoirs. The net result has been a reduction in diatom abundance and increase in other algae and cyanobacteria in many systems. Therefore, shifts in elemental ratios involving Si can influence phytoplankton community composition.

1.5 Influence of Nutrient Loading and Nutrient Ratios on Phytoplankton Composition

Evidence has suggested that phytoplankton species composition is particularly sensitive to nutrient load as nutrients become limited, specifically nitrogen and phosphorus. Subsequently, ecosystem productivity becomes affected with the manipulation of trophic level complexity and stability, and microbial community species richness and abundance distribution. Anthropogenic point source discharges, NH_4^+ and NO_3^- atmospheric deposition, and agricultural runoff have been known to elevate chlorophyll a (chl a), phytoplankton biomass, and TP content in lake systems (e.g. the Laurentian Great Lakes). Non-point nutrient loading (i.e. smaller tributaries discharges) may account for a predominate portion of the total nutrient loading (Smith *et. al.*, 2007).

Under eutrophic conditions, horizontal distribution of lake phytoplankton may be dominated by cyanobacteria (e.g. *Anabaena*) as wind currents may progressively move nutrients and microbial flock into the pelagic zone (Ishikawa, et. al, 1999). Cyanobacteria are also capable of utilizing bicarbonate (HCO_3^-) more efficiently than diatoms and green algae. Bicarbonate is the dominate species of dissolved inorganic carbon in many lakes (Filstrup *et. al.*, 2009). Eutrophic diatoms, *Fragilaria crontenensis* and *Aulacoseira*, may dominate lake regions of constant mixing or nutrient loading from rivers at certain times, particularly when water temperatures are colder (Liukkonen *et. al.*, 1993). Filamentous green algae *Spirogyra* may out compete aquatic macrophytes in response to more frequent but less intense nutrient additions (Simons, 1994; Van der Linden, 1989). Green algae may increase growth rate despite the low N:P ratio content in hypereutrophic lakes with high nutrient loading (Vrede *et. al.*, 2009).

Community composition and diversity shifts according to nutrient limitations where microbial adaptive qualities favour an increased contribution to total population. If a nutrient is less than half-saturation for uptake, then the environment would suggest a probable nutrient limitation scenario. Potential nutrient limitations (Baek *et. al.*, 2009; Justic *et. al.*, 1995) are shown as follows:

N limitation: DIN < 1μM; DIN:soluble reactive P < 10; Si:DIN > 1;
Dissolved organic nitrogen (nitrate, nitrite, and ammonium) < 1.0 μM.

P limitation: SRP < 1μM; DIN:SRP > 22; Si:SRP > 22;
SI:P > 20 and DIN:P > 20;
Phosphate < 0.2 μM

Si limitation: Si < 2 μM; Si:SRP < 10; Si:DIN < 1;
Si:P < 10 and Si:DIN < 1;
Silicates < 2.0 μM

Generally, low N:P ratios in whole-lake, mesocosms and laboratory studies produce cyanobacteria dominance (Horne & Commins, 1987; Vrede *et. al.*, 2009; Zevenboom, 1982; Zevenboom *et. al.*, 1982). Lake cyanobacteria N-fixation become favourable with N:P ratios lower than 16:1 and total inorganic N concentrations of less than 3.6-7.1 μM (Horne & Commins, 1987; Vrede *et. al.*, 2009). Often participating as an asscessory algae in phytoplankton communities, green algae dominance is defined by their adaptive strategies to endure unique aquatic niches instead of competiting against phytoplankton for limited nutrient resources. For example, filamentous *Spyrogyra sp.* may anchor to

shallow and turbulent lake areas where phytoplankton generally wash away (Hainz *et. al.*, 2009; Hoshaw & McCourt, 1988; Umrath, 1941).

1.6 Differences in Buoyancy and Sinking Rates of Different Phytoplankton

Differing plankton buoyancy may be advantageous during low nutrient situations, as cells may increase its nutrient uptake by migrating towards nutrient rich environments within the water column (Britton & Timm, 1993; Ebert *et. al.*, 2001; Fennel & Boss, 2003; Kolokolnikov *et. al.*, 2009; Shigesada & Okubo, 1981). Phytoplankton population is controlled by nutrient limitations, seasonal temperature, and light gradients in the water column. Internal loading of nutrients from sediment results in concentrations highest below the thermocline in the mid-late summer, while light decreases with depth. Phytoplankton that can maintain buoyancy are often found in greatest density near the thermocline where they optimize growth by balancing light and nutrient availability. A phenomenon then occurs, known as the deep chlorophyll maximum, when both gradients (light and nutrients) intersect at mid-water column. In subtropical and tropical oceanic environments, the chlorophyll maximum is around 100 m depth. Lake water has a shallower chlorophyll maximum as light penetration is much more turbid and internal loading of nutrients delivers nutrients to the thermocline. Within a shallow lake with sufficient light and moderate temperature, most phytoplankton biomass grows near the surface with a continuous population sinking towards the bottom (Kolokolnikov *et. al.*, 2009).

Phytoplankton groups may differ in buoyancy. In green algae, the carbon storage product (starch) induces cell sinking, whereas the energy storage product in diatoms (i.e. lipids) can create positive cell buoyancy. Euphotic zone nutrient depletion may decrease lipid production allowing an increased lipid degradation via metabolic ß-oxidation to occur causing diatoms to be less buoyant (Wilhelm *et. al.*, 2006). Diatom buoyancy may also be diminished by the uptake of silicates from the water column that increases frustule density. Depending on the amount of DSi converted to diatom BSi, a protective protein coat (frustule protection) may be formed and possibly slow down sinking rates with greater coating as it becomes degraded by environmental shearing (Sommer & Stabel, 1983). During stages of growth, diatom sinking rates could be at 0.3 to 3 m d^{-1} or the end of their living cycle at 1 to 10 m d^{-1}, or over 100 m d^{-1} in winter when larger diatom cells sink rapidly out of marine euphotic zones (D'Asaro, 2008). Intracellular gas vesicles that contain oxygen maintain buoyancy in cyanobacteria (Kinsman *et. al.*, 1991). Certain cyanobacteria are able to actively control their buoyancy by changing their cellular carbohydrates (Bormans & Condie, 1997).

Other morphological adaptations may reduce sinking in various phytoplankton. For example, production of chitin fibres in the marine diatom *Thalassiosira weissflogii* increases drag and reduces sinking rates (Durkin *et. al.*, 2009). Exterior algal formations of spines, fibres and mucus secretions may also reduce sinking rate. With other cases, algae sedimentation occurs regardless of adaptive advantages as is with the interaction of phytoplankton and calcite precipitation. Known as whiting events in Lake Ontario, rapid sedimentation proceeds as calcite crystals aggregates with phytoplankton algae and bacteria (Gälman *et. al.*, 2008). Typically, the larger the phytoplankton size, the greater

the sinking rate (Smayda, 1970), although as a whole, phytoplankton sinking rates (-0.4 to >2.2 m day^{-1}) may be determined by cell or colony density rather than phytoplankton sizes (<10 to >1000 um) as shown in the Dutch coastal zone of the North Sea (Peperzak *et. al.*, 2003).

Relevant to this thesis, diatoms and green algae are expected to sink more rapidly than cyanobacteria, resulting in greater export of organic matter (including organic N) to sediments. Diatoms and green algae are typically larger than cyanobacteria and have greater density due to carbohydrate storage product (green algae) or luxuriant Si uptake (diatoms). Nutrient loading conditions that favour diatoms and green algae relative to cyanobacteria would facilitate this transport of organic matter to sediments. This, in turn, could alter nitrogen cycling if nitrogen is recycled primarily in the water column (cyanobacteria dominated system) versus in the sediment (diatom or green algae dominated system). It should be noted that luxuriant Si uptake by diatoms may be a short-term. Diatom populations may adapt to high Si levels and uptake may exhibit saturation-type kinetics over time (Thamatrakoln & Hildebrand, 2008). Therefore, nutrient loading conditions that specifically favour green algae may have the greatest long-term effect on nitrogen transport to sediments.

1.7. Research Rationale and Approach

The majority of studies on nitrogen biogeochemistry are conducted under marine conditions with some findings carrying over to freshwater knowledge. Most commonly these studies have been carried out in microcosms, using sediment cores or sediment slurries. However, generalizations from controlled microcosm experiments can be

challenging to extrapolate to field conditions as scale of experimental systems can strongly influence outcome (Petersen & Hastings, 2001; Petersen *et. al.*, 2003). An important aspect of this thesis is that research in microcosms was repeated in field mesocosms to determine if results were scale dependent.

Past studies of controls on denitrification have focused on N-form assessments (i.e. NOx, NH_4^+, N_2O, N_2) and manipulated experimental conditions have attempted to directly explain denitrification rates (Balderston *et. al.*, 1976; Goering & Dugale, 1966; Kana, *et. al*, 1994; Laursen & Seitzinger, 2002; Meyer *et. al.*, 2001; Nielsen, 1992; Risgaard-Petersen, 2003; Seitzinger, 1988) on occasion relating N:P, C:N, and Si:N aspects to individual lake organisms (i.e. algae, bacteria, macrophytes, and invertebrates) (Bykova *et. al.*, 2006; Hopfensperger, *et. al*, 2009; Ishida *et. al.*, 2008; Koho *et. al.*, 2008; Liikanen & Martikainen, 2003; Ragueneau *et. al.*, 2002; Silvennoinen *et. al.*, 2008) or food web structure to denitrification (Hansen & Kristensen, 1998; Mermillod-Blondin *et. al.*, 2004; Welsh, 2003). There is a fundamental need to address the subtle influences of nutrient ratios on phytoplankton community as a whole and how they affect denitrification rates and nitrous oxide production in a controlled microcosm and field mesocosm set of experiments.

Recent denitrification studies have focused on sediment microcosm enclosures that involve the periodic subsampling of dissolved gases in water above the sediment. Microcosm setups may either record N_2 flux measurement within static incubation enclosures (Cornwell *et. al.*, 1999; Kana *et. al.*, 1994; Kana *et. al.*, 1998) or flow-through incubations, (Groffman *et. al.*, 2006; Nishio *et. al.*, 1982; Nishio *et. al.*, 1983), typically measuring N_2 flux based on N_2:Ar. In some cases, N_2-free gas, usually helium, was initially flushed into microcosm incubation

enclosures to remove background dinitrogen gas (Seitzinger *et. al.*, 1983; Seitzinger, 1988). Pre-incubation difficulties may include bottle effects produced by extended degassing periods and sediment sample decoupling from water column nitrate and carbon flow (Nowicki, 1994; Seitzinger *et. al.*, 1993). Steady state microcosms ideally run less than 12 hours at about 50% oxygen saturation to reduce oxygen effects on the nitrification/denitrification processes (Groffman *et. al.* 2006; Jenkins & Kemp, 1984).

Studies have showed that denitrification may be influenced by various environmental factors: organic carbon availability (Arango & Tank, 2008; Klump *et. al.*, 2009; Pfenning & McMahon, 1997), nitrogen availability (Bernot *et. al.*, 2006; Martin *et. al.*, 2001; Royer *et. al.*, 2004), substrate type (Groffman *et. al.*, 2006; Hopfensperger *et. al.*, 2009; Porter *et. al.*, 2006) and periphyton community (Heggie *et. al.*, 2008; Smith *et. al.*, 2007). However, microcosms encompass small sediment volumes and it is difficult to replicate the natural physical environment of lakes in microcosms, making it difficult to extrapolate results from microcosm experiments to real ecosystems.

In general, mesocosms, depending on experimental intentions, allow natural irradiation exposure, seasonal temperature and rain event effects, and gas exchange. Mesocosms have a larger volume than microcosms, encompass a greater sediment surface area, and do a better job replicating the physical environment being studied. Results from mesocosms may be easier to extrapolate to natural systems, although this comes at a cost in experimental control.

Aquatic systems are particularly susceptible to environmental variability and may not respond consistently with in-lab microcosm results. For example, seasonal light exposure may intensify microbial competition, and wind disturbances promote lake mixing that may increase phytoplankton diversity. Discrepancies between

microcosm/mesocosm studies were also found to include differing algal material, incubation temperatures, and the use of single versus double exponential decay models (Foree & McCarty, 1970; Gälman *et. al.*, 2008; Jewell & McCarty, 1971; Lehmann *et. al.*, 2002). Also, area specific nitrification/denitrification processes in aquatic systems may be patchy, and microcosms may capture hot spots or cold spots, whereas mesocosms integrate more surface area and rates measured are more likely to reflect natural rates.

1.8 Hypotheses

The research presented in this thesis was designed to test two primary hypotheses, each with three related sub-hypotheses. The research made use of both microcosm and mesocosm experiments to take advantage of greater experimental control offered by microcosms, and greater represention of natural systems offered by mesocosms. Results of microcosm experiments reflect potential response to changes in elemental loading ratios, while results from mesocosm experiments reflect the more likely responses in a more complex system.

Hypothesis 1: An increase in Si:N relative to Redfield ratio will cause an increase in diatom abundance relative to other photoautotrophs.

> **Hypothesis 1a:** An increase in diatom abundance relative to other photoautotrophs will result in greater sinking of organic matter to sediment.
>
> **Hypothesis 1b:** An increase in organic matter deposition will increase denitrification.
>
> **Hypothesis 1c:** An increase in organic matter deposition will increase N_2O production and evasion from mesocosms.

Hypothesis 2: An decrease in N:P relative to Redfield ratio would result in a relative increase in phytoplanktonic cyanobacteria.

Hypothesis 2a: An increase in Cyanobacteria abundance relative to other photoautotrophs will result in less sinking of organic matter to sediment.

Hypothesis 2b: A decrease in organic matter deposition will decrease denitrification.

Hypothesis 2c: A decrease in organic matter deposition will decrease N_2O production.

2. EXPERIMENTAL MATERIALS AND METHODS

2.1 Microcosm Experiment

General denitrification examination under microcosm setup is not representative of the absolute environmental values that the setup is simulating, but instead indicates the relative sediment chemical change of these conditions (Liikanen *et. al.*, 2002). Although stagnation is brought about by the slow water turnover and the gradual gas gradient, microbial interaction associated with nutrient ratio proceeds to influence denitrification rates.

2.1.1 Microcosm Experimental Setup

Microcosms contained silica sand (~ 7-8 cm depth) in 1.85 L straight-sided glass jars (8 cm diameter, 20 cm depth). Sand substrate was chosen because it was more conducive for microbial activity than the less porous clay sediment with pockets having limited nutrients and moisture. Denitrification rates in sandy sediments may have a greater value than those in muddy sediment, and may have a greater potential for observation (Ehrenhauss *et. al.*, 2004; Mermillod-Blondin *et. al.*, 2002; Rust *et. al.*, 2000). However, there have been numerous studies on substrate effects on denitrification and the results are equivocal. Sometimes sandy sediment seems to have a higher rate, where other occasions, silty sediment seems to have a higher rate. In a cross-system comparison, there was no systematic difference in rates (Seitzinger & Giblin, 1996). Nutrient-rich water was continually pumped through a peristaltic pump and delivered via a glass pipe into each microcosm in which the end was positioned 3 cm above the sediment surface. Glass microcosms were assumed inert with a minimal effect on silica loading (through leaching) and silica dissolution from sand likely constituted the majority of the background silica in

this experiment. All microcosms were contained in a single water bath to maintain a relatively stable daily temperature (20-23°C over the experimental period). Experimental duration simulated was 3 months (August – November 2007). Fluorescent lights were maintained on a 14:10 light:dark cycle mimicking summer photoperiod. Light intensity was 60 to 80 μmol m^{-2} s^{-1} at the water surface.

The experimental design consisted of six different nutrient treatment combinations of Si:N (high = 2:1, low 0.5:1) and N:P (high = 25:1, medium 15:1, low = 5:1). These ratios are within the range of measured nutrient ratios in freshwater systems. Nitrogen loading to each microcosm was constant (200 μmol N $mesocosm^{-1}$ d^{-1}), while Si and P loading varied among treatments (Table 2-1). Each treatment maintained four microcosm trials (Figure 2-1) that allowed for a 20% total volume nutrient renewal (370 ml d^{-1}). Nutrient stock was prepared in accordance to modified CHU-10 algae media (Appendix A, Part D), with concentrations of N, P, and Si modified to deliver target nutrient loading rates. Autoclaved nutrient stocks solutions were continually pumped by a multichannel peristaltic pump from 20L carboys (Figure 2-2). Simulating an open water system, gas exchange was allowed through the opening at the top where excess nutrients overflowed into the water bath reservoir. Physical disturbances were kept to a minimal as the microcosms were left to establish microbial communities.

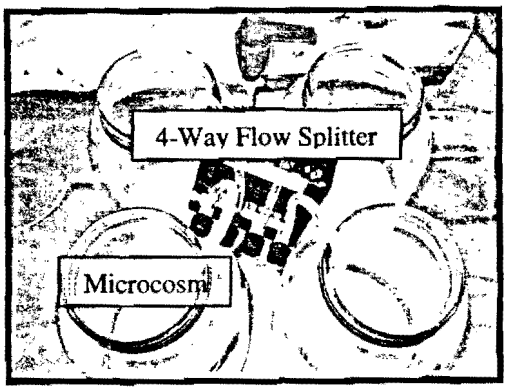

Figure 2-1. Microcosm setup: 4 trials per nutrient treatment

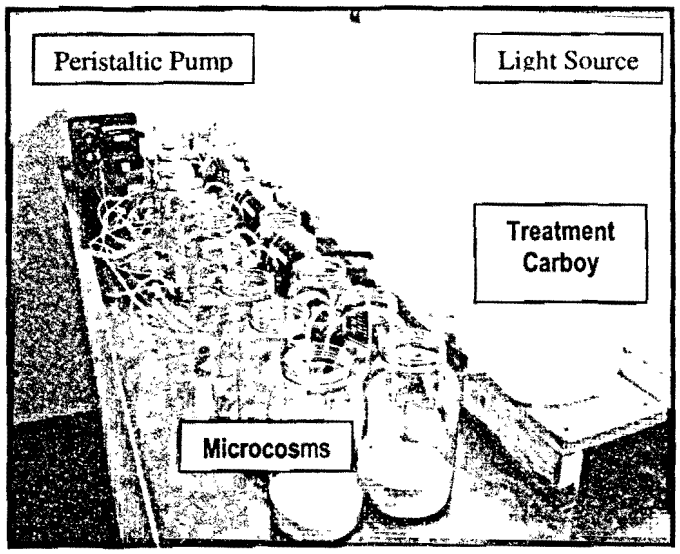

Figure 2-2. Nutrient Treatment (Carboy) Setup along a light source

Table 2-1. Nomial nutrient loading rates for microcosm experiments

Treatment	Nutrient Loading (μmol Si, N, or P d^{-1})		
	Si	N	P
Low Si, Low P	100	200	8
Low Si, Medium P	100	200	13
Low Si, High P	100	200	40
Hi Si, Low P	400	200	8
Hi Si, Medium P	400	200	13
Hi Si, Hi P	400	200	40

2.1.2 Microcosm Maintenance

Nutrient stock for each nutrient trial was replenished every week in each carboy, maintaining a nutrient media excess of 100ml to compensate for leaks, pump variation, and condensation within the interior carboy walls. Iron within the CHU-10 media periodically precipitated as a red layer at the bottom of the carboy. Iron resuspension involved the gentile mixing of the carboy within its immediate area and during media

renewal. Periodically, connecting tubes were cleared of algae and trapped air bubbles by removing and flushing lines with distilled water before reconnection. Microcosm flow rate gradually slowed down and was intermittently adjusted to maintain the 15 - 20% volume renewal per day.

2.1.3 Microcosm Setup

Treatment carboys were arranged in random order against a supporting wall, and equally spaced below a fluorescent light source producing all UV-spectra required for plant maintenance. Silica sand was washed repeatedly (minimum of 2 washes) with distilled water to remove floating particulates and was allowed to stand for 24 hours to permit air bubbles to settle out. Sand was then placed in each microcosm to a 1.5 cm depth and a height of 2.5 cm from the nutrient glass capillary. Although there is some evidence that would suggest that benthic algae may be able to metabolize SiO_2 from sand grains (Lewin, 1955), Carrick and Lowe (2007) analyzed algal growth with substrates containg silica and without and found that there was no statistical difference ($p > 0.05$) between each sediment. However, algal biomass was greater under silica supported substrate where it may be used to emphasize microbial population and adequately simulate lake environments.

Polyethylene tubing connecting to the water system (carboys, peristaltic pump, and microcosms) was filled with distilled water upon tube connection, which was also submerged in water to prevent air bubble entry that could disrupt flow. Water flow rates were adjusted using the peristaltic pump adjustment control and fine adjustment for each individual microcosm with a four-way channel splitter that contained a fine knob adjustment for each port. A 24 hour flow through of all water (distilled) filled carboys

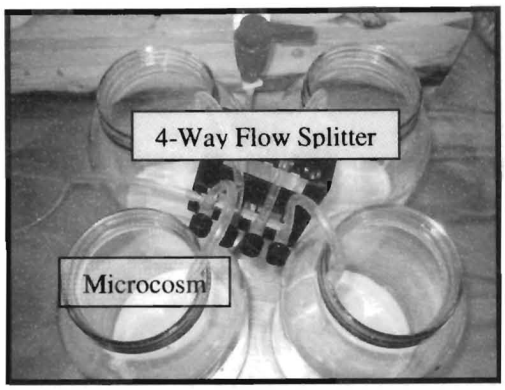

Figure 2-1. Microcosm setup: 4 trials per nutrient treatment

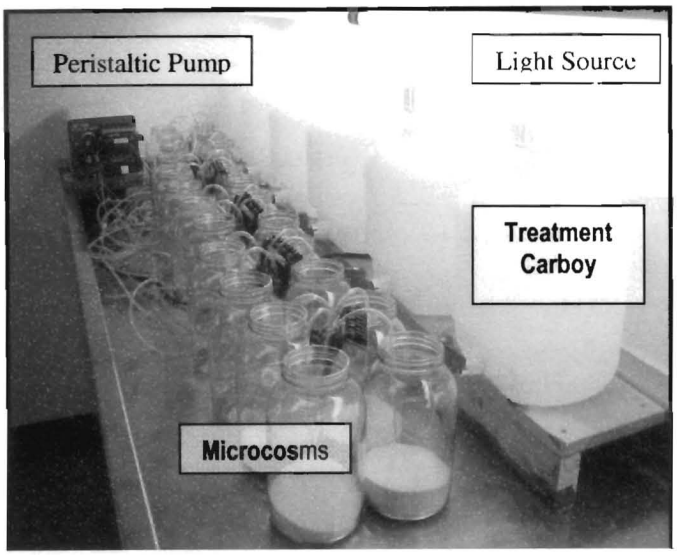

Figure 2-2. Nutrient Treatment (Carboy) Setup along a light source

Table 2-1. Nomial nutrient loading rates for microcosm experiments

Treatment	Nutrient Loading (μmol Si, N, or P d^{-1})		
	Si	N	P
Low Si, Low P	100	200	8
Low Si, Medium P	100	200	13
Low Si, High P	100	200	40
Hi Si, Low P	400	200	8
Hi Si, Medium P	400	200	13
Hi Si, Hi P	400	200	40

2.1.2 Microcosm Maintenance

Nutrient stock for each nutrient trial was replenished every week in each carboy, maintaining a nutrient media excess of 100ml to compensate for leaks, pump variation, and condensation within the interior carboy walls. Iron within the CHU-10 media periodically precipitated as a red layer at the bottom of the carboy. Iron resuspension involved the gentile mixing of the carboy within its immediate area and during media

renewal. Periodically, connecting tubes were cleared of algae and trapped air bubbles by removing and flushing lines with distilled water before reconnection. Microcosm flow rate gradually slowed down and was intermittently adjusted to maintain the 15 - 20% volume renewal per day.

2.1.3 Microcosm Setup

Treatment carboys were arranged in random order against a supporting wall, and equally spaced below a fluorescent light source producing all UV-spectra required for plant maintenance. Silica sand was washed repeatedly (minimum of 2 washes) with distilled water to remove floating particulates and was allowed to stand for 24 hours to permit air bubbles to settle out. Sand was then placed in each microcosm to a 1.5 cm depth and a height of 2.5 cm from the nutrient glass capillary. Although there is some evidence that would suggest that benthic algae may be able to metabolize SiO_2 from sand grains (Lewin, 1955), Carrick and Lowe (2007) analyzed algal growth with substrates containg silica and without and found that there was no statistical difference ($p > 0.05$) between each sediment. However, algal biomass was greater under silica supported substrate where it may be used to emphasize microbial population and adequately simulate lake environments.

Polyethylene tubing connecting to the water system (carboys, peristaltic pump, and microcosms) was filled with distilled water upon tube connection, which was also submerged in water to prevent air bubble entry that could disrupt flow. Water flow rates were adjusted using the peristaltic pump adjustment control and fine adjustment for each individual microcosm with a four-way channel splitter that contained a fine knob adjustment for each port. A 24 hour flow through of all water (distilled) filled carboys

was performed to ensure a constant rate before another 24 hour flow through was performed with the actual experimental nutrient treatments. Microbial inoculum was added without nutrient loading, sequentially to all microcosms. After 2 hours for settling time, nutrient flow commenced. This was done to prevent washout immediately after inoculation. A dilute bleach solution was added to the water bath to prevent algal growth from occurring within the water bath.

2.1.4. Microbial Inoculation

The algal community was selected to represent the Great Lakes microbial community (Figure 2-3): diatoms (i.e. *Navicula pelliculosa, Fragilaria crotonensis, & Aulacoseira sp.*), cyanobacteria (i.e. *Nostoc sp. & Anabaena sp.*), and green algae (*Chlorella vulgaris, Pseudokirchneriella subcapitata,* and *Spirogyra sp.*). *Navicula pelliculosa* is a common diatom within freshwater bodies as this genus has the greatest recorded taxa (Kociolek, 2005), whereas *Fragilaria crotonensis, & Aulacoseira sp* are commonly found in eutrophic lakes (Moos *et. al.*, 2009). Notably, *Chlorella* may potentially produce N_2O (Weathers, 1984). Most cultures were obtained from Ward's Scientific (St. Catharines, ON). *Fragilaria crotonensis* and *Aulacoseira sp.* cultures were obtained through University of Toronto Culture Collection of Algae and Cyanobacteria (UTCC), now the Canadian Phycological Culture Centre. Algae and cyanobacteria were cultured using CHU-10 media (Stein, 1973), modified according to J. Acreman (UTCC). All media was sterilized and cultures were transferred aseptically. Algal suspensions were maintained on a mixing table under a fixed light source (fluorescent grow lights) that simulated

scheduled an 8-hour daylight exposures. Algal concentrations were comparable to seasonal trends (i.e. spring and summer) of the Great Lakes.

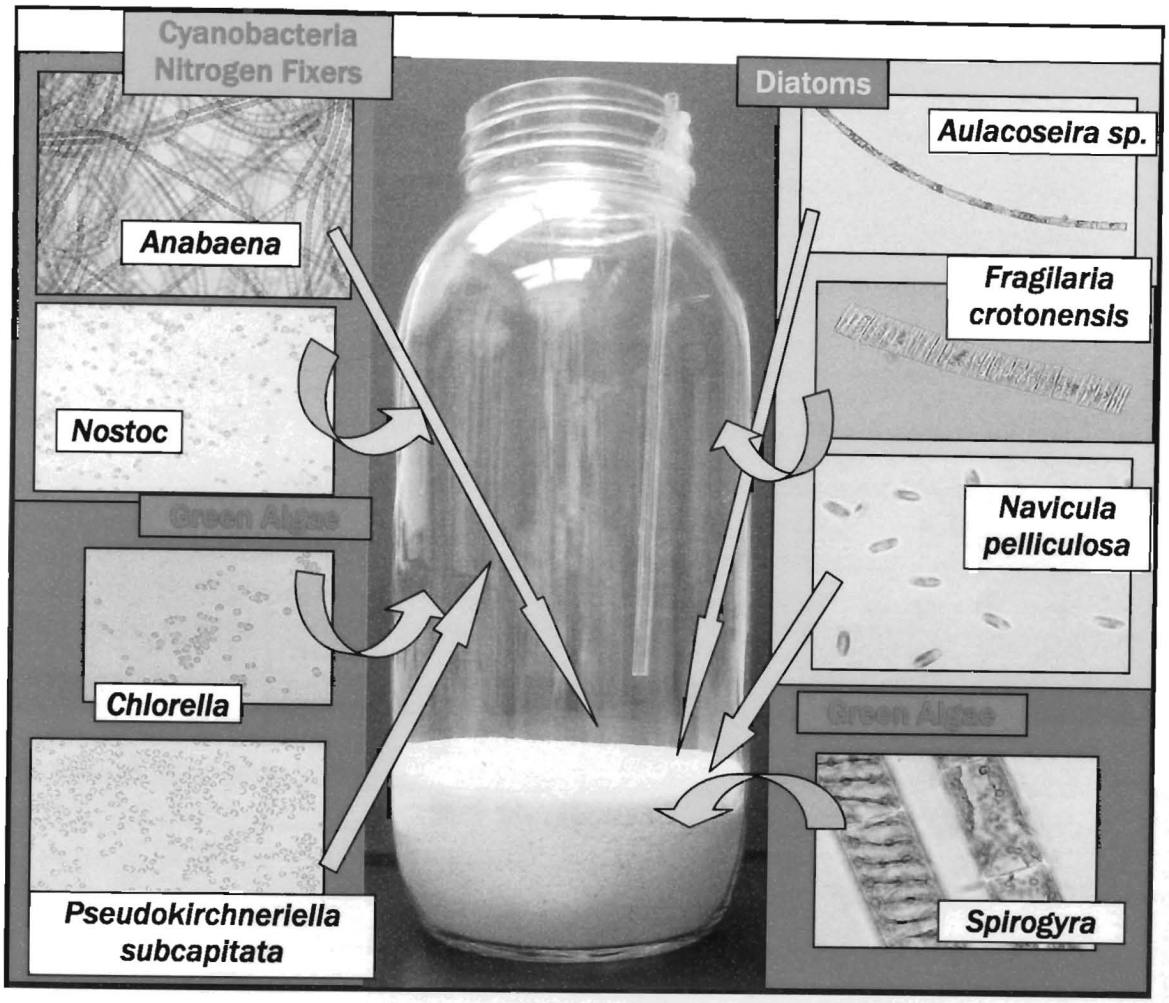

Figure 2-3. Microcosm Innocolum Set-up

Algal community densities that were used included:

Anabaena (1 x 10^5 cells/ml), *Aulacoseira sp.* (7200 Filaments/ml), *Chlorella* (1 x 10^6 cells/ml), *Fragilaria crotonensis* (3 x 10^5 cells/ml), *Navicula pelliculosa* (6 to 8 x 10^5 cells/ml), *Nostoc* (1 x 10^5 cells/ml), *Pseudokirchneriella subcapitata* (1 x 10^4 cells/ml), and *Spirogyra* (5 ml stock).

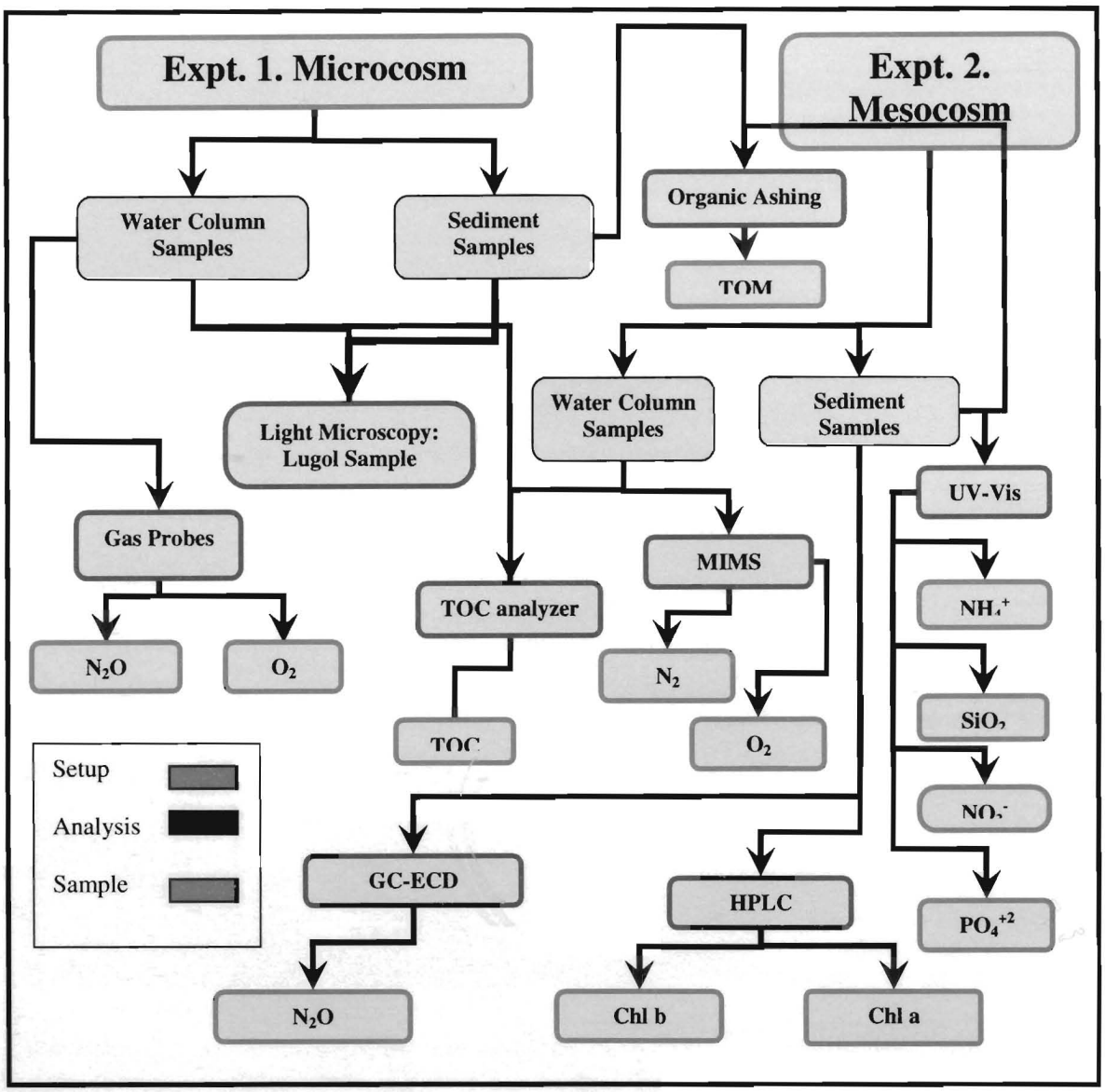

Figure 2-4. Microcosm/Mesocosm Sample Analysis Flowchart

2.1.5 Gas Measurements

Chemical analyses included NO_3^-, dissolved silica, ortho-phosphate, NH_4^+, and total organic carbon (TOC) as illustrated in figure 2-4. Oxygen and nitrous oxide probes were calibrated using two-point calibrations. Initially, distilled water at room temperature was

moderately sparged with air by an air bubbler in a beaker (~20 minutes). The signals (in pA) for 100% oxygen and nitrous oxide saturation were recorded for each probe. The beaker was then sparged with N_2 for ~ 20 minutes and the signals for 0% oxygen and nitrous oxide saturation were recorded. The temperature of this water standard was also taken to convert probe measurements from pA to μM concentrations.

Dissolved oxygen and nitrous oxide concentrations were measured using microsensors (Unisense A/S, Aarhus, Denmark). Preliminary microcosm gas preparation involved turning the light source off during the day for about 30 minutes, before turning the light on and recording gas values. Microsensors were submerged mid-depth for about 5-10 seconds until readings were stabilized before recording the next adjacent microcosm. The light cycle was recorded first (estimated at about 5 minutes to record all microcosm readings) before the lights were turned off where the dark cycle readings were recorded for the same duration. Conditions affecting gas exchange across the air-water interface (e.g. temperature, pressure, air circulation) were assumed constant across all microcosms, and gas flux was estimated according to:

$$\text{Flux} = k(\text{measured concentration} - \text{equilibrium concentration})$$

where flux is measured in mmol O_2 or N m^{-2} h^{-1}, k is a piston velocity (units of m h^{-1}) and gas concentrations have units of mmol O_2 or N m^{-3}. Equilibrium gas concentrations are calculated based on water temperature (Weiss, 1970; Weiss & Craig, 1973; Weiss & Price, 1980). Piston velocity is estimated from an empirical wind velocity-piston velocity relationship (Laursen & Seitzinger, 2005), using a wind velocity of 0 m s^{-1}. Respiration, net primary production, and net N_2O production were determined based on changes in

dissolved gas concentrations through time under constant conditions (e.g. measurements 3 hours apart under dark conditions or light conditions), and correcting for flux.

2.1.6 Organic Carbon

At the end of the 3 month experiment, water column samples were drawn from the mid-region of the water column and examined for their Total Organic Carbon content by the Shimadzu TOC-V (serial #: HS1104285065) analyzer and total organic content by the standard Ash technique. Water columns samples were collected on site and stored at freezing. Water samples were thawed later and examined by the TOC analyzer. Samples were drawn into the analyzer by a carrier gas (150 ml/min flowrate) into a combustion tube containing an oxidation catalyst and then heated to 680°C. As a result, carbon dioxide is formed from the burnt total carbon in the sample. The revenants of this sample are swept from the combustion tube to an electronic dehumidifier where it becomes dehydrated and cooled. After passing through a halogen scrubber, the carbon dioxide becomes quantified by a non-dispersive infrared gas analyzer (Shimadzu Corporation, 2001). Whereas, the latter procedure required 50mL water samples to be filtered through a pre-combusted Whatman GF/F syringe filter. The filter was dried, weighed, and ashed at 500°C for 24 hours to remove organics. The final mass was used to determine the organic content as mass lost on ignition.

2.2 Mesocosm Experiment

Small microcosm are acceptable for small scale variability due to their small sediment surface area, however, error values might extrapolate to larger scale problems. A small surface area may also limit water column microbial flock and biofilm formation that are

associated with late spring/summer ecosystem behaviour. Mesocosm setup (large scale microcosms, Figure 2-6) was carried out the following summer in order to coincide with environmental and temporal events experienced by local lake water bodies. This mesocosm framework was based on the microcosm setup of the previous summer. Mesocosm nutrient loading ratios were to follow the same nutrient ratio regime as the microcosm experiment, although loading rates were reduced for better representation of loading to natural systems (Table 2-2) (Cook *et. al.*, 2009; Downing & McCauley, 1993; Schindler *et. al.*, 2008; Turner, 2002). This was modified by removing the high N:P treatments, as microcosm experiments found no differences in oxygen consumption, production, or net N_2O production between high N:P (25:1) and middle-range N:P (15:1). Therefore, the mesocosm experimental design was restricted to 4 different treatments with triplicate mesocosms for each treatment for a total of 12 mesocosms at each location. Mesocosm chambers consisted of cylindrical plastic drums of equal size (50.8 cm diameter, 96.52 cm height, 163 L volume) arranged in random order in an open field. Two duplicate runs of this 12 mesocosm setup were conducted in two different field sites: Markham region and City of Hamilton. Water exchange (10% volume replacement) was conducted after weekly samples were collected. Water was removed from mesocosms and replaced with municipal tap water (Markham mesocosms) or with pond water (Stoney Creek mesocosms). The Stoney Creek mesocosms, then, had a continuous reinoculation with aquatic microorganisms, including algae and cyanobacteria. The experiment was conducted over an 8 week period in August and September of 2008.

Table 2-2. Nominal nutrient loading rates for mesocosm experiments

Treatment	Nutrient Loading (μmol Si, N, or P m^{-2} d^{-1})		
	Si	N	P
Low Si, Low P	200	400	27
Low Si, High P	200	400	80
Hi Si, Low P	800	400	27
Hi Si, High P	800	400	80

Silica sand was added to mesocosms, covering the bottom of each drum to a depth of ~10 cm. Sand was washed several times to eliminate floating particles and debris. Silty sediment was collected from Christie Lake in Dundas, ON using an Ekman dredge. This sediment was added to the mesocosms to a depth of ~ 3 cm, providing finer particles, organic matter, and natural microbial inoculum. Mesocosms were filled with municipal tap-water. Mesocosms were assigned trial treatments and were randomized on the experimental field. Mesh was fitted at the opening to limit access by mosquitoes while still allowing gas exchange and light penetration. Mesocosms were allowed to settle for one week to allow silt to settle, stratification to begin, and the release of trapped air bubbles before nutrient loading began.

Within the first 24 hours, sediment traps (two per mesocosm) that consisted of a 50ml centrifuge tube were deployed at the bottom of each mesocosm (Figure 2-5). They were inserted in sediment and later collected using a rod with a centrifuge cap glued to the end. Each centrifuge tube contained 2-3 marbles to prevent floating. In theory, a dense periphyton layer will accumulate during experimental operation and will add to benthic organic content and sediment microbial community present.

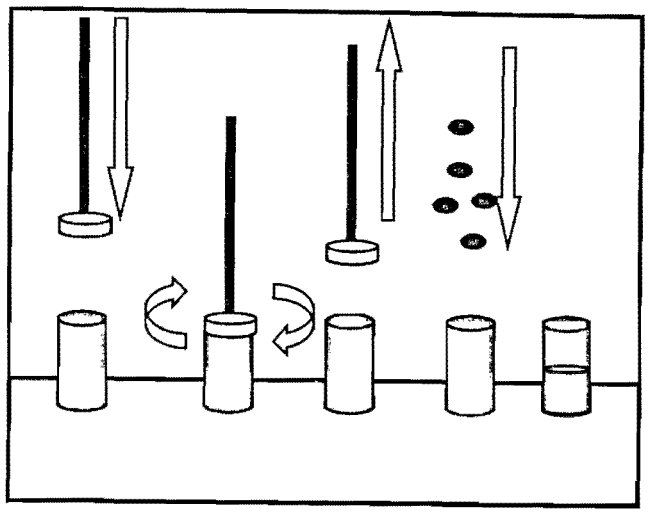

Figure 2-5. Benthic algae trap deployment and algae collection

Figure 2-6. Outdoor Mesocosm Setup under rainy conditions

2.2.1 Weekly Sampling of Mesocosms

Nutrients were replenished within each mesocosm by removing 10% of the water column and replacing it with municipal tap water (Markham) or pond water (Stoney Creek), and adding nutrients from stock solutions. Water column samples were collected using a siphon tube and gravity filling of sample vessels. Water samples were collected from mid-depth. Samples for nutrient analyses (50 ml) were filtered (Whatman GF/F) and frozen before nutrients were replenished in mesocosms in order to assess the previous week's conditions. Water samples were taken from the water supplies used for volume replacement (tap and pond water) as well as precipitation whenever rain events occurred during the week. Precipitation measurements were based on Pearson Airport/Buttonville Airport and Hamilton Airport, for Markham and Hamilton areas respectively. Volumes of water exchanged and concentrations of nutrients in water exchanged (by replacement,

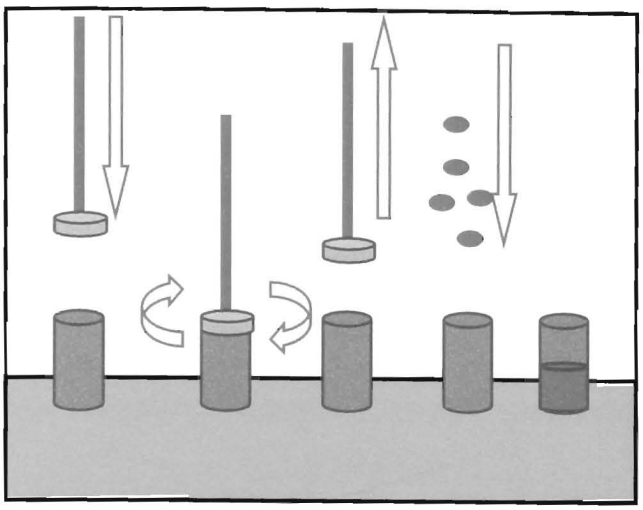

Figure 2-5. Benthic algae trap deployment and algae collection

Figure 2-6. Outdoor Mesocosm Setup under rainy conditions

2.2.1 Weekly Sampling of Mesocosms

Nutrients were replenished within each mesocosm by removing 10% of the water column and replacing it with municipal tap water (Markham) or pond water (Stoney Creek), and adding nutrients from stock solutions. Water column samples were collected using a siphon tube and gravity filling of sample vessels. Water samples were collected from mid-depth. Samples for nutrient analyses (50 ml) were filtered (Whatman GF/F) and frozen before nutrients were replenished in mesocosms in order to assess the previous week's conditions. Water samples were taken from the water supplies used for volume replacement (tap and pond water) as well as precipitation whenever rain events occurred during the week. Precipitation measurements were based on Pearson Airport/Buttonville Airport and Hamilton Airport, for Markham and Hamilton areas respectively. Volumes of water exchanged and concentrations of nutrients in water exchanged (by replacement,

nutrient amendment, and rainfall) were used to calculate actual nutrient loading to mesocosms. Samples for N_2O were processed by the gentle gravity filling of 10 ml water sample, into a syringe, from the siphon tube. The sample was transferred immediately into a 20 ml serum bottle previously flushed with N_2 (minimum 20 volumes flushed). This serum bottles were then vigorously shaken to equilibrate the gas between the water sample and the headspace. After 5 minutes of shaking, a syringe was used to withdraw 10 ml of gas was and transfer it to an N_2-flushed exetainer. Samples for dissolved O_2, N_2, and Ar were collected by gentle gravity filling of exetainers, inserting the siphon tube into the bottom of the exetainer and allowing three volumes to overflow the exetainer before removing the tube. Samples were preserved by pipetting in concentrated $ZnCl_2$ solution to a final concentration of 0.5% volume/volume (20 μL into 4 ml water sample). Exetainers were capped, taking care to avoid trapping bubbles, and were stored under water in a refrigerator. Temperature readings were recorded by using a temperature probe at mid-depth in the water column. Temperature was used to determine headspace equilibrium for N_2O analyses and to determine theoretical gas equilibrium concentrations. Gases were analyzed as described below.

2.2.2 Mesocosm Location

Summer mesocosms were located in two different locations: Markham township and Hamilton region. Separate locations determined if differing water supply, continuous versus one-time direct inoculum with aquatic microorganisms, and geographical location in field were causative factors that would influence biogeochemistry and phytoplankton community structure. Temporal seasonal effects and general geographical location were shared between the two experimental sites.

2.2.2.1 Markham

Markham is a township north of the city of Toronto. The municipal water codes comply with the Ontario Drinking Water System Regulation. Under Ontario Regulation 170/03, water samples are collected by provincially approved York-Durham regional environmental laboratories certified with Waterworks licences. Tested drinking water from all water municipalities maintained a consistent amount of nitrite and nitrate levels that were 0.010 mg/L and 0.590 mg/L respectively (The Corporation of the Town of Markham Annual Regulatory Water Quality Report, 2008).

2.2.2.2 Turtle Pond

Situated in Stoney Creek (municipality of Hamilton), Turtle pond is a small (~ 10 ha) flood basin pond of Lake Ontario. The pond is shallow (~ 1.3 m) with very turbid water. Turtle pond experiences frequent blooms of cyanobacteria during the summer and autumn.

2.3 Organic Carbon and Sediment Analysis

Water column organics were measured by collecting 250ml water samples. Within 24 hours, suspended organics were collected by vacuum filtration and filters (pre-combusted GF/F) were dried, weighed, and combusted at 500°C. Ashed filters were reweighed to determine mass lost on ignition (organic fraction). Sediment traps and sediment cores were collected by gently draining the mesocosms (siphon tubes) until less than 20 cm water depth was present. Sediment cores were collected using a centrifuge tube with the end cut off, forming an open barrel that could be inserted and then capped to maintain

suction while the core was removed. Three sediment cores were collected from each mesocosm (random locations), transferred to a plastic jar, and homogenized as a composite sample. Sediment samples were stored at -20°C. Sediment core and sediment samples were used for organic carbon analysis (combustion as above) and phytopigment analysis.

2.4 Chemical and Gas Analysis

2.4.1 N_2, O_2, and Ar - Membrane Inlet Mass Spectrometry

Dissolved gas samples were drawn from the mid-region water column of each mesocosm via siphoning from a Tygon tube into a 5ml glass vial. Gentle water transfer was maintained until vial overflow to ensure that air bubbles were not formed and that water samples were not degassed. A supersaturated $ZnCl_2$ solution was added to the water sample and was encapsulated allowing no air bubbles to be trapped inside. This was performed to preserve the gaseous content within the water sample and to prevent the metabolic breakdown of the gas. Samples were refrigerated for storage instead of frozen to prevent degassing.

Samples were analyzed for N_2, O_2, and Ar using membrane inlet mass spectrometry (MIMS) (Kana *et. al.*, 1994, 1998). With high N_2 background associated with gas analysis, MIMS becomes an appropriate gas technique as it measures N_2 directly under *in situ* conditions. Gas ratios (N_2:Ar and O_2:Ar) are measured by mass spectrometry as ratios can be measured with much greater precision (<0.05% CV among replicates) than direct measurement of individual gases. Ar is a non-reactive, relatively abundant gas and is generally assumed present at 100% saturation with respect to

temperature. N_2 and O_2 can then be calculated from measured gas ratios assuming Ar to be at equilibrium.

The instrument was standardized using a gently and continuously mixed distilled water sample, held in a water bath and equilibrated for several hours. The standard was assumed to be at 100% saturation with respect to all three gases at the temperature of the water bath. Measured ratios in the standard were normalized to theoretical gas ratios at equilibrium (Weiss, 1970). This normalization was applied to ratios measured in gas samples to determine in situ gas ratios. N_2 and O_2 were then calculated from ratios assuming Ar was at equilibrium at the time the sample was collected given the measured sample water temperature.

Samples were first drawn in the MIMS by a peristaltic pump where gas molecules from this water sample were then swept through a semi-permeable microbore silicone membrane by an internal turbomolecular vacuum pump. The gas sample was drawn into a loop inserted into a liquid nitrogen trap to capture water vapour and carbon dioxide from the main gas stream. The remaining N_2, O_2, and Ar are detected by a quadrapole mass spectrometer. Using Ar as the inert internal standard, N_2:Ar and O_2:Ar ratios determined gas concentrations as ratio measurements were more precise than individual concentration values. Dissolved gas concentrations were determined from equations derived by (Weiss, 1970).

Under direct N_2:Ar measurement of microcosm waters by N-isotopes, solubility equations of Ar concentrations at air saturation (Colt, 1983; Weiss, 1970) may calculate the change in dinitrogen gas. The differences in dinitrogen gas concentration produced will define denitrified N_2 flux as analyzed by mass spectrometers. Sequence batch reactors determine N_2:Ar

between inlet and outlet water, flow rate and core surface area produce a more dynamic nutrient effect than steady-state conditions. However, batch trials may require a more complicated setup that may run for several days or weeks.

Microcosm studies have identified the positive influence of algal and bacterial community (i.e. structure and biomass) on benthic periphyton. Microphytobenthos and benthic bacteria may be compared within these sediment deposits. By alternating periphyton characteristics (e.g. nutrient load, sediment substrate, redox potential, etc), sediment denitrification rates will be affected (Ishida *et. al.*, 2008). Although stagnation is brought about by the slow water turnover and the gradual gas gradient, microbial interaction associated with nutrient ratio proceeds to influence denitrification rates.

2.4.2 Ammonia Assay

The combination of ammonia sample with hypochlorite and indophenol reagents forms a blue colour that is analyzed using a UV-Vis spectrometer. This phenol reaction is catalyzed by sodium nitroprusside. Analysis was conducted using a UV-Vis spectrometer at 640nm. Protocol details are as listed in Appendix A. part A.1 (Greenberg *et. al.*, 1999; Solarzano, 1969).

2.4.3 Nitrate Assay

Nitrate analysis was performed by running prepared samples through a cadmium column that quantitatively reduces nitrate to nitrite. A peristaltic pump was used to maintain constant flow. This nitrogen union with sulphanilamide and N-(1-napthyl)-ethylenediamine dihydrochloride creates an azo-dye that is a vibrant pink colour. Sample concentrations are determined through UV spectroscopy at 543nm. Protocol details are as

listed in Appendix A. part A.2 (Methods for chemical analysis of water and wastes.1979; Greenberg *et. al.*, 1999; Wood *et. al.*, 1967).

2.4.4 Ortho-Phosphate Assay

The ascorbic acid method was used to determine dissolved orthophosphate (phosphorus) concentrations. A molybdenum blue is developed with reduction of heteropholy acid (phosphomolybdic acid) from the reaction of ammonium molybdate and potassium antimonyl tartrate with orthophosphate in the presence. Molybdenum blue intensity is reciprocal to orthophosphate concentration, which is analyzed under the UV-Vis spectrometer at 880nm. Protocol details are as listed in Appendix A. part A.3 (Edwards *et. al.*, 1965; Greenberg *et. al.*, 1999; Murphy & Riley, 1962).

2.4.5 Dissolved Silica Assay

The molybdosilicate method was used for SiO_2 analysis. In this assay, silica and phosphate are reacted with ammonium molybdate (pH 1.2) to form heteropoly acids. The phosphate aspect (molybdophosphoric acid) is eliminated with the addition of oxalic acid leaving the molybdosilicic acid intact. A yellowish colour is produced in proportion to molybdosilicici acid content and is read at 410 nm using the UV-Vis spectrometer. The detailed nutrient assay was based on wastewater treatment standards and are noted in Appendix A, part A.4 (Eaton *et. al.*, 1995; Greenberg *et. al.*, 1999).

2.4.6 GC-ECD N_2O Analysis

Perkin Elmer Autosystem XL gas chromatography was installed with a Supelco Plot 1010 column for sample analysis. A hydrogen gas carrier gas was used at a flow rate of

45.0 ml/min with a general air flowrate at 450.0 ml/min. The split ratio was set a default of zero reading and was adjusted according to the gas pressure. The oven temperature was set on a 35°C isothermal temperature program. Samples were injected at a injector temperature of 185°C with sample detector temperature set at 200°C. Protocol details are as listed in Appendix A. part B.

2.5 Microbial Analysis

2.5.1 Lugol Sample/Light Microscopy

Microbial community is monitored individually or as individuals of a whole community. Microbial samples were stored using lugol iodine solution. The Lugol solution consisted of 10g potassium iodide and 5g iodine for every 100ml water mixture.

Two Lugol samples were taken at a mid-intermediate period (established community) and near the termination of the experiment (community maturity). Characterization was accomplished by identification through a light microscope and then numerated based on haemocytometer counts that determined microbial cell density.

2.5.2. Phytopigmentation Analysis

Mesocosm sediment cores and sediment traps would be sent to DHI organisation (independent, international and research organisation) for phytopigmentation analysis which is approved and controlled by the Danish Accreditation Scheme (DANAK). Samples will be stored in liquid nitrogen after being filtered onto GF/F filters. Upon analysis, samples will be analyzed by a Shimadzu LC-10A HPLC system according to methodology described by Wright, *et. al.* (1991). Protocol details are as listed in Appendix A. part C.

2.6 Statistical Analyses

Statistical analyses were performed using SYSTAT (2008) software for PC computers. Repeated-measures analysis was used to assess differences in mesocosm nutrient (PO_4^{-2}, Si, NO_3^-, NH_4^+) concentrations, microcosm TOC and TOM concentrations, N_2O and O_2 microcosm readings, mesocosm $\%N_2$ saturation, and $\%O_2$ saturation. The different microcosm/mesocosm assay results as stated were defined as experimental units, with N:P loading, N:Si loading, location effects were taken as the between-unit factors and the time, time x location, time x N:P, time x Si:P taken as the within-unit factors. The general linear model was performed on mesocosm inorganic nitrogen loss, mesocosm SiO_2 loss, and mesocosm PO_4^{-2} loss.

3. RESULTS AND DISCUSSION

3.1 Microcosm Experiment

After the initial two weeks of microbial inoculation, a consistent green colour from primary producers was visible throughout the 3-month experimental duration on the sediment surface. Benthic growth was visible in all microcosm trials (Figure 3-1); however, growth density was subject to nutrient loading regime, as a thin growth layer was present in low nutrient loading treatments, or when flow was disrupted due to tube blockage. Microbial growth consistency was re-established once nutrient flow continued (Figure 3-2). Gas concentrations were measured weekly using Unisense A/S dissolved oxygen and nitrous oxide microsensors directly above the sediment in the water column (Figure 3-3).

Figure 3-1. Microcosm set-up in laboratory. Reservoir with nutrient stock is visible in background, tubing, and water bath

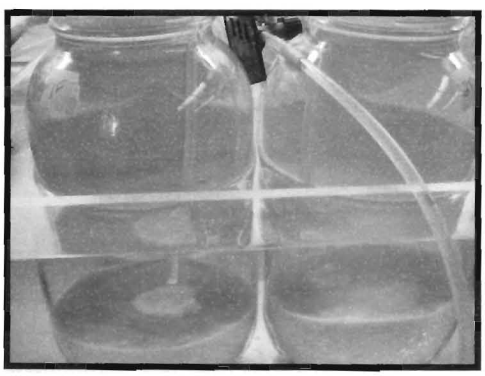

Figure 3-2. Nutrients applied by glass capillary above sediment

Figure 3-3. Gas probe analysis of microcosms

3.1.1 Nitrous oxide production

ANOVA indicated different trends in nitrous oxide production between the light and dark cycles as shown in Figure 3-4 (a and b). Both Si:N and N:P loading ratios affected N_2O production in the light, but only N:P affected N_2O production in the dark (Table 3-1). Regarding P loading (figure 3-4), it would seem that nitrous oxide production during the light cycle generally increase with increasing P load (relative to N). For example, low Si:N = 0.5 and low N:P =5 initially produces ~18 nmol N_2O m^{-2} h^{-1} and then decreases to ~8 nmol m^{-2} h^{-1} N_2O at Redfield N:P = 15 and at high Si:N = 2. Also, low N:P produces N_2O ~28 nmol m^{-2} h^{-1} (high Si:N, yellow bar, Figure 3-4 a.) that decreases to ~10 nmol m^{-2} h^{-1} occuring at the high N:P ratio. High N:P, which should favour green algae over cyanobacteria, resulted in lower N_2O production which is not consistent with hypothesis 2, 2a, and 2c.

Increased Si:N loading on the other hand showed a general increase of nitrous oxide production at low N:P, but a reduction in N_2O production at high N:P. Redfield N:P ratio showed the greatest difference between Si loading with ~8nmol m^{-2} h^{-1} N_2O produced at low Si:N = 0.5 in comparison to the high Si:N = 2 with ~15 nmol m^{-2} h^{-1} N_2O produced.

The effect of Si:N loading on N_2O production was strongly dependent on N:P loading, as shown by significant Si x P interaction terms ($p < 0.001$ in light, $p = 0.002$ in dark) (i.e. the tendency for high silica to increase N_2O production was reversed where N:P was high). Increased N_2O production with high silica loading at low N:P was consistent with hypothesis 1, and 1c as the competitive balance was tipped from cyanobacteria more toward diatoms. The results of reduced N_2O production at high N:P

are also consistent with the predictions of hypothesis 2, and 2c. While low N:P favours cyanobacteria, high N:P with low silica loading should favour green algae, which are generally denser than diatoms or cyanobacteria, and sink exporting carbon and organic N to sediments. High N:P with high silica loading should favour diatoms, which are less likely to sink than green algae due to carbon storage as lipids. This should reduce organic N export to sediments, and therefore N_2O production by denitrification.

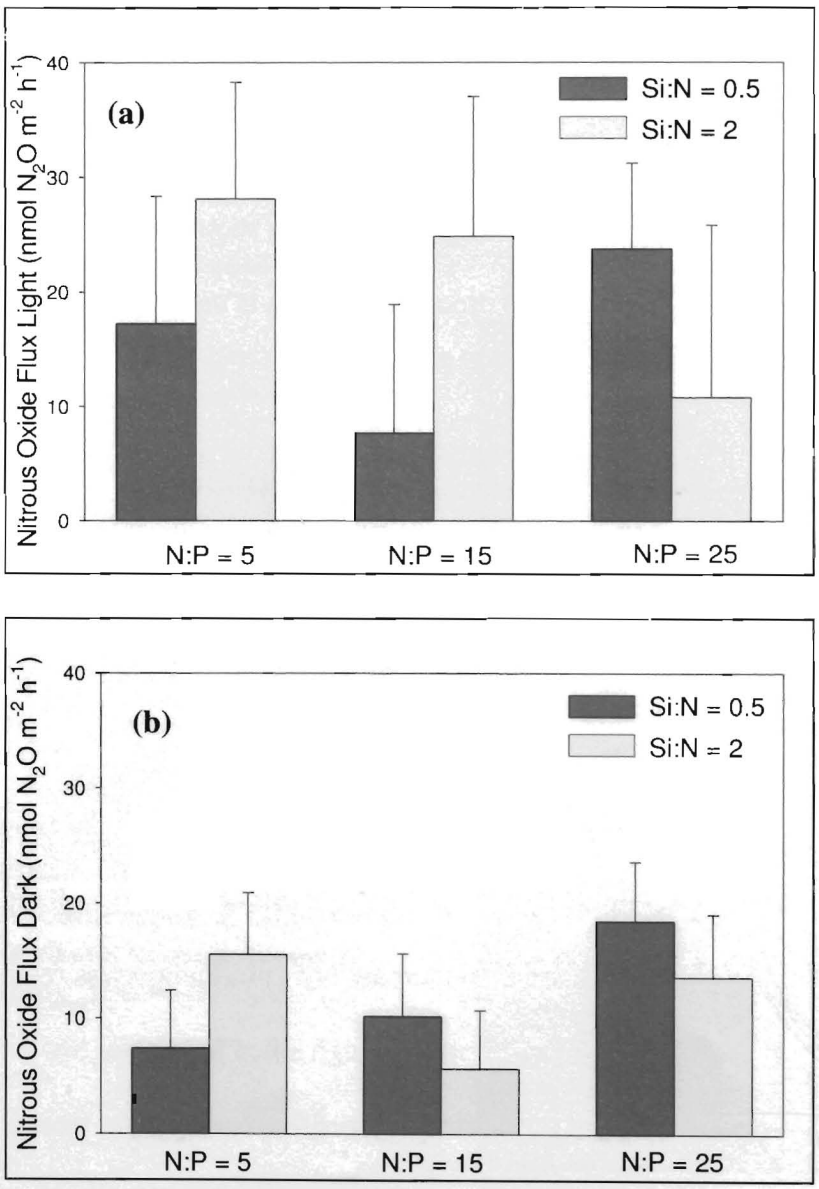

Figure 3-4. Net O_2 flux in light (a) and dark (b) in relation to nutrient loading ratios

Values of N_2O production in the dark cycle were generally lower in magnitude compared to their light cycle counterparts. Statistical evidence also showed that N_2O flux changed over time in both the light and dark situations, as indicated by the significant effect of date.

Similar to other diural studies, overall dark nitrous oxide flux values were relatively lower than their light cycle counterparts, which would suggest a greater importance of autotrophic influence on denitrification processes during the day. Although nitrifiers are light sensitive, photosynthesized oxygen may increase the sediment oxic layer and support denitrification via coupling with nitrification (Risgaard-Petersen *et. al.*, 2005; Rysgaard *et. al.*, 1994). As shown in figure 3-4b (dark conditions), denitrification may have become relatively less important in the dark.

Table 3-1 Statistical results of repeated measures analysis of variance for N_2O flux from microcosms in light and dark

Effect	Test Statistic	Probability
Light		
Silica loading	$F_{1,72} = 5.66$	0.020
Phosphorus loading	$F_{2,72} = 3.48$	0.036
Date	$F_{3,72} = 458.74$	< 0.001
Silica loading x phosphorus loading	$F_{2,724} = 18.65$	< 0.001
Silica loading x Date	$F_{3,724} = 24.62$	< 0.001
Phosphorus loading x Date	$F_{6,72} = 4.68$	< 0.001
Silica loading x Phosphorus loading x Date	$F_{6,72} = 30.12$	< 0.001
Dark		
Silica loading	$F_{1,72} = 0.07$	0.799
Phosphorus loading	$F_{2,72} = 8.41$	0.001
Date	$F_{3,72} = 65.97$	0.001
Silica loading x phosphorus loading	$F_{2,724} = 7.00$	0.002
Silica loading x Date	$F_{3,724} = 77.15$	0.001
Phosphorus loading x Date	$F_{6,72} = 9.76$	0.001
Silica loading x Phosphorus loading x Date	$F_{6,72} = 12.29$	0.001

ANOVA model: N_2O flux = constant + Si + P + Date + Si*P + Si*Date + P*Date + Si*P*Date + error

3.1.2 Photosynthesis/Respiration

High silica loading relative to nitrogen consistently increased oxygen flux, both in light (Figure 3-5a) and in the dark (Figure 3-5b). Phosphorus loading (relative to nitrogen) had no effect on oxygen flux under light conditions, however increased P loading (relative to N) did increase oxygen consumption by sediments in the dark ($p = 0.033$) (Table 3-2). The increased loading of silica appears to have stimulated overall metabolic activity, perhaps by selecting for a more productive community of photosynthetic organisms, particularly diatoms. As discussed, diatom biomass will contribute to the periphyton layer with increasing Si:N loading. The potential for reducing agents (i.e. organic carbon) within this layer may rise and possibly account for the increase in respiration rate with this shift in loading ratio.

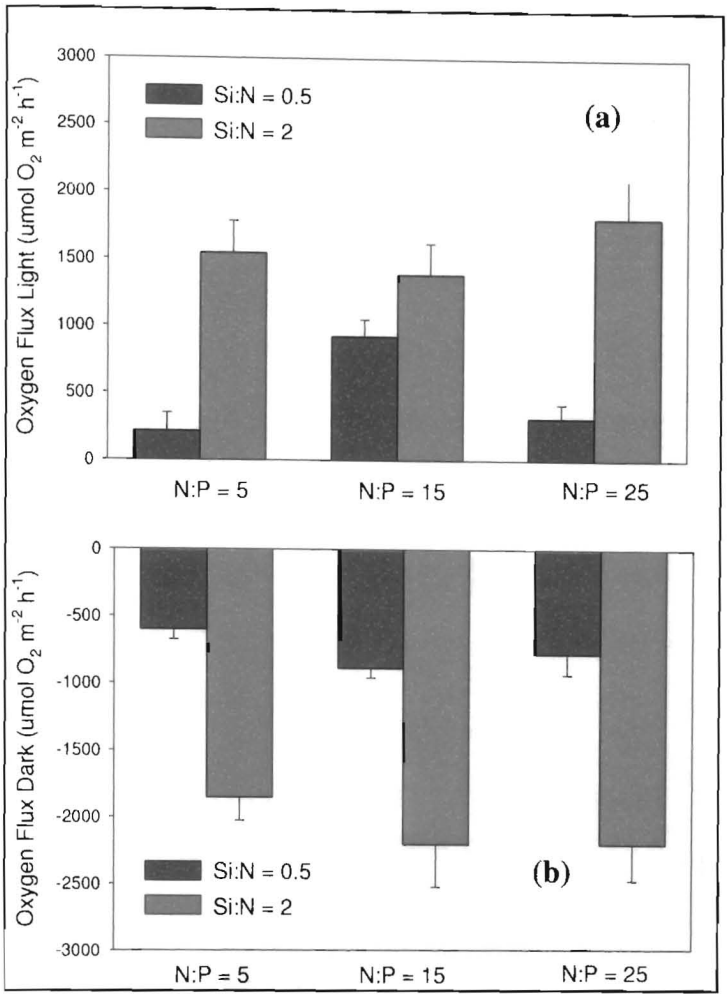

Figure 3-5. Net O_2 flux in light (a) and dark (b) in relation to nutrient loading ratios

Table 3-2 Statistical results of repeated measures analysis of variance for O_2 flux from microcosms in light and dark

Effect	Test Statistic	Probability
Light		
Silica loading	$F_{1,174} = 69.54$	0.001
Phosphorus loading	$F_{2,174} = 0.98$	0.381
Date	$F_{7,174} = 15.97$	0.001
Silica loading x phosphorus loading	$F_{2,174} = 5.40$	0.005
Dark		
Silica loading	$F_{1,174} = 135.9$	0.001
Phosphorus loading	$F_{2,174} = 3.49$	0.033
Date	$F_{7,174} = 9.45$	0.001
Silica loading x phosphorus loading	$F_{2,174} = 2.83$	0.062

ANOVA model: O_2 flux = constant + Si + P + Date + Si*P + error

3.1.3 Total Organic Carbon

Total organic carbon analysis of samples from the water column is a proxy for microbial biomass, and would be expected to correlate with phytoplankton biomass. Organic carbon decreased as phosphorus loading (relative to N loading) decreased (Figure 3-6; Table 3-3). However, as noted in the previous section, decreased P loading did not reduce oxygen production during the day. This suggests that either community with high N:P loading is more productive, per unit biomass, or that much of the production in these communities is benthic. The latter possibility would also be consistent with expectations of hypothesis 2a. However, total organic matter (TOM) in sediments did not increase with higher N:P loading (Table 3-4; Figure 3-7) as would be expected from hypothesis 2b. Further, sediment TOM decreased with increased Si:N loading, contrary to expectations from hypothesis 1b.

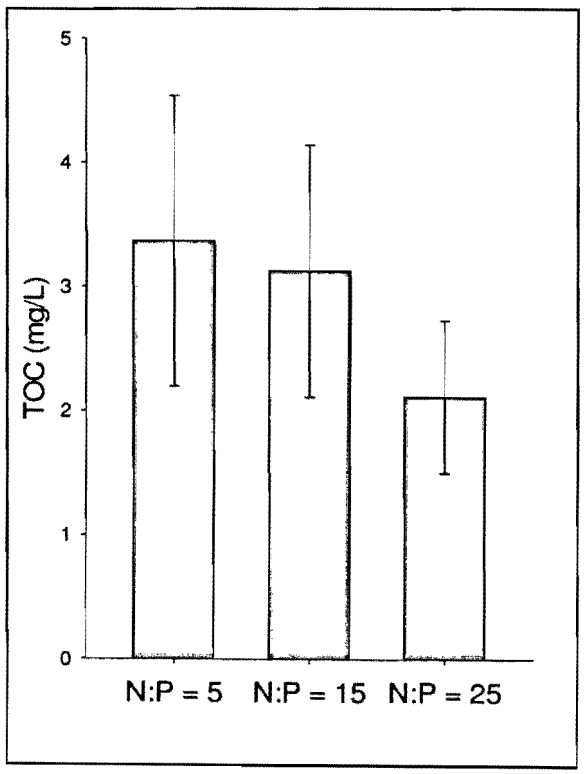

Figure 3-6. Microcosm Water Column TOC (Final Sample)

Table 3-3. Statistical results of an one-way analysis of variance for dissolved organic carbon in microcosms

Effect	Test Statistic	Probability
Light		
Silica loading	$F_{1,18} = 0.300$	0.591
Phosphorus loading	$F_{2,18} = 3.339$	0.058
Silica loading x phosphorus loading	$F_{2,18} = 0.054$	0.948

ANOVA model: TOC = constant + Si + P + Si*P + error

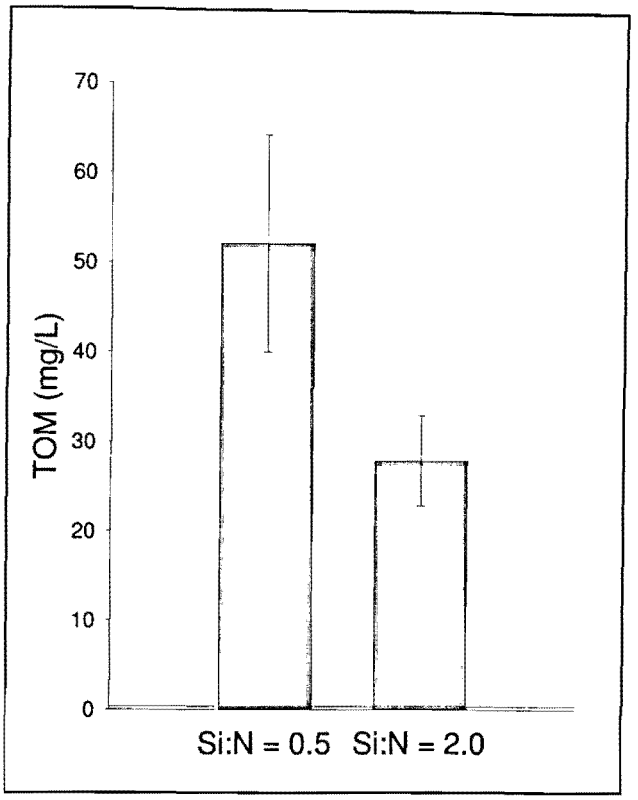

Figure 3-7. Microcosm Sediment TOM (Final Sample)

Table 3-4. Statistical results of an one-way analysis of variance for sediment organic matter in microcosms

Effect	Test Statistic	Probability
Light		
Silica loading	$F_{1,15} = 3.621$	0.076
Phosphorus loading	$F_{2,15} = 1.787$	0.201
Silica loading x phosphorus loading	$F_{2,15} = 0.589$	0.567

ANOVA model: TOM = constant + Si + P + Si*P + error

3.1.4 Community Composition Analysis

Preserved samples were characterised using light microscopy and cells were enumerated with a haemocytometer. Primary producers were identified by their size, cellular shape and internal membrane structure, which were visually enhanced by iodine staining characteristics of cellular components. Given that samples were seeded with eight morphologically distinct microphytes, identification of cells in mixed communities may potentially be relatively simple. Community composition was defined by the percent contribution of each type of microphyte to the mixed culture. These percentage contributions were used as the dependent variables in the MANOVA analysis.

The MANOVA full model found that community composition did vary significantly among nutrient loading treatments and over time (Table 3-5; full model, $p < 0.001$). Silica loading (relative to N) did not have a significant effect on commnity composition ($p = 0.449$), however P loading (relative to N) did have a marginally significant effect on community composition ($p = 0.084$). The temporal effect ($p < 0.001$), on the other hand, showed a significant difference between the initial results with those taken three months later.

Generally, an increase in P loading relative to N resulted in a decrease in the relative abundance of green algae and an increase in the abundance of cyanobacteria (Figure 3-8); consistent with hypothesis 2, and 2a. An increase in relative abundance of diatoms was expected with an increase in Si loading. This was not observed and diatoms were consistently a minor part of microphyte community composition. Small diatoms may be very difficult to observe and identify with general light microscopy (i.e. not using phase contrast and sediment-free samples). It is likely that diatom abundance was under

reported. The results, while not supportive of the hypothesis that increased Si:N loading would favour diatom dominance, should not be taken as evidence against the hypothesis as there is extensive research supporting this issue (Carrick & Lowe, 2007; Schelske *et. al.*, 1986, 2006).

Upon further statistical analysis, univariate F tests showed that *Navicula* (diatom, $p < 0.001$) and *Nostoc* (cyanobacteria, $p = 0.032$) were the genera that were most responsive to treatment, and best explained the overall community response to different treatments. Considering that diatoms readily take up silica as part of their frustule structure and cyanobacteria can store large amounts of phosphorus in polyphosphate granules within their cells, microbial cultures of *Navicula* and *Nostoc* may be most effectively linked to alterations in Si:N and N:P. Again, *Navicula* were probably undercounted and the *Nostoc* results may be the most robust from this data set. Nostoc was sensitive to N:P loading and was greatly reduced in dominance when N:P loading increased to 25 (Figure 3-8). A comparison between panels (Figure 3-8a and 3-8b) showed that the green algae may have slowly increase in microcosms and become more dominate during the latter stages of the experiment. Although *Spirogyra* was inoculated into all microcosms, it was not detected in any September or December samples.
It also appeared that the medium N:P loading (15:1) produced the lowest diatom dominance as compared to the other N:P treatments that created relatively similar diatom abundance. Redfield nutrient ratio is ideal for general microbial growth and may create competition for resources in a limited spaced microcosm. For this reason, cyanobacteria and green algae may have a competitive advantage as their free-floating nature accesses a greater water surface area for nutrients in the water column over benthic diatoms. Low

flow conditions (5 cm/s average horizontal velocity) such as this microcosm setup would lead to buoyant cyanobacteria species (i.e. *Anabaena*) (Bormans & Condie, 1997). Nonetheless, the ability of diatoms to specifically utilize Si and its ease of buoyancy manipulation due to their relatively high surface area may give competitive advantages over other species under extreme N:P conditions. Regardless, cyanobacteria dominance was shown to be relatively consistent among microcosm nutrient loading regimes.

Table 3-5. Statistical results of multivariate analysis of variance for microphyte community composition

Effect	Test Statistic	Probability
Multivariate Models	F = 2.77	<0.001
Full Model		
Silica loading	F = 0.97	0.449
Phosphorus loading	F = 1.72	0.084
Date	F = 2.77	<0.001
Univariate Models		
Navicula	F = 8.03	<0.001
Nostoc	F = 2.94	0.032
Chlorella	F = 1.70	0.168
Pseuodkirschneriella	F = 2.10	0.099
Anabaena	F = 0.18	0.948

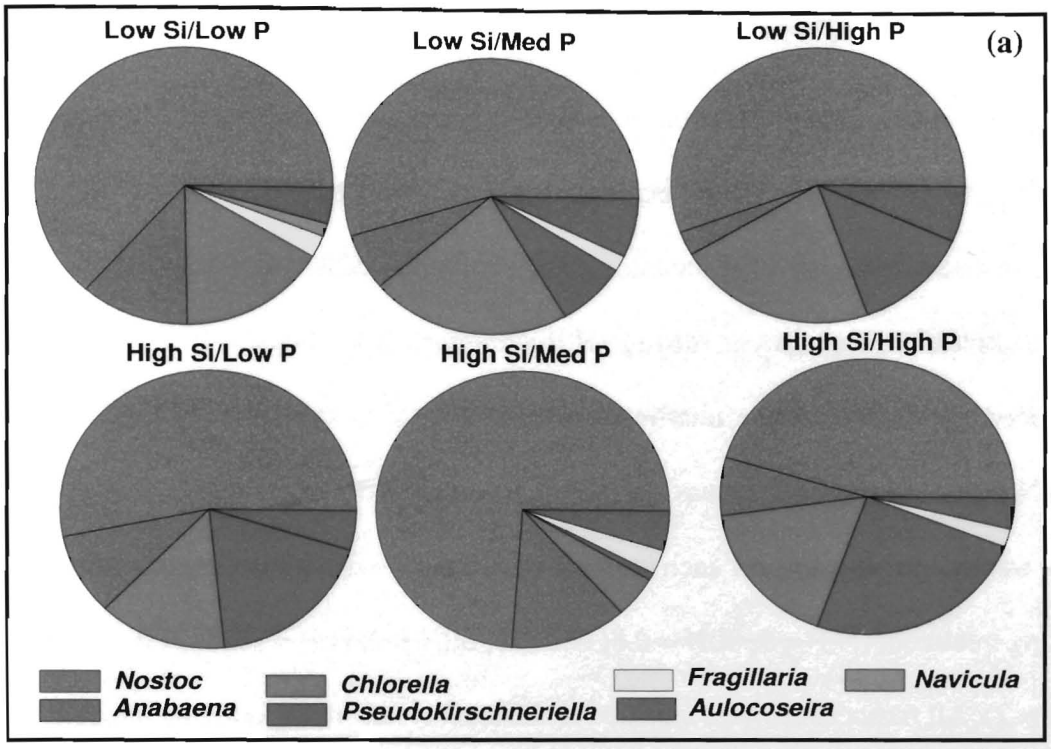

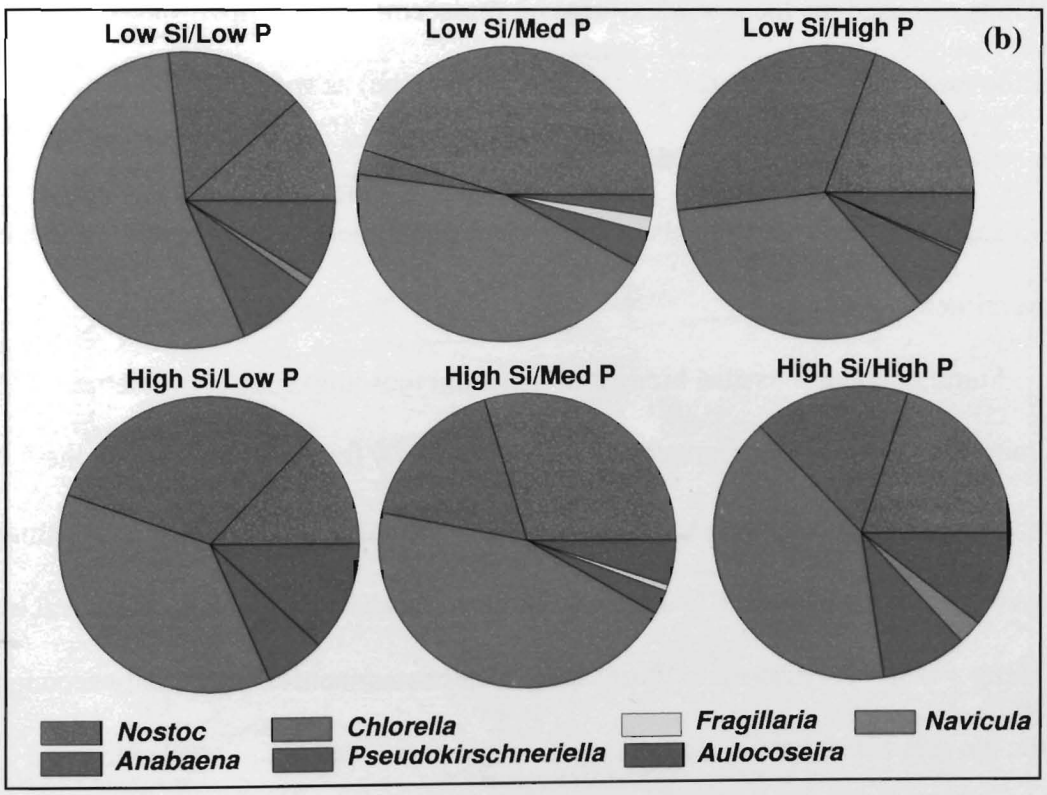

Figure 3-5. Microcosm Microbial Diversity in Mid-Experiment (Sept 16 '07) (a) and Final Experimental (Dec 12 '07) (b)

3.2 Mesocosm Experiments

Large scale mesocosms were setup in outdoor fields of two locations, Markham and Hamilton, and simulated indoor microcosm parameters from the previous summer. Through statistical analysis of the microcosms it was concluded that there was no significant difference between the high N:P nutrient trial in comparison to the medium N:P (Redfield) nutrient ratio in terms of nitrous oxide and oxygen flux. Therefore, the high N:P loading ratio (25:1) was not included in mesocosm experiments. Altogether, there were 12 mesocosms for each location with 3 mesocosm trials for each nutrient loading treatment (N:P = 5, Si:N = 0.5; N:P = 5, Si:N = 2; N:P = 15, Si:N = 0.5; N:P = 15, Si:N = 2). All mesocosms were exposed to the local weather, surrounding temperature conditions and used the local water system for replacement (municipal water). The Hamilton mesocoms used nearby lake water (Turtle pond) as well as the local municipal water system for replacement, as described in the Methods section. The Hamilton mesocosms, then, had a continuous inoculation of pond microphytes over the course of the experiment.

Summer conditions also brought up potential mosquito control problems. Mosquitoes were prevented from entering mesocosms by fixing net barriers on the mesocosm openings. Although large insect vectors were efficiently denied entry, smaller insects (i.e. midges) were able to spawn within the Markham mesocosms. Removal by net sifting was the only means of eliminating such contaminants and can only account for visible, moving insect larvae. Barriers were only removed for sample collection and nutrient replacement each week.

3.2.1 Denitrification

A Membrane Inlet Mass Spectrometer (MIMS) at the University of Montreal was used to analyze water samples for dissolved N_2 and O_2 as described in the Methods section. Denitrification rates were not directly measured, but relative differences in denitrification can be inferred from differences in saturation of water with respect to N_2. Similarly, differences in respiration can be inferred from differences in saturation of water with respect to O_2.

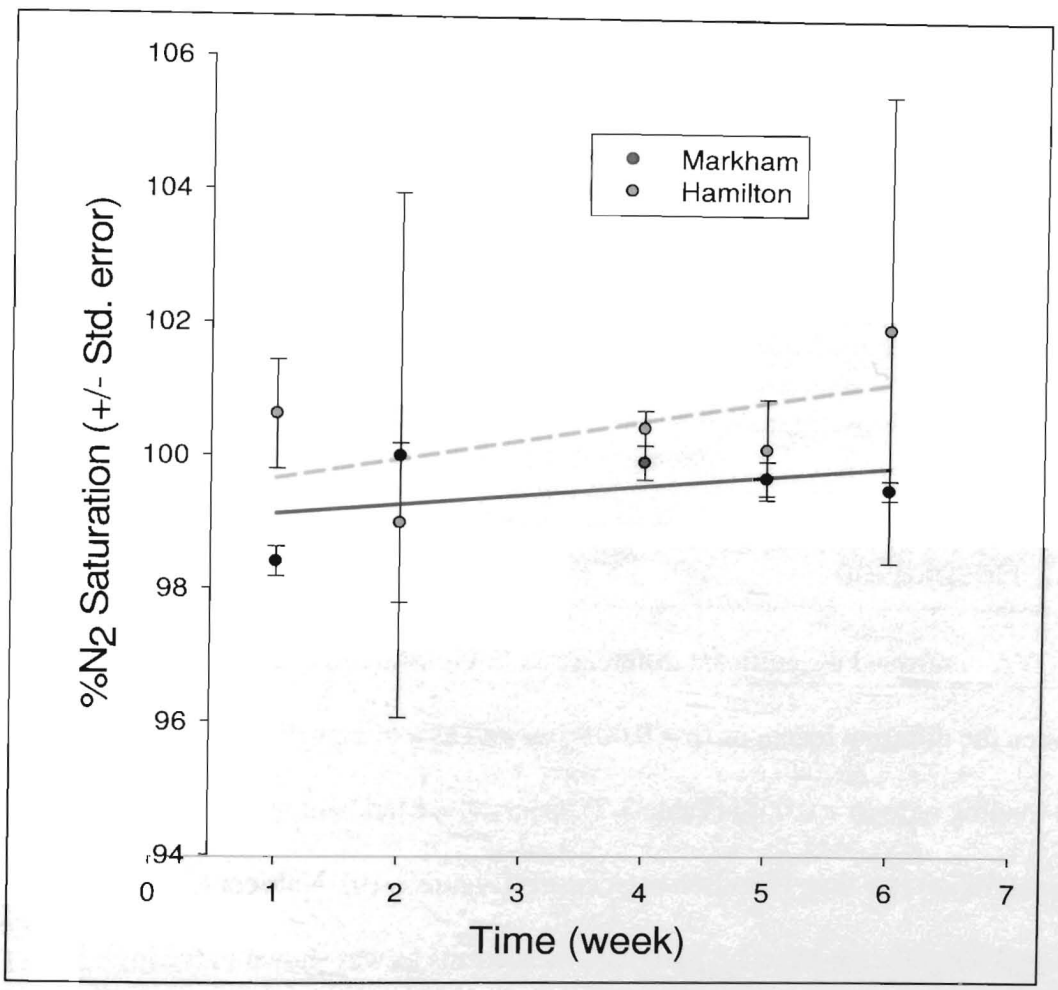

Figure 3-9. Mesocosm N_2 (%Saturation)

ANOVA found that the only significant effect on $\%N_2$ saturation was the differing locations ($p = 0.022$) (Table 3-6). With a high denitrification rate, a greater degree of N_2 product becomes saturated in the water column, hence an increase in $\%N_2$ saturation value. Hamilton mesocosms can be inferred to have had generally greater denitrification rates than Markham mesocosms (Figure 3-9).

Table 3-6. Statistical results of repeated measures analysis of variance for dissolved N_2 (as % saturation) in mesocosms

Effect	Test Statistic	Probability
Primary Factors		
Location	$F_{1,16} = 6.465$	0.022
Silica loading	$F_{1,16} = 0.432$	0.521
Phosphorus loading	$F_{1,16} = 0.431$	0.521
Time	$F_{4,64} = 0.908$	0.465
Multivariate Models		
Time x Location	$F_{4,64} = 2.212$	0.094
Time x Silica loading	$F_{4,64} = 0.807$	0.525
Time x Phosphorus loading	$F_{4,64} = 0.819$	0.518

ANOVA model: N_2 (% saturation) = constant + Location + Si + P + time + time*Si + time*P + time*location + error

3.2.2 Respiration

ANOVA confirmed a significant difference in $\%\ O_2$ saturation of mesocosm water between the different locations ($p = 0.001$), as well as a marginally significant effect of Si:N loading ratio ($p = 0.065$) (Table 3-7). Generally, Markham mesocosms had a greater $\%O_2$ saturation rate than Hamilton mesocosms (Figure 3-10). Nutrient loading involving Si:N had a significant effect on Markham mesocosms as was shown in the high Si:N nutrient ratio trial that produced a greater oxygen staturation rate than the low Si:N trial. Hamilton mesocosm Si:N nutrient trials were comparable and showed no difference.

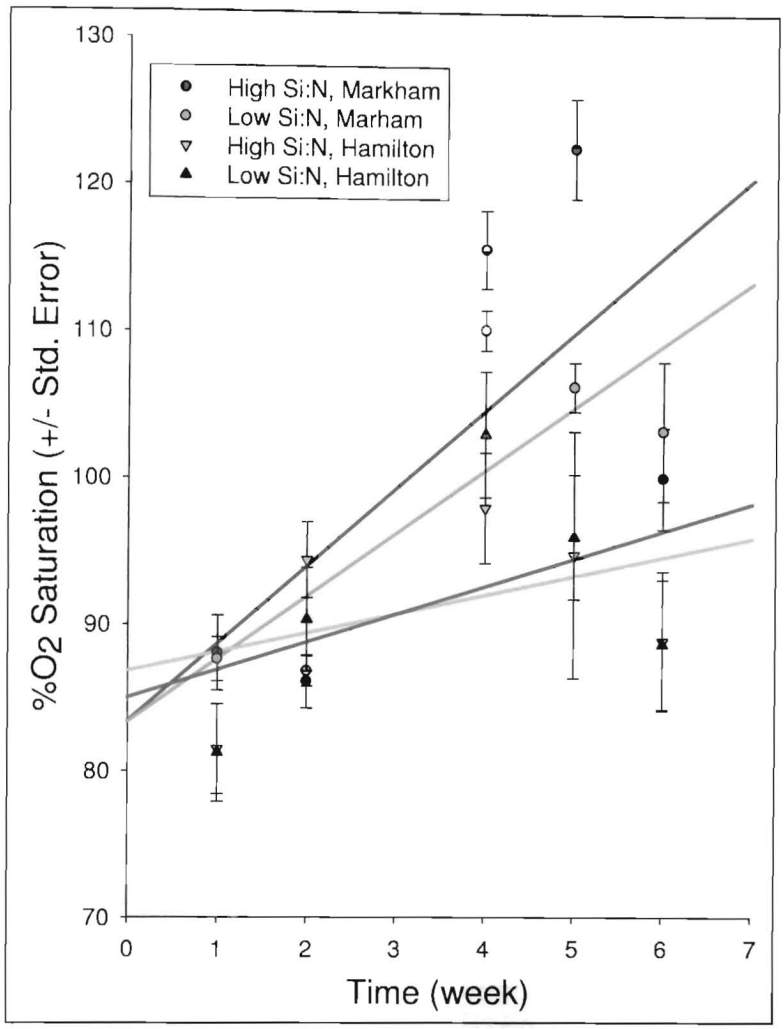

Figure 3-10. Mesocosm O_2 (% Saturation)

Table 3-7. Statistical results of repeated measures analysis of variance for dissolved O_2 (as % saturation) in mesocosms

Effect	Test Statistic	Probability
Primary Factors		
Location	$F_{1,16} = 15.716$	0.001
Silica loading	$F_{1,16} = 2.478$	0.135
Phosphorus loading	$F_{1,16} = 0.205$	0.657
Time	$F_{4,64} = 36.8$	0.000
Multivariate Models		
Time x Location	$F_{4,64} = 15.865$	0.000
Time x Silica loading	$F_{4,64} = 2.333$	0.065
Time x Phosphorus loading	$F_{4,64} = 0.696$	0.597

ANOVA model: O_2 (% saturation) = constant + Location + Si + P + time + time*Si + time*P + time*location + error

High silica loading may have favoured a productive benthic periphyton layer dominated by diatoms in the Markham mesocosms, explaining the difference in % O_2 saturation during the day between Si:N loading regimes. However, phytopigment analysis of sediments must be completed to provide support for this.

3.2.3 Nitrous Oxide Production

Nitrous oxide production was not measured directly; however, differences in dissolved N_2O concentrations can be used to infer differences in net production. ANOVA results showed that experimental treatments (nutrient loading ratios) had no significant effects in mesocosm trials (Table 3-8). Nitrous oxide concentrations were shown to decrease with time (Figure 3-11), despite cooling of water, which would increase solubility. This suggests that net production rates decreased through the late summer into early autumn.

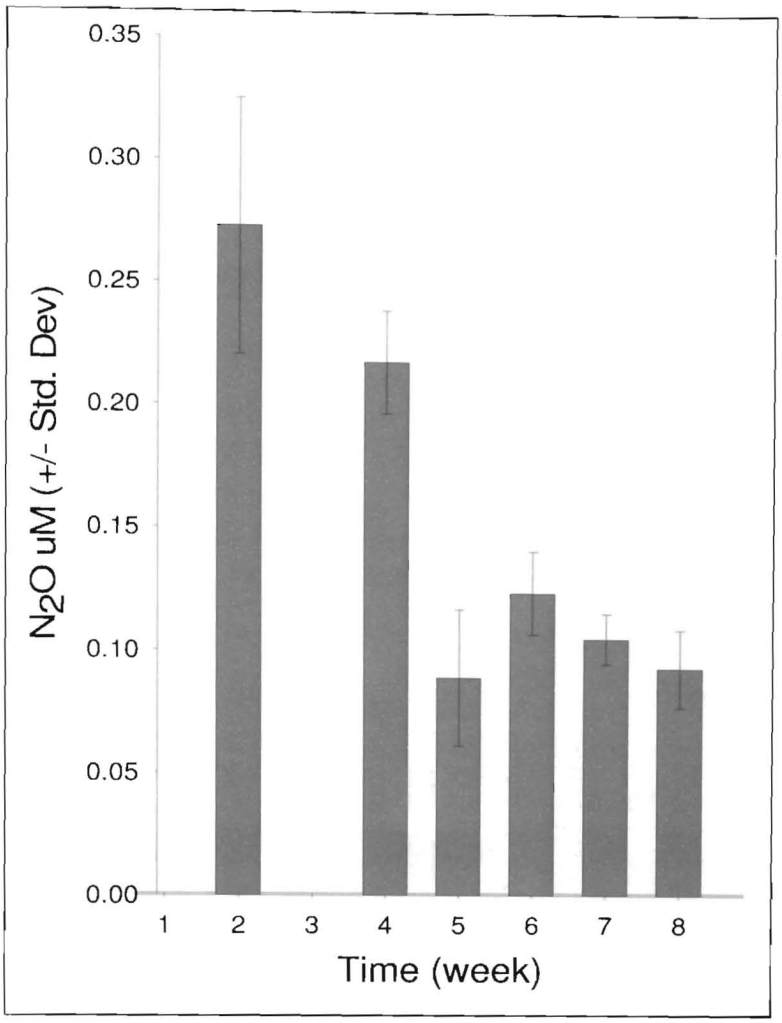

Figure 3-11. Mesocosm Nitrous Oxide

Table 3-8. Statistical results of repeated measures analysis of variance for dissolved N_2O concentration in mesocosms

Effect	Test Statistic	Probability
Primary Factors		
Location	$F_{1,16} = 0.606$	0.448
Silica loading	$F_{1,16} = 0.266$	0.613
Phosphorus loading	$F_{1,16} = 0.033$	0.858
Time	$F_{5,80} = 6.511$	0.000
Multivariate Models		
Time x Location	$F_{5,80} = 0.232$	0.948
Time x Silica loading	$F_{5,80} = 0.374$	0.865
Time x Phosphorus loading	$F_{5,80} = 0.227$	0.950

ANOVA model: N_2O = constant + Location + Si + P + time + time*Si + time*P + time*location + error

3.2.4 Nutrient Analysis

A general pattern for nutrient concentrations is that there is a significant difference between site locations and temporally. Nutrient assay results are categorized by location, according to Markham or Hamilton results. The nutrient and organic assays involved in this study were TOC, NH_4^+, NO_3^-, Si, and PO_4^{-2} (Figure 2-4).

3.2.4.1 Water Column Total Organic Carbon (TOC)

TOC in mesocosm water samples was shown to vary between locations (Table 3-9). Mesocosms located in Hamilton generally had higher TOC concentrations on any given date than Markham mesocosms (Figure 3-12). Although TOC concentrations varied among dates within each location, there was no clear temporal pattern as seen for N_2O concentrations, suggesting net carbon production was more temporally variable than net N_2O production.

Their periphyton layers may ultimately define mesocosm denitrification rates and sediment metabolism. Periphyton organic matter may act as an electron donor for utilization of heterotrophic bacteria including denitrifiers. Hamilton mesocosms (~7 TOC $\mu g\ L^{-1}$) generally have greater water column TOC content than Markham (~5 TOC $\mu g\ L^{-1}$) throughout experimentation, which may translate to more carbon available in the periphyton or sediment layers. This organic carbon availability could account for the higher % saturation of N_2 and lower % saturation of O_2 seen in Hamilton mesocosms relative to Markham mesocosms.

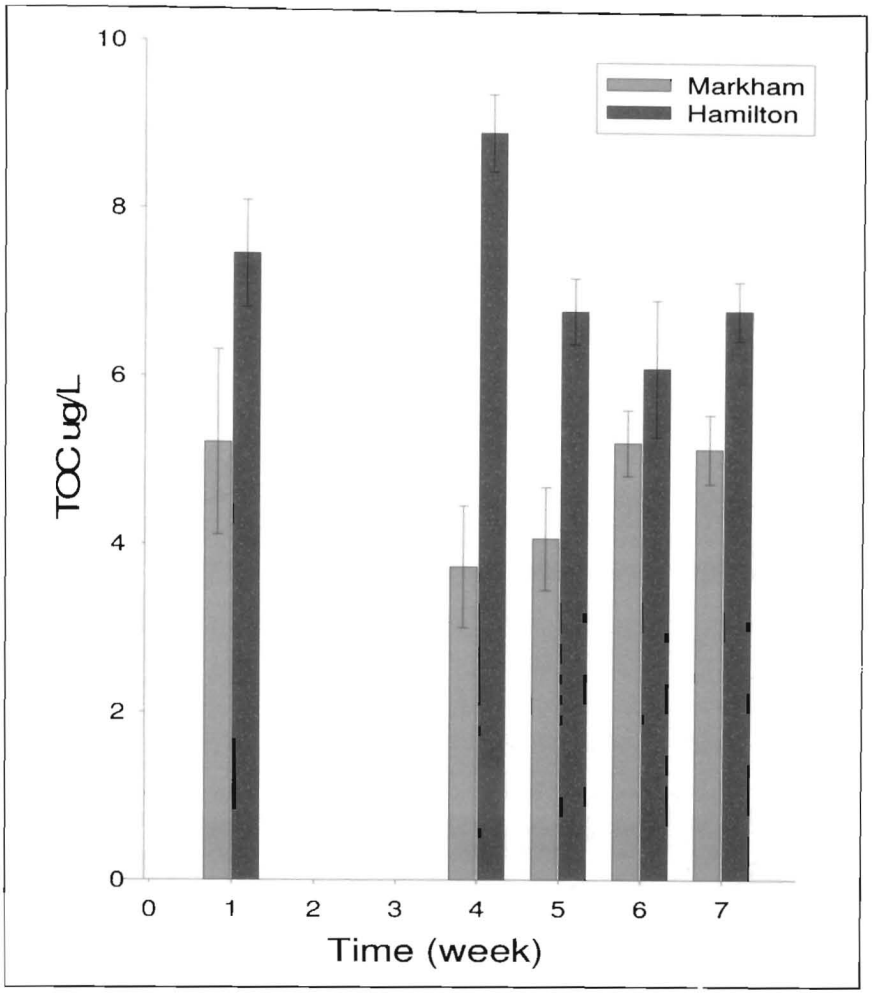

Figure 3-12. Mesocosm Total Organic Carbon

Table 3-9. Statistical results of repeated measures analysis of variance for total organic carbon concentration in mesocosms

Effect	Test Statistic	Probability
Primary Factors		
Location	$F_{1,9} = 9.210$	0.014
Silica loading	$F_{1,9} = 2.689$	0.135
Phosphorus loading	$F_{1,9} = 0.601$	0.458
Time	$F_{4,36} = 2.742$	0.043
Multivariate Models		
Time x Location	$F_{4,36} = 1.991$	0.117
Time x Silica loading	$F_{4,36} = 0.629$	0.645
Time x Phosphorus loading	$F_{4,36} = 0.069$	0.991

ANOVA model: TOC = constant + Location + Si + P + time + time*Si + time*P + time*location + error

3.2.4.2 Ammonium

Being a readily bio-available source of nitrogen, Markham and Hamilton NH_4^+ concentration trends decreased with time (Figure 3-13). Ammonium concentrations in Hamilton mesocosm experienced a parabolic relationship with respect to ammonium concentration, where week 4 and 5 showed the lowest concentrations. Ammonium concentrations were significantly different between locations with Markham mesocosms having generally higher concentrations. Nutrient loading ratios had no effect on ammonium available for biomass production (Table 3-10).

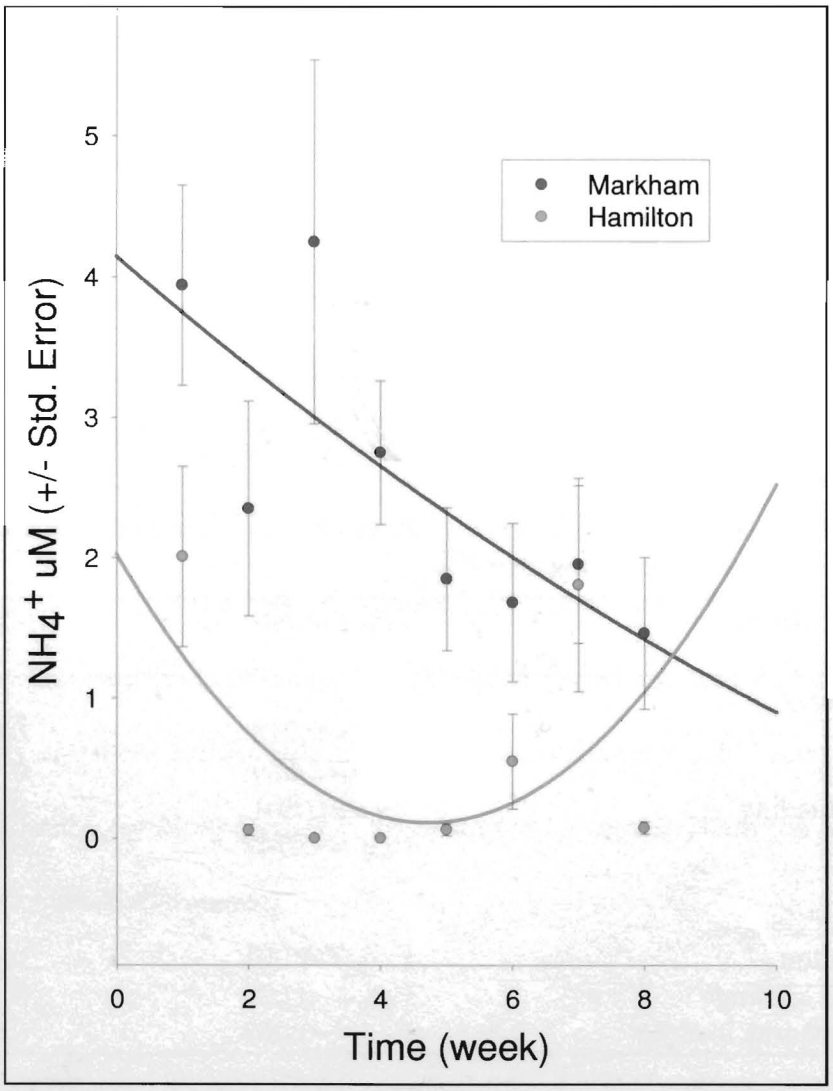

Figure 3-13. Mesocosm Ammonium

Table 3-10. Statistical results of repeated measures analysis of variance for ammonium concentration in mesocosms

Effect	Test Statistic	Probability
Primary Factors		
Location	$F_{1,16} = 32.54$	0.000
Silica loading	$F_{1,16} = 0.435$	0.519
Phosphorus loading	$F_{1,16} < 0.001$	0.983
Time	$F_{7,112} = 2.965$	0.007
Multivariate Models		
Time x Location	$F_{7,112} = 2.024$	0.058
Time x Silica loading	$F_{7,112} = 1.160$	0.331
Time x Phosphorus loading	$F_{7,112} = 0.210$	0.984

ANOVA model: NH_4^+ = constant + Location + Si + P + time + time*Si + time*P + time*location + error

3.2.4.3 Nitrate

ANOVA results for nitrate showed a temporal and location effect (Table 3-11). Similarly, with Hamilton ammonium concentration trends, nitrate concentrations had a parabolic relationship within each location where week 6 showed the lowest nitrate concentration recorded before increasing slightly (Figure 3-14). In contrast to ammonium concentrations, nitrate concentrations were generally higher in Hamilton mesocosms than in Markham mesocosms. Taken together, these results suggest that net nitrification rates may be generally higher in Hamilton mesocosms than in Markham mesocosms.

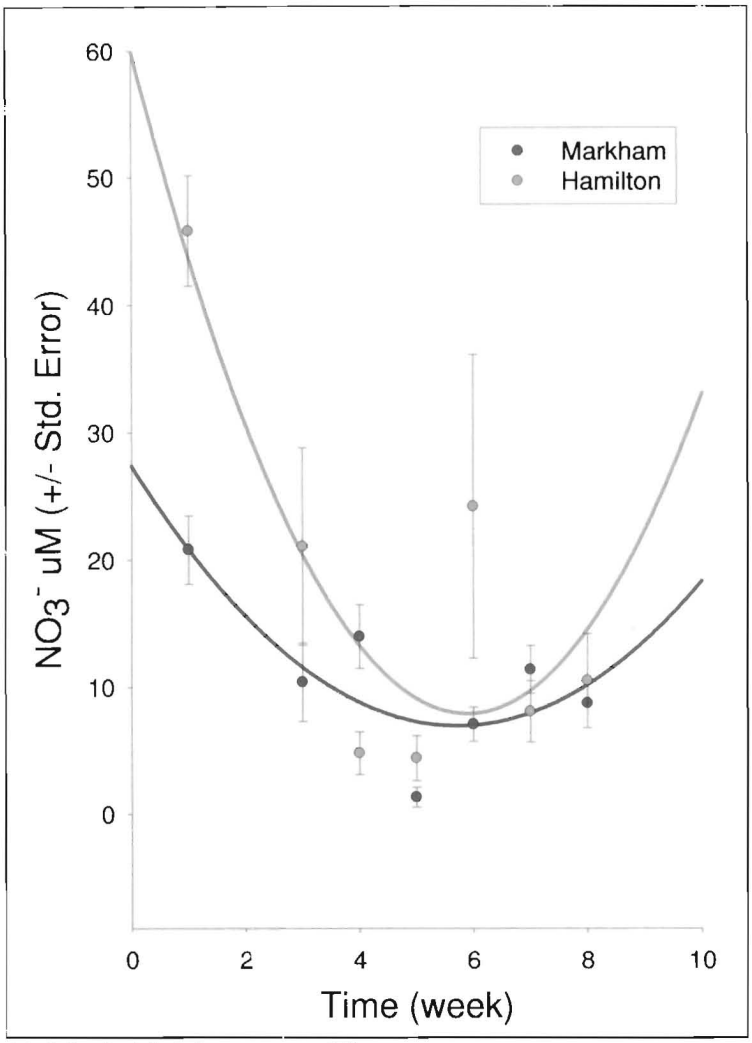

Table 3-14. Mesocosm Nitrate

Table 3-11. Statistical results of repeated measures analysis of variance for nitrate concentration in mesocosms

Effect	Test Statistic	Probability
Primary Factors		
Location	$F_{1,14} = 5.407$	0.036
Silica loading	$F_{1,14} = 0.082$	0.779
Phosphorus loading	$F_{1,14} = 0.051$	0.824
Time	$F_{6.84} = 17.348$	0.000
Multivariate Models		
Time x Location	$F_{6.84} = 5.272$	0.000
Time x Silica loading	$F_{6.84} = 0.838$	0.544
Time x Phosphorus loading	$F_{6.84} = 1.753$	0.119

ANOVA model: NO_3^- = constant + Location + Si + P + time + time*Si + time*P + time*location + error

3.2.4.4 Dissolved Inorganic Nitrogen Loss

Possible inorganic nitrogen fates could be sediment burial, microbial biomass assimilation, and loss by denitrification (either directly or through coupled nitrification/denitrification). The lag growth of seeded microbial community in each mesocosm may be a probable explanation to initially high nutrient values. As the microbial community, including phytoplankton, matures and becomes established, more nutrients may be removed contributing to dissolved inorganic nitrogen loss. ANOVA results showed a significant difference in nitrogen loss from mesocosms based on location (Table 3-12). Loss of dissolved inorganic nitrogen (ammonium + nitrate + nitrite) was generally greater from Hamilton than from Markham mesocosms. This was particularly true during the first four weeks of the experiment, with no difference between locations beyond week 5 (Figure 3-15). While loss could be attributed in part to burial or assimilation, the results are consistent with the higher % N_2 saturation data and, taken together, suggest denitrification rates were not affected by nutrient loading ratios but were affected by location.

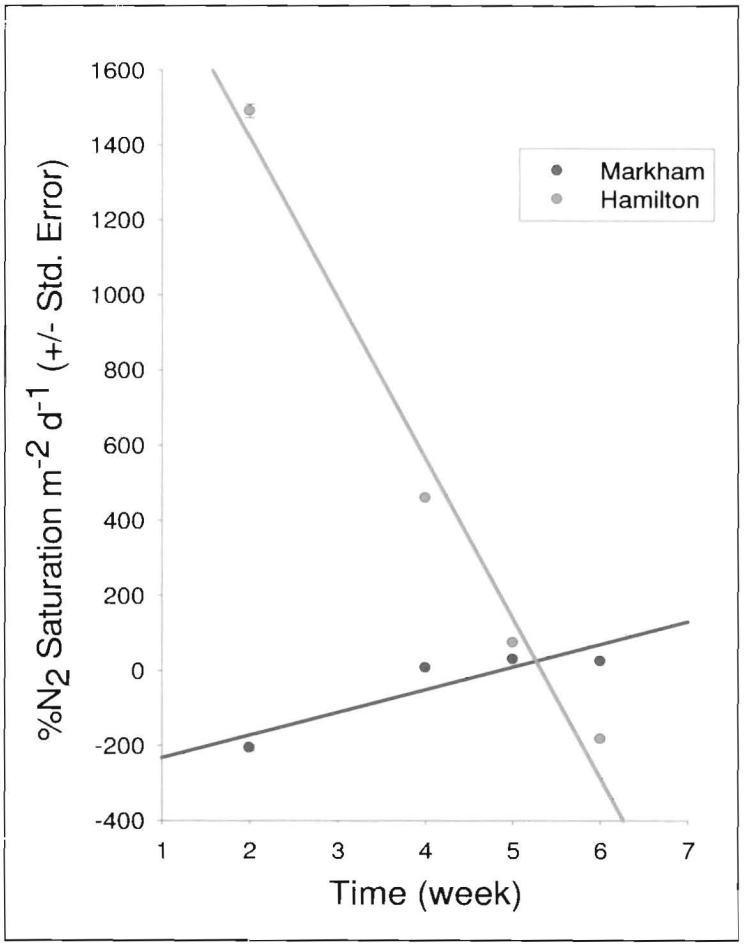

Table 3-14. Mesocosm Inorganic Nitrogen Loss

Table 3-12. Statistical results of repeated measures analysis of variance for dissolved inorganic nitrogen loss from mesocosms

Effect	Test Statistic	Probability
Primary Factors		
Location	$F_{1,14} = 46.60$	0.002
Silica loading	$F_{1,14} = 0.971$	0.380
Phosphorus loading	$F_{1,14} = 0.735$	0.440
Time	$F_{3,12} = 3.025$	0.071
Multivariate Models		
Time x Location	$F_{3,12} = 10.10$	0.001
Time x Silica loading	$F_{3,12} = 1.666$	0.227
Time x Phosphorus loading	$F_{3,12} = 0.962$	0.442

ANOVA model: DIN loss = constant + Location + Si + P + time + time*Si + time*P + time*location + error

3.2.4.5 Silica

The Si:N loading ratio as well as time and location had a signficant effects on dissolved silica concentrations in mesocosms (Table 3-13). All mesocosms showed a general decrease in silica concentration with time. As expected, Si:N loading ratio of 2 consistently resulted in higher silica concentrations than Si:N loading of 0.5. Hamilton mesocosms generally had higher concentrations of silica than Markham mesocosms, and typically Hamilton mesocosms with Si:N loading of 0.5 had higher dissolved silica concentrations than Markham mesocosms with Si:N loading of 2 (Figure 3-16).

Silica loss was also related to Si:N loading ratio (Table 3-14; Figure 3-17). Higher silica loading resulted in a greater rate of silica loss, perhaps by stimulating diatom growth and the silica uptake associated with these microphytes. Diatom-dominated communites would be expected to have high silica uptake. The loss of silica from all mesocosms, regardless of location and nutrient loading regime, may suggest a general movement toward dominance by diatoms in later summer to early autumn. That Markham mesocosms have lower silica may also suggest these mesocosms have generally greater diatom abundance. If this is the case, it might be consistent with hypothesis that a diatom dominated community (Markham) may export less carbon to sediments and have lower denitrification rates than green algae dominated communities (Hamilton), although the results of phytoplankton analysis in support of this is not yet available.

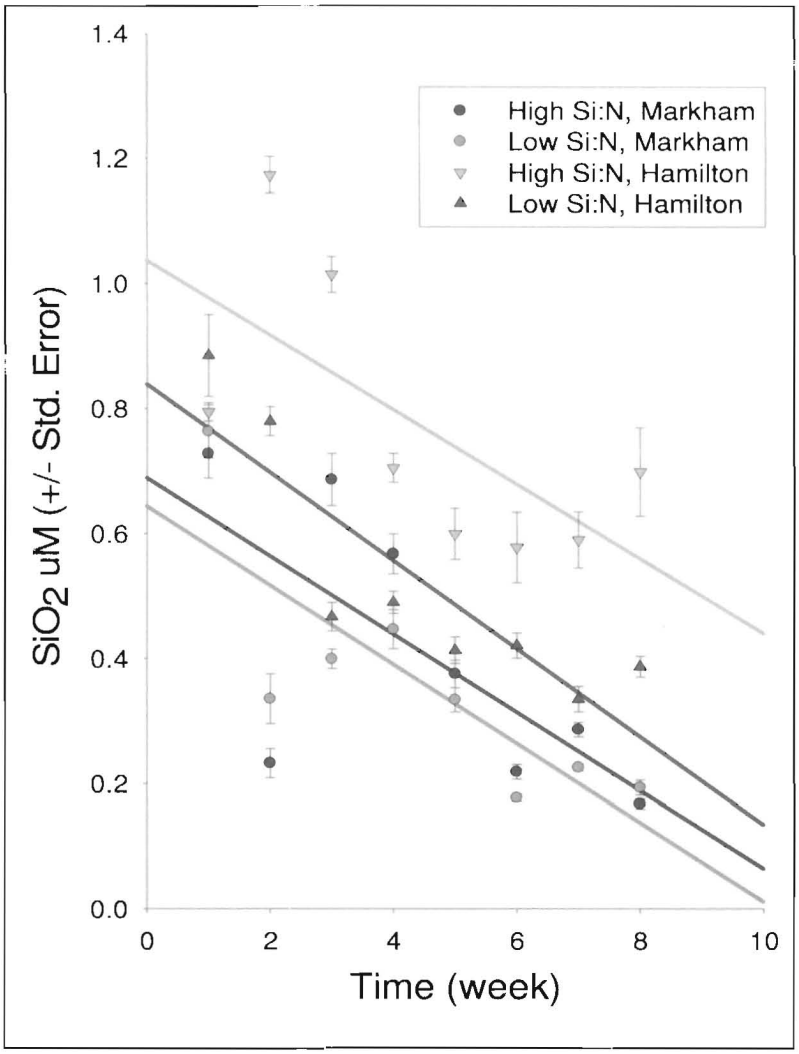

Figure 3-16. Mesocosm Silica

Table 3-13. Statistical results of repeated measures analysis of variance for dissolved silica in mesocosms

Effect	Test Statistic	Probability
Primary Factors		
Location	$F_{1,14} = 25.13$	0.000
Silica loading	$F_{1,14} = 6.270$	0.025
Phosphorus loading	$F_{1,14} = 0.108$	0.747
Time	$F_{7,98} = 20.331$	0.000
Multivariate Models		
Time x Location	$F_{7,98} = 5.997$	0.000
Time x Silica loading	$F_{7,98} = 3.400$	0.007
Time x Phosphorus loading	$F_{7,98} = 0.859$	0.542

ANOVA model: SiO_2 = constant + Location + Si + P + time + time*Si + time*P + time*location + error

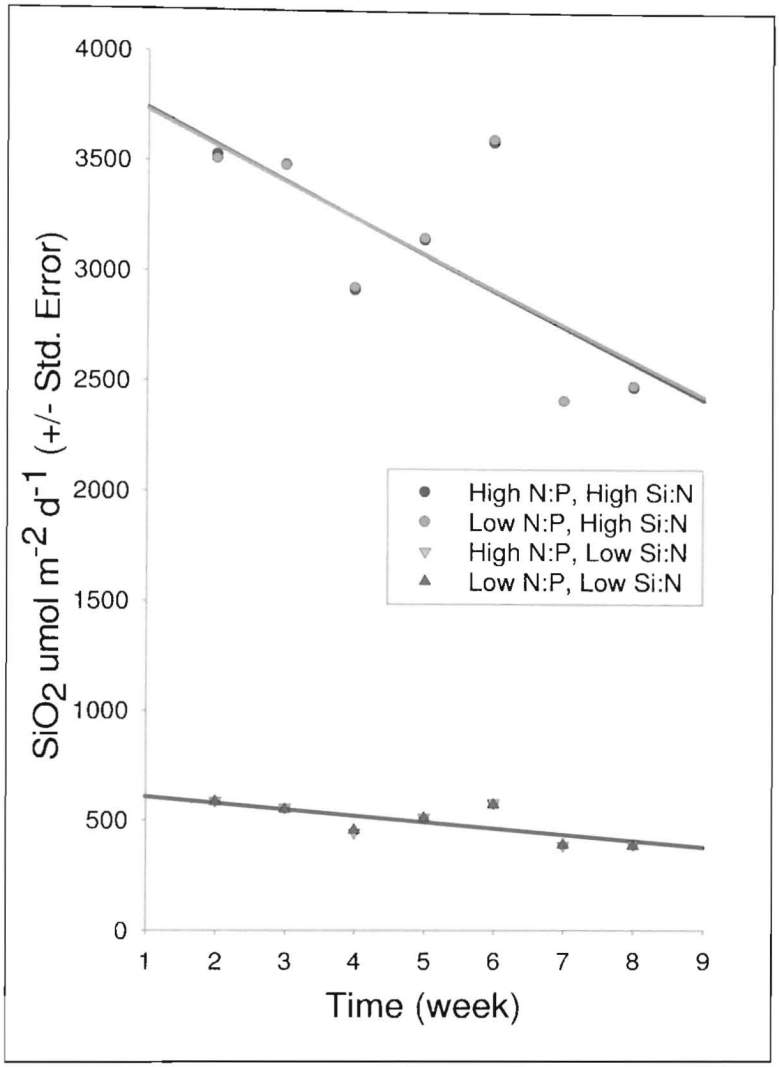

Table 3-17. Mesocosm SiO_2 Loss

Table 3-14. Statistical results of repeated measures analysis of variance for dissolved silica loss from mesocosms

Effect	Test Statistic	Probability
Primary Factors		
Location	$F_{1,14} = 0.000$	0.996
Silica loading	$F_{1,4} = 7476.7$	0.000
Phosphorus loading	$F_{1,14} = 12.985$	0.023
Time	$F_{6,24} = 4.549$	0.003
Multivariate Models		
Time x Location	$F_{6,24} = 0.001$	1.000
Time x Silica loading	$F_{6,24} = 4.750$	0.003
Time x Phosphorus loading	$F_{6,24} = 7.475$	0.000

ANOVA model: SiO_2 loss = constant + Location + Si + P + time + time*Si + time*P + time*location + error

3.2.4.6 Phosphate

Ortho-phosphate concentrations were influenced by location and time according to the ANOVA results (Table 3-15). Hamilton mesocosms had generally higher concentrations of phosphate than Markham mesocosms (Figure 3-18). Phosphate concentrations decreased through time with concentrations in Hamilton mesocosms decreasing at a greater rate than Markham mesocosms. Interestingly, N:P loading ratio had no influence on phosphate concentrations. It should be noted that phosphate concentrations were consistently near the detection limit and patterns should be interpreted cautiously.

ANOVA results showed a significant effect of N:P loading ratio and location on phosphorus loss in mesocosms (Table 3-16). Although P uptake decreased with time at both locations and for both N:P loading ratios, uptake under the low N:P loading regime (i.e. higher P loading) was of greater magnitude as might be expected (Figure 3-19). The decline in P uptake was sharper in Markham mesocosms than in Hamilton mesocosms, perhaps suggesting Markham mesocosms were more rapidly approaching a balance between primary production and remineralization.

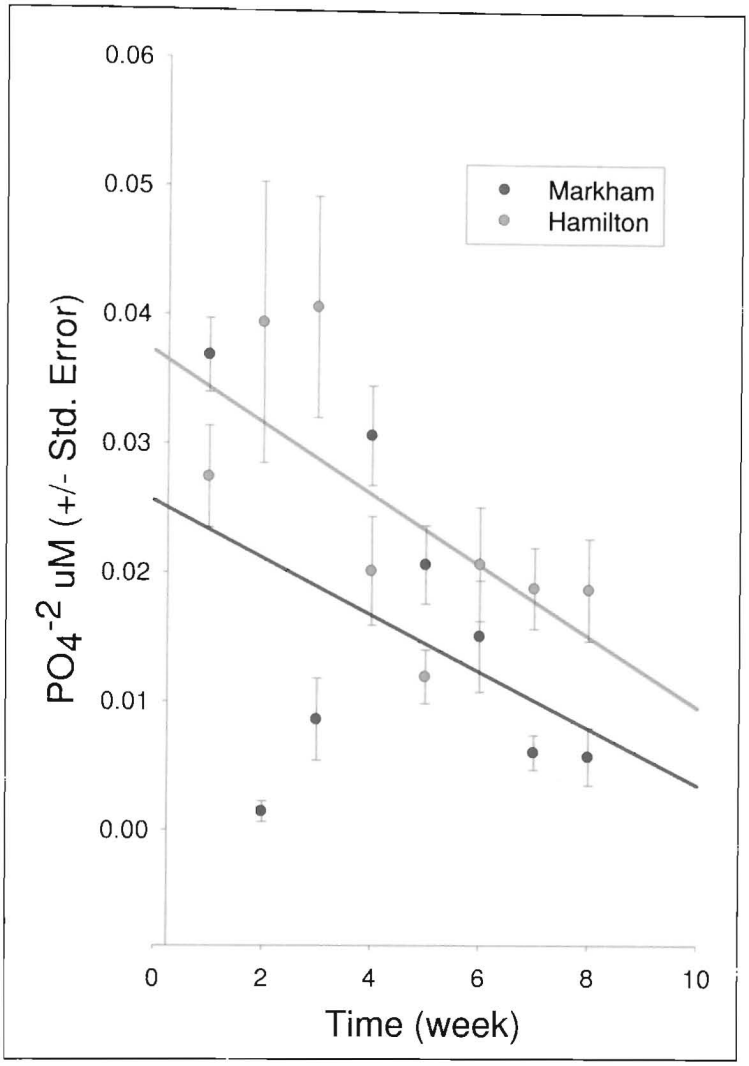

Table 3-18. Mesocosm Phosphorus

Table 3-15. Statistical results of repeated measures analysis of variance for ortho-phosphate in mesocosms

Effect	Test Statistic	Probability
Primary Factors		
Location	$F_{1,16} = 7.013$	0.018
Silica loading	$F_{1,16} = 0.279$	0.604
Phosphorus loading	$F_{1,16} = 0.384$	0.544
Time	$F_{7,112} = 6.042$	0.000
Multivariate Models		
Time x Location	$F_{7,112} = 11.106$	0.000
Time x Silica loading	$F_{7,112} = 1.879$	0.080
Time x Phosphorus loading	$F_{7,112} = 1.538$	0.162

ANOVA model: PO_4^{3-} = constant + Location + Si + P + time + time*Si + time*P + time*location + error

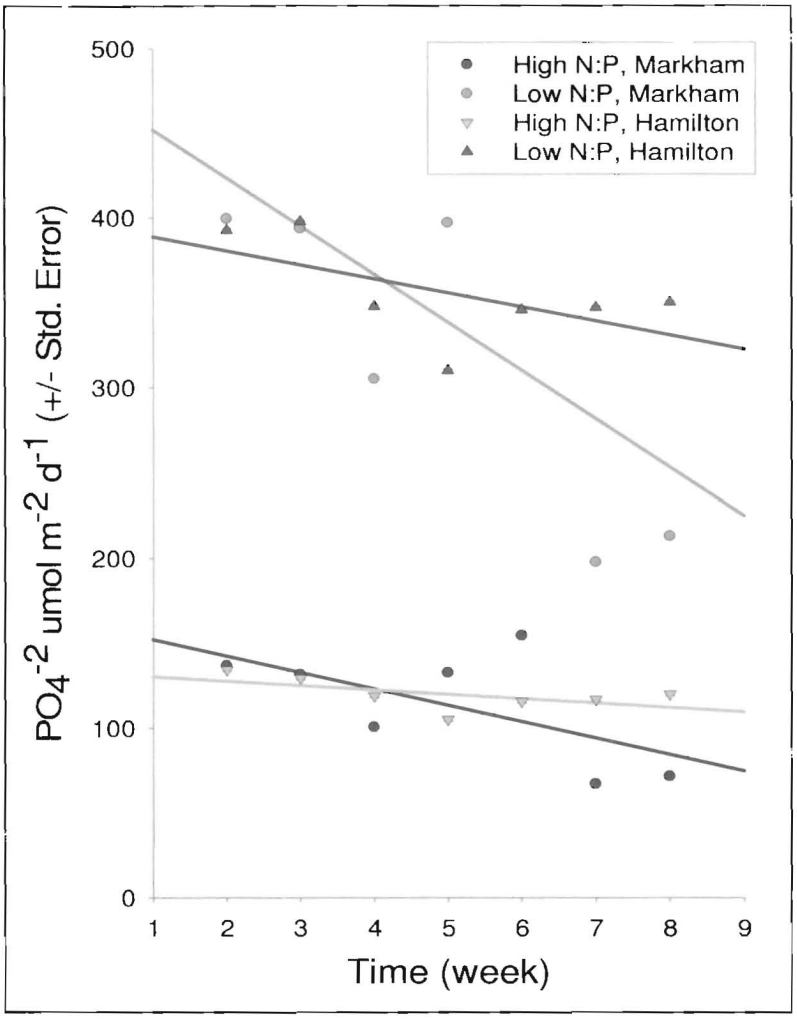

Table 3-19. Mesocosm PO_4^{-2} Loss

Table 3-16. Statistical results of repeated measures analysis of variance for phosphate loss from mesocosms

Effect	Test Statistic	Probability
Primary Factors		
Location	$F_{1,14} = 19.439$	0.012
Silica loading	$F_{1,14} = 0.001$	0.982
Phosphorus loading	$F_{1,14} = 7155.5$	0.000
Time	$F_{7,112} = 9.931$	0.000
Multivariate Models		
Time x Location	$F_{7,112} = 16.261$	0.000
Time x Silica loading	$F_{7,112} = 0.006$	1.000
Time x Phosphorus loading	$F_{7,112} = 4.872$	0.002

ANOVA model: PO_4^{3-} loss = constant + Location + Si + P + time + time*Si + time*P + time*location + error

3.3 Conclusions

3.3.1 Hypothesis 1: An increase in Si relative to Redfield ratio will cause an increase in diatom abundance relative to other photoautotrophs.

Diatom niches may uniquely improve their nutritional uptake of surrounding inorganic nitrogen under high Si:N load, relative to the Redfield ratio. Such an accumulation of silica by diatom frustules would suggest a competitive advantage over other photoautotrophs as silica is essential for diatom division, consequently improving their number and density. On the other hand, lugol counts via light microscopy indicated the contrary as cyanobacteria became the dominate photoautotroph. This may be attributed to the physical constraints of contrasting microbes that may hinder microbe identification; as a result, diatom numbers were underestimated. This would support the use of phytopigment analysis, which would be implemented during succeeding mesocosm sediment analysis, where the results are not yet available. Microcosm nitrous oxide results supported this hypothesis as N_2O increased with increased Si:N load. However, silica load may have induced a greater diatom population in the water column as sediment TOM accumulation declined under the low Si:N nutrient treatment. Mesocosm experiments experienced silica loss between experimental weeks, however, Si load was shown to have no significant difference between trials.

Hypothesis 1a: An increase in diatom abundance relative to other photoautotrophs will result in greater sinking of organic matter to sediment.

While the evidence leading towards a shift in microbial diatom dominance to other photoautotrophs (e.g. cyanobacteria and green algae) may be inconclusive, comparable mesocosm measurements using sediment traps, and organic C analysis of sediments (ash-free dry mass) may prove otherwise. Under similar high Si:N treatments, these mesocosms experienced an increased TOM (sediment organics) and DOC (water column organics) concentration, in association with elevated chlorophyll c (fucoxanthin diatom phytopigment) content (Mandrapilias, 2009).

Hypothesis 1b: An increase in organic matter deposition will increase denitrification.

Mesocosms experienced an incline in percent N_2 saturation within the water column that would indicate an improved denitrification rate throughout experimentation. Hamilton produced a greater denitrification rate (%N_2 saturation) in comparison to Markham mesocosms, which may be directly linked to the benthic region where the periphyton layer is located. However, organic sediment analysis is pending. Analysis of specific dates apart from the averages calculated may yield promising results.

Hypothesis 1c: An increase in organic matter deposition will increase N_2O production and evasion from mesocosms.

Early microcosm experimentation showed evidence that high Si:N, in association with low N:P, results in a greater N_2O production, which would suggest that diatomaceous organic matter settled downwards to support the periphyton layer. However, this was not the case as microcosm TOM decreased with increased Si:N treatment, which would indicate that nitrous oxide production might not have been stimulated by silica-based organics.

On the other hand, the larger scale mesocosms indicated that nutrient treatments showed no significant effects on nitrous oxide production, which could be attributed to the issue of scale, and experimental parameters that adequately represent environmental conditions. Mesocosms are inherently distorted representations of nature. Experimental scale may be an issue, as they are of short duration, subject to reduced biological material and energetic exchange, exposed temporal and spatial variability, simplification of complex physical and biological processes, prone to enclosure effects (large edge effects) which may compromise natural lake system results (Englund & Cooper, 2003; Schindler, 1998). Conversely, mesocosms allow for a greater degree of control, replication and repeatability than whole ecosystems or environmental plots (Kareiva, 1989; Kemp *et. al.*, 1980). Peterson, *et. al.* (2005) explains that there must be functional similarity where experimental conditions, relationships and behaviours are made similar to nature in order to test hypothesis (Petersen & Englund, 2005).

The problem of scale with respect to data collection, either from the microcosm parameters translated to the mesocosm setup, or the setups as a whole extrapolating their

findings to the environment, may be categorized as the microcosm/mesocosm spatial scale relative to their natural counterparts, their reduced temporal scale, and the degree of ecological complexity these containments are capable of simulating. Experimental scale becomes an issue where results become significant (stable) with increasing mesocosm size as variability between trials decreases. However, there is a need to adjust variables (light penetration) influenced by scale since the ratio of edge perimeter to the internal mesocosm area decreases with increasing size (Petersen *et. al.*, 1999). The great strength of these mulitscale setups (microcosm and mesocosm) is that factors, such as nutrient load, may be constant so that specific variables under certain conditions may be directly extrapolated into natural systems without the issue of scaling effects. Peterson and Hastings (2001) and Langhaar (1951) had mentioned that these factors are significant aspects to a dimensional approach to mesocosm design that translates specific attributes of interest to larger environmental conditions. Temporal distortion between microcosm and mesocosm may not be an issue as both were conducted under a 3-month period, nonetheless, this brief period is only a small aspect of conditions lakes experience seasonally year after year.

Yet, intimate biological and physical conditions present in microcosms may not translate well to larger scale mesocosms due to their lower ecological complexity. Mesocosms may undergo depth scale effects that may involve benthic-pelagic coupling (Hargrave, 1973; Oviatt *et. al.*, 1986), primary production productivity (per unit area), and differences in light and gas flux per unit volume according to depth (Petersen *et. al.*, 1997). Due to this complexity, regions of data collection (i.e. N_2O) from different depths within the mesocosm water column may be variable. Whereas, the small scale microcosm

may produce consistent results at depth at the cost of variable results between trials. Consequently, scaling distortion issues concerning the microcosm light source may occur and significantly effect the photoautrophic microphytobenthic organisms (Petersen & Hastings, 2001). For example, mean field-approximations of insignificant spatial or temporal variability (e.g. light intensity, temperature, etc.) were assigned to microcosm setups which may offer a degree of control with lower variability (Petersen *et. al.*, 2003). Under shallow depth and transparent boundaries, microcosms were significantly effect as they were exposed to increased light intensity, elevated sediment light, consistent light exposure, increased benthic-water column interactions, reduced surface-bottom mixing, and increased nutrient delivery to the benthic surface (Petersen *et. al.*, 1997). Chen *et. al.*, (1997, 2000) also mentions that microcosm may experience a high ratio of periphyton layer area to water volume, creating greater sediment metabolic potential as nutrient uptake is also increased. This may encourage microphytobenthic interactions with denitrification via organic contribution, thus stimulating nitrous oxide production.

Since microcosm systems may be less complex, they may not fully represent the full effect of seasonal variability experienced by mesocosms (Petersen *et. al.*, 2003). Opposed to the controlled continuous nutrient delivery within the microcosm setup, the weekly load nutrient renewal in mesocosms may be influenced by variable environmental conditions as nutrients were possibly consumed by phytoplankton that are favoured in larger radius containers (Chen *et. al.*, 2000); subject to sediment burial under cold temperatures; or taken up periphytic organisms along the mesocosm walls (Chen *et. al.*, 1997; Harte *et. al.*, 1980). Nevertheless, mesocosm walls were not cleaned as the influence of wall growth decreases with increasing mesocosm radius (Chen *et. al.*, 1997).

Microcosm wall growth was shown to be minimal. Numerous studies had experienced an increased difficulty in parameter control (i.e. temperature and light regulation) when mesocosm size has increased (Brockmann, 1990; Kemp *et. al.*, 1980; Petersen *et. al.*, 1999; Whittaker, 1961). It would seem that a controlled environment (microcosm) might lead towards a more conclusive distinction between Si:N load and N_2O production than a more turbulent and possible nutrient starved environment that the mesocosm setup may be exposed to.

3.3.2 Hypothesis 2: An increase in P relative to Redfield ratio would result in a relative increase in phytoplanktonic Cyanobacteria.

Cyanobacteria becomes dominate under nutrient restricted conditions (low N:P) as they are able to utilize atmospheric N and saturated N_2 in water via heterocyst structures. However, nitrous oxide yield decreased with decreasing N:P load in the microcosm experiment which was opposed the hypothesis statement. Under low N:P load in microcosms, lugol counts confirmed the abundance of cyanobacteria and decrease of green algae in phytoplankton although numbers may be undervalued as stated earlier. Diatom dominance in phytoplankton may also occur under high N:P and high Si:N, where cyanobacteria become out competed. On the other hand, green algae may proliferate and sink to the benthic region as it becomes dense under high N:P (low Si:N). Similarly to Si load, mesocosm experimentation showed no significant effect of P load among treatment trials.

Hypothesis 2a: An increase in Cyanobacteria abundance relative to other photoautotrophs will result in less sinking of organic matter to sediment.

Microbial characterization and numeration of lugol samples via light microscopy have indicated a direct link with cyanobacteria dominance to low N:P load in the microcosm experiment. Although N:P loading showed no significant effect on phosphate within the larger mesocosm setup, N:P loading ratio and location were influential on water column phosphorus loss. There was a greater P-loss under low N:P than high N:P treatments within both locations (Figure 3-19) which may suggest a stimulated cyanobacteria activity, and a possible circulation of nutrients within its water column niche. This water column cyanobacteria productivity was further supported in the microcosm setup as there was a greater TOC content in the low N:P trial than in the high N:P treatment.

Hypothesis 2b: A decrease in organic matter deposition will decrease denitrification.

Hamilton mesocosm contained a greater TOC quantity within the water column than Markham mesocosms, which may suggest that Hamilton nitrogen saturation rates were generally greater due to an increased organic potential. Similarly to hypothesis 1b, there is a need to analyze sediment organics in order to directly link microbial dominance to nutrient load in order to characterize the events in both the water column and the bethic region.

Hypothesis 2c: A decrease in organic matter deposition will decrease N_2O production.

Cycled water column nutrients by cyanobacteria in mesocosm may suggest a lower organic accumulation from the water column to the sediment, hence a generally lower nitrous oxide concentration. However, there were no direct links between benthic organics endorsed by nutrient loads (N:P and Si:N) with nitrous oxide production as mesocosm N_2O production was not affected by nutrient loading rates, according to ANOVA results (Table 3-8). Instead, N_2O production was a result of denitrification effects that may be seasonally influenced and location dependent.

3.3.3 Further Study

A need to emphasize a direct connection between microbial dominance to nutrient load with respect to the Redfield ratio must be further studied. Analysis of water column and specifically sediment samples through additional phytopigmentation and chlorophyll become significant. Specifically, the HPLC quantification of zeaxanthin (cyanobacteria); lutein and chlorophyll b (green algae); and fucoxanthin and chlorophyll c (diatom) would quantify microbial abundance. Manipulation of temporal data based on nutrient load effects of each week instead of data averages may also yield significant conclusions.

Considering that the coupling of nitrification to denitrification is sensitive to the sediment oxic layer, depth profiles may be conducted in small scale microcosm sediment in order to determine immediate heterotrophic effects on periphyton thickness, oxygen demand, and denitrification rates. Ecosystem effects involving food webs may also define microbial effects on denitrification, as predator prey and competition models may characterize sediment organic disposition, consequently influencing N_2O via denitrification. Variations of the large scale mesocosm approach should also explore aquatic chambers within littoral zones of different eutrophic lakes. This may illustrate environmental effects sensitive to seasonal properties, with an on-going yearly mesocosm setup to historically track seasonal changes. Current biogeochemical analytical techniques and experimental designs are always open for discussion.

4. References

Abeling, U., & Seyfried, C. F. (1992). Anaerobic-aerobic treatment of high-strength ammonium wastewater - nitrogen removal via nitrite. *Water Science and Technology, 26*(5-6), 1007-1015.

Alexander, R. B., Elliott, A. H., Shankar, U., & McBride, G. B. (2002). Estimating the sources and transport of nutrients in the Waikato river basin, New Zealand. *Water Resources Research, 38*(12), 41-423.

Aller, R. C. (1994). Bioturbation and remineralization of sedimentary organic matter: Effects of redox oscillation. *Chemical Geology, 114*(3-4), 331-345.

Anderson, N. J. (2000). Miniview: Diatoms, temperature and climatic change. *European Journal of Phycology, 35*(4), 307-314.

Andersson, M. G. I., Brion, N., & Middelburg, J. J. (2006). Comparison of nitrifier activity versus growth in the Scheldt estuary - A turbid, tidal estuary in northern europe. *Aquatic Microbial Ecology, 42*(2), 149-158.

Arango, C. P., & Tank, J. L. (2008). Land use influences the spatiotemporal controls on nitrification and denitrification in headwater streams. *Journal of the North American Benthological Society, 27*(1), 90-107.

Baek, S. H., Shimode, S., Kim, H., Han, M., & Kikuchi, T. (2009). Strong bottom-up effects on phytoplankton community caused by a rainfall during spring and summer in sagami bay, Japan. *Journal of Marine Systems, 75*(1-2), 253-264.

Baeseman, J. L., Smith, R. L., & Silverstein, J. (2006). Denitrification potential in stream sediments impacted by acid mine drainage: Effects of pH, various electron donors, and iron. *Microb Ecol, 51*(2), 232-241.

Balderston, W. L., Sherr, B., & Payne, W. J. (1976). Blockage by acetylene of nitrous oxide reduction in pseudomonas perfectomarinus. *Applied and Environmental Microbiology, 31*(4), 504-508.

Bergström, A., Blomqvist, P., & Jansson, M. (2005). Effects of atmospheric nitrogen deposition on nutrient limitation and phytoplankton biomass in unproductive Swedish lakes. *Limnology and Oceanography, 50*(3), 987-994.

Bergström, A., & Jansson, M. (2006). Atmospheric nitrogen deposition has caused nitrogen enrichment and eutrophication of lakes in the northern hemisphere. *Global Change Biology, 12*(4), 635-643.

Bernot, M. J., Tank, J. L., Royer, T. V., & David, M. B. (2006). Nutrient uptake in streams draining agricultural catchments of the midwestern united states. *Freshwater Biology, 51*(3), 499-509.

Blackburn, T. H., & Blackburn, N. D. (1993). Coupling of cycles and global significance of sediment diagenesis. *Marine Geology, 113*(1-2), 101-110.

Blackburn, T. H., Blackburn, N. D., Jensen, K., & Risgaard-Petersen, N. (1994). Simulation model of the coupling between nitrification and denitrification in a freshwater sediment. *Applied and Environmental Microbiology, 60*(9), 3089-3095.

Blackburn, T. H., & Henriksen, K. (1983). Nitrogen cycling in different types of sediments from danish waters. *Limnology & Oceanography, 28*(3), 477-493.

Bodelier, P. L. E., Libochant, J. A., Blom, C. W. P. M., & Laanbroek, H. J. (1996). Dynamics of nitrification and denitrification in root-oxygenated sediments and adaptation of ammonia-oxidizing bacteria to low-oxygen or anoxic habitat. *Applied and Environmental Microbiology, 62*(11), 4100-4107.

Bormans, M., & Condie, S. A. (1997). Modelling the distribution of *Anabaena* and melosira in a stratified river weir pool. *Hydrobiologia, 364*(1), 3-13.

Bouwman, A. F., Van Der Hoek, K. W., & Olivier, J. G. J. (1995). Uncertainties in the global source distribution of nitrous oxide. *Journal of Geophysical Research, 100*(D2), 2785-2800.

Brady, N. C., & Weil, R. R. (2002). *The nature and properties of soil* (13th ed.). New Jersey: Prentice Hall.

Bratbak, G. (1987). Carbon flow in an experimental microbial ecosystem. *Mar.Ecol.Prog.Ser., 36*, 267-276.

Britton, N. F., & Timm, U. (1993). Effects of competition and shading in planktonic communities. *J.Math.Biol., 31*, 655-673.

Brooks, A. S., & Edgington, D. N. (1994). Biogeochemical control of phosphorus cycling and primary production in lake michigan. *Limnology and Oceanography, 39*(4), 961-968.

Brzezinski, M. A. (1985). The Si:C:N ratio of marine diatoms: Interspecific variability and the effect of some environmental variables. *Journal of Phycology, 21*, 347-357.

Bulgakov, N. G., & Levich, A. P. (1999). The nitrogen: Phosphorus ratio as a factor regulating phytoplankton community structure. *Archiv Fur Hydrobiologie, 146*(1), 3-22.

Burgin, A. J., & Hamilton, S. K. (2007). Have we overemphasized the role of denitrification in aquatic ecosystems? A review of nitrate removal pathways. *Frontiers in Ecology and the Environment, 5*(2), 89-96.

Bykova, O., Laursen, A., Bostan, V., Bautista, J., & McCarthy, L. (2006). Do zebra mussels (*Dreissena polymorpha*) alter lake water chemistry in a way that favours *Microcystis* growth? *Science of the Total Environment, 371*(1-3), 362-372.

Canfield, D. E., Kristensen, E., & Thamdrup, B. (2005). *Marine biology: Aquatic geomicrobiology*. California: Elsevier Inc.

Carrick, H. J., & Lowe, R. L. (2007). Nutrient limitation of benthic algae in Lake Michigan: The role of silica. *Journal of Phycology, 43*(2), 228-234.

Conley, D. J., Carstensen, J., Vaquer-Sunyer, R., & Duarte, C. M. (2009). Ecosystem thresholds with hypoxia. *Hydrobiologia, 629*(1), 21-29.

Cornwell, J. C., Kemp, W. M., & Kana, T. M. (1999). Denitrification in coastal ecosystems: Methods, environmental controls, and ecosystem level controls, a review. *Aquatic Ecology, 33*(1), 41-54.

Curie, F., Ducharne, A., Sebilo, M., & Bendjoudi, H. (2009). Denitrification in a hyporheic riparian zone controlled by river regulation in the Seine river basin (France). *Hydrological Processes, 23*(5), 655-664.

D'Asaro, E. A. (2008). Convection and the seeding of the north Atlantic bloom. *Journal of Marine Systems, 69*(3-4), 233-237.

Davidson, E. A., Chorover, J., & Dail, D. B. (2003). A mechanism of abiotic immobilization of nitrate in forest ecosystems: The ferrous wheel hypothesis. *Global Change Biology, 9*(2), 228-236.

De Bie, M. J. M., Middelburg, J. J., Starink, M., & Laanbroek, H. J. (2002). Factors controlling nitrous oxide at the microbial community and estuarine scale. *Marine Ecology Progress Series, 240*, 1-9.

De Wilde, H. P. J., & De Bie, M. J. M. (2000). Nitrous oxide in the schelde estuary: Production by nitrification and emission to the atmosphere. *Marine Chemistry, 69*(3-4), 203-216.

DeDuve, C. (1991). *Blueprint for a cell: The nature and origin of life*. Burlington, N.C.: Neil Patterson Publishers.

DeLong, E. F., & Karl, D. M. (2005). Genomic perspectives in microbial oceanography. *Nature, 437*(7057), 336-342.

Delwiche, C. C. (1981). The nitrogen cycle and nitrous oxide. *Denitrification, nitrification, and atmospheric nitrous oxide.* New York: Wiley.

DeSimone, L. A., & Howes, B. L. (1998). Nitrogen transport and transformations in a shallow aquifer receiving wastewater discharge: A mass balance approach. *Water Resources Research, 34*(2), 271-285.

Dolan, D. M., & McGunagle, K. P. (2005). Lake Erie total phosphorus loading analysis and update: 1996-2002. *Journal of Great Lakes Research, 31*(SUPPL. 2), 11-22.

Dong, L. F., Nedwell, D. B., & Stott, A. (2006). Sources of nitrogen used for denitrification and nitrous oxide formation in sediments of the hypernutrified colne, the nutrified humber, and the oligotrophic conwy estuaries, United Kingdom. *Limnology and Oceanography, 51*(1 II), 545-557.

Duff, J. H., Tesoriero, A. J., Richardson, W. B., Strauss, E. A., & Munn, M. D. (2008). Whole-stream response to nitrate loading in three streams draining agricultural landscapes. *Journal of Environmental Quality, 37*(3), 1133-1144.

Durkin, C. A., Mock, T., & Armbrust, E. V. (2009). Chitin in diatoms and its association with the cell wall. *Eukaryotic Cell, 8*(7), 1038-1050.

Ebert, U., Arrayás, M., Temme, N., Sommeijer, B., & Huisman, J. (2001). Critical conditions for phytoplankton blooms. *Bulletin of Mathematical Biology, 63*(6), 1095-1124.

Eyre, B. D., & Ferguson, A. J. P. (2002). Comparison of carbon production and decomposition, benthic nutrient fluxes and denitrification in seagrass, phytoplankton, benthic microalgae and macroalgae dominated warm temperate Australian lagoons. *Marine Ecology Progress Series, 229*, 43-59.

Fanning, J. C. (2000). The chemical reduction of nitrate in aqueous solution. *Coordination Chemistry Reviews, 199*(1), 159-179.

Farías, L. (2003). Remineralization and accumulation of organic carbon and nitrogen in marine sediments of eutrophic bays: The case of the bay of concepcion, Chile. *Estuarine, Coastal and Shelf Science, 57*(5-6), 829-841.

Fennel, K., & Boss, E. (2003). Subsurface maxima of phytoplankton and chlorophyll: Steady-state solutions from a simple model. *Limnology and Oceanography, 48*(4), 1521-1534.

Fernández, M. L., Estrin, D. A., & Bari, S. E. (2008). Theoretical insight into the hydroxylamine oxidoreductase mechanism. *Journal of Inorganic Biochemistry, 102*(7), 1523-1530.

Filstrup, C. T., Scott, J. T., & Lind, O. T. (2009). Allochthonous organic matter supplements and sediment transport in a polymictic reservoir determined using elemental and isotopic ratios. *Biogeochemistry, 96*(1), 87-100.

Focht, D. D., & Verstraete, W. (1977). Biochemical ecology of nitrification and denitrification. *Advances in Microbial Ecology, 1*, 135-214.

Foree, E. G., & McCarty, P. L. (1970). Anaerobic decomposition of algae. *Environmental Science and Technology, 4*(10), 842-849.

Fortunato, C. S., Carlini, D. B., Ewers, E., & Bushaw-Newton, K. L. (2009). Nitrifier and denitrifier molecular operational taxonomic unit compositions from sites of a freshwater estuary of Chesapeake Bay. *Canadian Journal of Microbiology, 55*(3), 333-346.

Fransz, H. G., & Verhagen, J. H. G. (1985). Modeling research on the production cycle of phytoplankton in the southern bight of the North Sea in relation to riverborne nutrient load. *Netherlands Journal of Sea Research, 19*(3-4), 241-250.

Freney, J.R., Ivanov, M.V., and Rodnhe, H. (1983). Gaseous loss of nitrogen from plant-soil systems. Dr. W. Junk Publishers.

Froelich, P. N., Klinkhammer, G. P., Bender, M. L., Luedtke, N. A., Heath, G. R., Cullen, D., Dauphin, P., Hammond, D., Hartman, B., & Maynard, V. (1979). Early oxidation of organic matter in pelagic sediments of the eastern equatorial Atlantic: Suboxic diagenesis. *Geochimica Et Cosmochimica Acta, 43*(7), 1075-1090.

Galloway, J. N., Schlesinger, W. H., Levy II, H., Michaels, A., & Schnoor, J. L. (1995). Nitrogen fixation: Anthropogenic enhancement-environmental response. *Global Biogeochemical Cycles, 9*(2), 235-252.

Gälman, V., Rydberg, J., De-Luna, S. S., Bindler, R., & Renberg, I. (2008). Carbon and nitrogen loss rates during aging of lake sediment: Changes over 27 years studied in varved lake sediment. *Limnology and Oceanography, 53*(3), 1076-1082.

Garnier, J., & Billen, G. (2007). Production vs. respiration in river systems: An indicator of an "ecological status". *Science of the Total Environment, 375*(1-3), 110-124.

Goering, J. J., & Dugale, V. A. (1966). Estimates of the rates of denitrification in a Subarctic lake. *Limnol.Oceanogr., 11*, 113-116.

Goreau, T. J., Kaplan, W. A., & Wofsy, S. C. (1980). Production of NO_2^- and N_2O by nitrifying bacteria at reduced concentrations of oxygen. *Applied and Environmental Microbiology, 40*(3), 526-532.

Granger, J., & Ward, B. B. (2003). Accumulation of nitrogen oxides in copper-limited cultures of denitrifying bacteria. *Limnology and Oceanography, 48*(1 I), 313-318.

Granhall, U., & Lundgren, A. (1971). Nitrogen fixation in Lake Erken. *Limnol.Oceanogr., 16*, 711-719.

Groffman, P. M., Altabet, M. A., Böhlke, J. K., Butterbach-Bahl, K., David, M. B., Firestone, M. K., Giblin, A. E., Kana, T. M., Nielsen, L. P., & Voytek, M. A. (2006). Methods for measuring denitrification: Diverse approaches to a difficult problem. *Ecological Applications, 16*(6), 2091-2122.

Guillard, R. R. L., & Kilham, P. (1977). The ecology of marine planktonic diatoms. *The Biology of Diatoms,* 372-469.

Hainz, R., Wöber, C., & Schagerl, M. (2009). The relationship between spirogyra (*zygnematophyceae, streptophyta*) filament type groups and environmental conditions in central europe. *Aquatic Botany, 91*(3), 173-180.

Hall, B. D., Dutton, G. S., & Elkins, J. W. (2007). The NOAA nitrous oxide standard scale for atmospheric observations. *Journal of Geophysical Research D: Atmospheres, 112*(9)

Hansen, K., & Kristensen, E. (1998). The impact of the polychaete nereis diversicolor and enrichment with macroalgal (*Chaetomorpha linum*) detritus on benthic metabolism and nutrient dynamics in organic-poor and organic-rich sediment. *Journal of Experimental Marine Biology and Ecology, 231*(2), 201-223.

Harrison, J. A., Maranger, R. J., Alexander, R. B., Giblin, A. E., Jacinthe, P. -., Mayorga, E., Seitzinger, S. P., Sobota, D. J., & Wollheim, W. M. (2008). The regional and global significance of nitrogen removal in lakes and reservoirs. *Biogeochemistry,* 1-15.

Hartog, N., van Bergen, P. F., de Leeuw, J. W., & Griffioen, J. (2004). Reactivity of organic matter in aquifer sediments: Geological and geochemical controls. *Geochimica Et Cosmochimica Acta, 68*(6), 1281-1292.

Heggie, D. T., Logan, G. A., Smith, C. S., Fredericks, D. J., & Palmer, D. (2008). Biogeochemical processes at the sediment–water interface, bombah broadwater, Myall lakes. *Hydrobiologia, 608*(1), 49-67.

Hem, J. D. (1985). Study and Interpreation of the Chemical Characteristics of Natural water.

Henriksen, K., & Kemp, W. M. (1988). Nitrification in estuarine and coastal marine sediments. *Nitrogen Cycling in Coastal Marine Environments,* 207-249.

Hodell, D. A., & Schelske, C. L. (1998). Production, sedimentation, and isotopic composition of organic matter in Lake Ontario. *Limnology and Oceanography, 43*(2), 200-214.

Holmer, M., & Storkholm, P. (2001). Sulphate reduction and sulphur cycling in lake sediments: A review. *Freshwater Biology, 46*(4), 431-451.

Holt, L. M. (2007). The Ecological Effects of Land-Applying Municipal Biosolids on Nitrogen-Fixing Bacteria, Ryerson University. Masters Thesis.

Hopfensperger, K. N., Kaushal, S. S., Findlay, S. E. G., & Cornwell, J. C. (2009). Influence of plant communities on denitrification in a tidal freshwater marsh of the Potomac river, united states. *Journal of Environmental Quality, 38*(2), 618-626.

Horne, A. J., & Commins, M. L. (1987). Macronutrient controls on nitrogen fixation in planktonic cyanobacterial populations. *New Zealand Journal of Marine & Freshwater Research, 21*(3), 413-423.

Hoshaw, R. W., & McCourt, R. M. (1988). The *zygnemataceae* (chlorophyta): A twenty-year update of research. *Phycologia, 27*, 511-548.

Howard, J. B., & Rees, D. C. (1996). Structural basis of biological nitrogen fixation. *Chemical Reviews, 96*(7), 2965-2982.

Howarth, R. W., & Marino, R. (2006). Nitrogen as the limiting nutrient for eutrophication in coastal marine ecosystems: Evolving views over three decades. *Limnology and Oceanography, 51*(1 II), 364-376.

Howe, R. L., Rees, A. P., & Widdicombe, S. (2004). The impact of two species of bioturbating shrimp (*Callianassa subterranea* and *Upogebia deltaura*) on sediment denitrification. *Journal of the Marine Biological Association of the United Kingdom, 84*(3), 629-632.

Hulth, S., Aller, R. C., & Gilbert, F. (1999). Coupled anoxic nitrification/manganese reduction in marine sediments. *Geochimica Et Cosmochimica Acta, 63*(1), 49-66.

Igarashi, R. Y., & Seefeldt, L. C. (2003). Nitrogen fixation: The mechanism of the mo-dependent nitrogenase. *Critical Reviews in Biochemistry and Molecular Biology, 38*(4), 351-384.

Ishida, C. K., Arnon, S., Peterson, C. G., Kelly, J. J., & Gray, K. A. (2008). Influence of algal community structure on denitrification rates in periphyton cultivated on artificial substrata. *Microbial Ecology, 56*(1), 140-152.

Ishikawa, K., Kumagai, M., Nakano, S., & Nakahara, H. (1999). The influence of wind on the horizontal distribution of bloom-forming cyanobacteria in Akanoi Bay, Lake Biwa. *Japanese Journal of Limnology, 60*(4), 531-538.

Jacinthe, P., Groffman, P. M., & Gold, A. J. (2003). Dissolved organic carbon dynamics in a riparian aquifer: Effects of hydrology and nitrate enrichment. *Journal of Environmental Quality, 32*(4), 1365-1374.

Jahnke, R. A., & Jahnke, D. B. (2000). Rates of C, N, P and Si recycling and denitrification at the US mid-Atlantic continental slope depocenter. *Deep Sea Research Part I: Oceanographic Research Papers, 47*(8), 1405-1428.

James, W. F., Richardson, W. B., & Soballe, D. M. (2008). Contribution of sediment fluxes and transformations to the summer nitrogen budget of an upper Mississippi river backwater system. *Hydrobiologia, 598*(1), 95-107.

Jenkins, M. C., & Kemp, W. M. (1984). The coupling of nitrification and denitrification in two estuarine sediments. *Limnol.Oceanogr., 29*(3), 609-619.

Jensen, K., Sloth, N. P., Risgaard-Petersen, N., Rysgaard, S., & Revsbech, N. P. (1994). Estimation of nitrification and denitrification from microprofiles of oxygen and nitrate in model sediment systems. *Applied and Environmental Microbiology, 60*(6), 2094-2100.

Jewell, W. J., & McCarty, P. L. (1971). Aerobic decomposition of algae. *Environmental Science and Technology, 5*(10), 1023-1031.

Jordan, M. A., Welsh, D. T., Dunn, R. J. K., & Teasdale, P. R. (2009). Influence of trypaea australiensis population density on benthic metabolism and nitrogen dynamics in sandy estuarine sediment: A mesocosm simulation. *Journal of Sea Research, 61*(3), 144-152.

Jørgensen, K. S., Jensen, H. B., & Sørensen, J. (1984). Nitrous oxide production from nitrification and denitrification in marine sediment at low oxygen concentrations. *Can J Microbiol, 30*, 1073-1078.

Jørgensen, P. R., Urup, J., Helstrup, T., Jensen, M. B., Eiland, F., & Vinther, F. P. (2004). Transport and reduction of nitrate in clayey till underneath forest and arable land. *Journal of Contaminant Hydrology, 73*(1-4), 207-226.

Joye, S. B., & Hollibaugh, J. T. (1995). *Influence of sulfide inhibition of nitrification on nitrogen regeneration in sediments*

Justic, D., Rabalais, N. N., Turner, R. E., & Dortch, Q. (1995). Changes in nutrient structure of river-dominated coastal waters: Stoichiometric nutrient balance and its consequences. *Estuarine, Coastal and Shelf Science, 40*(3), 339.

Kana, T. M., Darkangelo, C., Oldham, J. B., Bennett, G. E., & Cornwell, J. C. (1994). Membrane inlet mass spectrometer for rapid high-precision determination of N_2, O_2, and are in environmental water samples. *Analytical Chemistry, 66*(23), 4166-4170.

Kana, T. M., Sullivan, M. B., Cornwell, J. C., & Groszkowski, K. M. (1998). Denitrification in estuarine sediments determined by membrane inlet mass spectrometry. *Limnology and Oceanography, 43*(2), 334-339.

Karl, D. M. (2007). The marine phosphorus cycle. In C. J. Hurst, R. L. Crawford, J. L. Garland, D. A. Lipson, A. L. Mills & L. D. Stetzenbach (Eds.), *Manual of environmental microbiology* (3rd ed.,). Washington, D.C.: ASM Press.

Karlson, K. (2007). Diurnal bioturbating activities of monoporeia affinis: Effects on benthic oxygen and nutrient fluxes. *Marine Ecology Progress Series, 331*, 195-205.

Kemp, W. M., Sampou, P., Caffrey, J., Mayer, M., Henriksen, K., & Boynton, W. R. (1990). Ammonium recycling versus denitrification in Chesapeake bay sediments. *Limnology & Oceanography, 35*(7), 1545-1563.

Kester, R. A., De Boer, W., & Laanbroek, H. J. (1997). Production of NO and N_2O by pure cultures of nitrifying and denitrifying bacteria during changes in aeration. *Applied and Environmental Microbiology, 63*(10), 3872-3877.

Khalil, M. A. K., & Rasmussen, R. A. (1992). The global sources of nitrous oxide. *Journal of Geophysical Research, 97*(D13), 14,651-14,660.

Kim, H. J., Graham, D. W., DiSpirito, A. A., Alterman, M. A., Galeva, N., Larive, C. K., Asunskis, D., & Sherwood, P. M. A. (2004). Methanobactin, a copper-acquisition compound from methane-oxidizing bacteria. *Science, 305*(5690), 1612-1615.

Kinsman, R., Ibelings, B. W., & Walsby, A. E. (1991). Gas vesicle collapse by turgor pressure and its role in buoyancy regulation by anabaena flos-aquae. *Journal of General Microbiology, 137*(5), 1171-1178.

Klump, J. V., Fitzgerald, S. A., & Waplesa, J. T. (2009). Benthic biogeochemical cycling, nutrient stoichiometry, and carbon and nitrogen mass balances in a eutrophic freshwater bay. *Limnology and Oceanography, 54*(3), 692-712.

Kociolek, J. P. (2005). A checklist and preliminary bibliography of the recent, freshwater diatoms of inlands environments of teh continental united states. *Proceedings of the California Academy of Sciences, 56*(27), 395-525.

Koho, K. A., Langezaal, A. M., van Lith, Y. A., Duijnstee, I. A. P., & van der Zwaan, G. J. (2008). The influence of a simulated diatom bloom on deep-sea benthic

foraminifera and the activity of bacteria: A mesocosm study. *Deep-Sea Research Part I: Oceanographic Research Papers, 55*(5), 696-719.

Kolokolnikov, T., Ou, C., & Yuan, Y. (2009). Phytoplankton depth profiles and their transitions near the critical sinking velocity. *Journal of Mathematical Biology, 59*(1), 105-122.

Korom, S. F. (1992). Natural denitrification in the saturated zone: A review. *Water Resources Research, 28*(6), 1657-1668.

Krause-Jensen, D., Christensen, P. B., & Rysgaard, S. (1999). Oxygen and nutrient dynamics within mats of the filamentous macroalga chaetomorpha linum. *Estuaries, 22*(1), 31-38.

Krishnan, K. P., & Loka Bharathi, P. A. (2009). Organic carbon and iron modulate nitrification rates in mangrove swamps of Goa, south west coast of india. *Estuarine, Coastal and Shelf Science, 84*(3), 419-426.

Laanbroek, H. J., Bodelier, P. L. E., & Gerards, S. (1994). Oxygen consumption kinetics of nitrosomonas europaea and nitrobacter hamburgensis grown in mixed continuous cultures at different oxygen concentrations. *Archives of Microbiology, 161*(2), 156-162.

Laursen, A. E., & Seitzinger, S. P. (2002). The role of denitrification in nitrogen removal and carbon mineralization in mid-atlantic bight sediments. *Continental Shelf Research, 22*(9), 1397-1416.

Lavery, P. S., & McComb, A. J. (1991). Macroalgal-sediment nutrient interactions and their importance to macroalgal nutrition in a eutrophic estuary. *Estuarine, Coastal and Shelf Science, 32*(3), 281-295.

Lavery, P. S., Oldham, C. E., & Ghisalberti, M. (2001). The use of fick's first law for predicting porewater nutrient fluxes under diffusive conditions. *Hydrological Processes, 15*(13), 2435-2451.

Lawson, D. R. (1988). The nitrogen species methods comparison study: An overview. *Atmospheric Environment (1967), 22*(8), 1517.

Lehmann, M. F., Bernasconi, S. M., Barbieri, A., & McKenzie, J. A. (2002). Preservation of organic matter and alteration of its carbon and nitrogen isotope composition during simulated and in situ early sedimentary diagenesis. *Geochimica Et Cosmochimica Acta, 66*(20), 3573-3584.

Levine, S. N., & Schindler, D. W. (1999). Influence of nitrogen to phosphorus supply

ratios and physicochemical conditions on cyanobacteria and phytoplankton species composition in the experimental lakes area, Canada. *Canadian Journal of Fisheries and Aquatic Sciences, 56*(3), 451-466.

Lewin, J. C. (1955). Silicon metabolism in diatoms. II. sources of silicon for growth of navicula pelliculosa. *Plant Physiol, 30*, 129-134.

Liikanen, A., Flojt, L., & Martikainen, P. (2002). Gas dynamics in eutrophic lake sediments affected by oxygen, nitrate, and sulfate. *Journal of Environmental Quality [H.W.Wilson - AST], 31*(1), 338.

Liikanen, A., & Martikainen, P. J. (2003). Effect of ammonium and oxygen on methane and nitrous oxide fluxes across sediment–water interface in a eutrophic lake. *Chemosphere, 52*(8), 1287-1293.

Liukkonen, M., Kairesalo, T., & Keto, J. (1993). Eutrophication and recovery of lake vesijarvi (South Finland): Diatom frustules in varved sediments over a 30-yr period. *Hydrobiologia, 269-270*, 415-426.

Logan, J. A. (1985). Tropospheric ozone: Seasonal behavior, trends, and anthropogenic influence. *Journal of Geophysical Research, 90*(D6), 10463-10482.

Lorenzen, J., Larsen, L. H., Klær, T., & Revsbech, N. (1998). Biosensor determination of the microscale distribution of nitrate, nitrate assimilation, nitrification, and denitrification in a diatom- inhabited freshwater sediment. *Applied and Environmental Microbiology, 64*(9), 3264-3269.

Ludwig, W., Dumont, E., Meybeck, M., & Heussner, S. (2009). River discharges of water and nutrients to the mediterranean and black sea: Major drivers for ecosystem changes during past and future decades? *Progress in Oceanography, 80*(3-4), 199-217.

Lundholm, N., Hansen, P. J., & Kotaki, Y. (2004). Effect of pH on growth and domoic acid production by potentially toxic diatoms of the genera pseudo-*Nitzschia* and *Nitzschia. Marine Ecology Progress Series, 273*, 1-15.

Machefert, S. E., Dise, N. B., Goulding, K. W. T., & Whitehead, P. G. (2002). Nitrous oxide emission from a range of land uses across Europe. *Hydrology and Earth System Sciences, 6*(3), 325-337.

Mandrailias, D. (2009) Effects of Community Composition and Elemental Loading Ratios on Lake Sediment Chemical Characteristics. Ryerson University, Undergraduate Thesis Project.

Martin, L. A., Mulholland, P. J., Webster, J. R., & Valett, H. M. (2001). Denitrification potential in sediments of headwater streams in the southern Appalachian mountains, USA. *Journal of the North American Benthological Society, 20*(4), 505-519.

Masukawa, H., Inoue, K., & Sakurai, H. (2007). Effects of disruption of homocitrate synthase genes on nostoc sp. strain PCC 7120 photobiological hydrogen production and nitrogenase. *Applied and Environmental Microbiology, 73*(23), 7562-7570.

McCarthy, M. J., Lavrentyev, P. J., Yang, L., Zhang, L., Chen, Y., Qin, B., & Gardner, W. S. (2007). Nitrogen dynamics and microbial food web structure during a summer cyanobacterial bloom in a subtropical, shallow, well-mixed, eutrophic lake (lake Taihu, China). *Hydrobiologia, 581*(1), 195-207.

McGucken, W. (2000). *Lake Erie Rehabilitated: Controlling Cultural Eutrophication,* 1960s-11990.

Megmw, S. R., & Knowles, R. (1987). Active methanotrophs suppress nitrification in a humisol. *Biology and Fertility of Soils, 4*(4), 205-212.

Mengis, M., Gachter, R., & Wehrli, B. (1996). Nitrous oxide emissions to the atmosphere from an artificially oxygenated lake. *Limnology and Oceanography, 41*(3), 548-553.

Mengis, M., Gächter, R., Wehrli, B., & Bernasconi, S. (1997). Nitrogen elimination in two deep eutrophic lakes. *Limnology and Oceanography, 42*(7), 1530-1543.

Mermillod-Blondin, F., Gaudet, J., Gerino, M., Desrosiers, G., Jose, J., & Creuzé Des Châtelliers, M. (2004). Relative influence of bioturbation and predation on organic matter processing in river sediments: A microcosm experiment. *Freshwater Biology, 49*(7), 895-912.

Mermillod-Blondin, F., Lemoine, D., Boisson, J., Malet, E., & Montuelle, B. (2008). Relative influences of submersed macrophytes and bioturbating fauna on biogeochemical processes and microbial activities in freshwater sediments. *Freshwater Biology, 53*(10), 1969-1982.

Meyer, R. L., Allen, D. E., & Schmidt, S. (2008). Nitrification and denitrification as sources of sediment nitrous oxide production: A microsensor approach. *Marine Chemistry, 110*(1-2), 68-76.

Meyer, R. L., Kjaer, T., & Revsbech, N. P. (2001). Use of NOx^- microsensors to estimate the activity of sediment nitrification and NOx^- consumption along an estuarine salinity, nitrate, and light gradient. *Aquatic Microbial Ecology, 26*, 181-193.

Miranda, J., Balachandran, K. K., Ramesh, R., & Wafar, M. (2008). Nitrification in Kochi backwaters. *Estuarine, Coastal and Shelf Science, 78*(2), 291-300.

Moore, R. M., Punshon, S., Mahaffey, C., & Karl, D. (2009). The relationship between dissolved hydrogen and nitrogen fixation in ocean waters. *Deep-Sea Research Part I: Oceanographic Research Papers, 56*(9), 1449-1458.

Morton, S. C., Glindemann, D., Wang, X., Niu, X., & Edwards, M. (2005). Analysis of reduced phosphorus in samples of environmental interest. *Environmental Science and Technology, 39*(12), 4369-4376.

Moos, M. T., Laird, K. R., & Cumming, B. F. (2009). Climate-related eutrophication of a small boreal lake in northwestern ontario: A palaeolimnological perspective. *Holocene, 19*(3), 359-367.

Naqvi, S. W. A., Jayakumar, D. A., Narvekar, P. V., Naik, H., Sarma, V. V. S. S., D'Souza, W., Joseph, S., & George, M. D. (2000). Increased marine production of N_2O due to intensifying anoxia on the Indian continental shelf. *Nature, 408*(6810), 346-349.

Nielsen, L. P. (1992). Denitrification in sediment determined from nitrogen isotope pairing. *FEMS Microbiology Ecology, 86*(4), 357-362.

Nishio, T., Koike, I., & Hattori, A. (1982). Dentrification, nitrate reduction, and oxygen consumption in coastal and estuarine sediments. *Applied and Environmental Microbiology, 43*(3), 648-653.

Nishio, T., Koike, I., & Hattori, A. (1983). Estimates of denitrification and nitrification in coastal and estuarine sediments. *Appl.Environ.Microbiol., 45*(2), 444-450.

Nowicki, B. L. (1994). The effect of temperature, oxygen, salinity, and nutrient enrichment on estuarine denitrification rates measured with a modified nitrogen gas flux technique. *Estuarine, Coastal and Shelf Science, 38*(2), 137-156.

Nriagu, J. O., & Moore, P. B. (1984). *Phosphate minerals*. New York: Springer-Verlag.

Ottley, C. J., Davison, W., & Edmunds, W. M. (1997). Chemical catalysis of nitrate reduction by Iron(II). *Geochimica Et Cosmochimica Acta, 61*(9), 1819-1828.

Owens, N. J. P., & Stewart, W. D. P. (1983). Enteromorpha and the cycling of nitrogen in a small estuary. *Estuarine, Coastal and Shelf Science, 17*(3), 287-296.

Passell, H. D., Dahm, C. N., & Bedrick, E. J. (2007). Ammonia modeling for assessing potential toxicity to fish species in the Rio Grande, 1989-2002. *Ecological Applications, 17*(7), 2087-2099.

Peperzak, L., Colijn, F., Koeman, R., Gieskes, W. W. C., & Joordens, J. C. A. (2003). Phytoplankton sinking rates in the rhine region of freshwater influence. *Journal of Plankton Research, 25*(4), 365-383.

Petersen, J. E., & Hastings, A. (2001). Dimensional approaches to scaling experimental ecosystems: Designing mousetraps to catch elephants. *American Naturalist, 157*(3), 324-333.

Petersen, J. E., Kemp, W. M., Bartleson, R., Boynton, W. R., Chen, C., Cornwell, J. C., Gardner, R. H., Hinkle, D. C., Houde, E. D., Malone, T. C., Mowitt, W. R., Murray, L., Sanford, L. P., Stevenson, J. C., Sundberg, K. L., & Suttles, S. E. (2003). Multiscale experiments in coastal ecology: Improving realism and advancing theory. *Bioscience, 53*(12), 1181-1197.

Pfenning, K. S., & McMahon, P. B. (1997). Effect of nitrate, organic carbon, and temperature on potential denitrification rates in nitrate-rich riverbed sediments. *Journal of Hydrology, 187*(3-4), 283-295.

Porter, E. T., Owens, M. S., & Cornwell, J. C. (2006). Effect of sediment manipulation on the biogeochemistry of experimental sediment systems. *Journal of Coastal Research, 22*(6), 1539-1551.

Poughon, L., Dussap, C., & Gros, J. (2001). Energy model and metabolic flux analysis for autotrophic nitrifiers. *Biotechnology and Bioengineering, 72*(4), 416-433.

Présing, M., Herodek, S., Preston, T., & Vörös, L. (2001). Nitrogen uptake and the importance of internal nitrogen loading in lake balaton. *Freshwater Biology, 46*(1), 125-139.

Quigg, A., Finkel, Z. V., Irwin, A. J., Rosenthal, Y., Ho, T., Reinfelder, J. R., Schofield, O., Morel, F. M. M., & Falkowski, P. G. (2003). The evolutionary inheritance of elemental stoichiometry in marine phytoplankton. *Nature, 425*(6955), 291-294.

Rabalais, N. N., Turner, R. E., Justić, D., Dortch, Q., Wiseman, W. J., & Sen Gupta, B. K. (2000). Gulf of Mexico biological system responses to nutrient changes in the mississippi river. *Estuarine Science,* 241-268.

Ragueneau, O., Chauvaud, L., Moriceau, B., Leynaert, A., Thouzeau, G., Donval, A., Le Loc'h, F., & Jean, F. (2005). Biodeposition by an invasive suspension feeder impacts the biogeochemical cycle of si in a coastal ecosystem (bay of Brest, France). *Biogeochemistry, 75*(1), 19-41.

Ragueneau, O., Lancelot, C., Egorov, V., Vervlimmeren, J., Cociasu, A., Déliat, G., Krastev, A., Daoud, N., Rousseau, V., Popovitchev, V., Brion, N., Popa, L., & Cauwet, G. (2002). Biogeochemical transformations of inorganic nutrients in the mixing zone between the Danube river and the North-Western Black Sea. *Estuarine, Coastal and Shelf Science, 54*(3), 321-336.

Ragueneau, O., Varela, E. D., Treguer, P., Queguiner, B., & Delamo, Y. (1994). Phytoplankton dynamics in relation to the biogeochemical cycle of silicon in a coastal ecosystem of western europe. *Marine Ecology Progress Series, 106*(1-2), 157-172.

Ravishankara, A. R., Daniel, J. S., & Portmann, R. W. (2009). Nitrous oxide (N_2O): The dominant ozone-depleting substance emitted in the 21st century. *Science,* doi:10.1126/science.1176985

Redfield, A. C. (1934). On the proportion of organic derivations in sea water and their relation to the composition of plankton. R. J. Daniel (Ed.), University Press of Liverpool. pg. 177-192.

Redfield, A. C. (1958). The biological control of chemical factors in the environment. am. sci. *The Biological Control of Chemical Factors in the Environment,* 205-221.

Rees, D. C., & Howard, J. B. (2000). Nitrogenase: Standing at the crossroads. *Current Opinion in Chemical Biology, 4*(5), 559-566.

Revsbech, N. P., Jorgensen, B. B., & Blackburn, T. H. (1980). Oxygen in the sea bottom measured with a microelectrode. *Science, 207,* 1355-1356.

Risgaard-Petersen, N., Rysgaard, S., Nielsen, L. P., & Revsbech, N. P. (1994). Diurnal variation of denitrification and nitrification in sediments colonized by benthic microphytes. *Limnology and Oceanography, 39*(3), 573-579.

Risgaard-Petersen, N. (2003). Coupled nitrification-denitrification in autotrophic and heterotrophic estuarine sediments: On the influence of benthic microalgae. *Limnology and Oceanography, 48*(1, Part 1), 93-105.

Rivett, M. O., Buss, S. R., Morgan, P., Smith, J. W. N., & Bemment, C. D. (2008). Nitrate attenuation in groundwater: A review of biogeochemical controlling processes. *Water Research, 42*(16), 4215-4232.

Rockwell, D. C., Warren, G. J., Bertram, P. E., Salisbury, D. K., & Burns, N. M. (2005). The U.S. EPA Lake Erie indicators monitoring program 1983-2002: Trends in phosphorus, silica, and chlorophyll a in the central basin. *Journal of Great Lakes Research, 31*(SUPPL. 2), 23-34.

Routh, J., Choudhary, P., Meyers, P. A., & Kumar, B. (2008). A sediment record of recent nutrient loading and trophic state change in Lake Norrviken, sweden. *Journal of Paleolimnology,* , 1-17.

Royer, T. V., Tank, J. L., & David, M. B. (2004). Transport and fate of nitrate in headwater agricultural streams in Illinois. *Journal of Environmental Quality, 33*(4), 1296-1304.

Rust, C. M., Aelion, C. M., & Flora, J. R. V. (2000). Control of pH during denitrification in subsurface sediment microcosms using encapsulated phosphate buffer. *Water Research, 34*(5), 1447-1454.

Rysgaard, S., Christensen, P. B., & Nielsen, L. P. (1995). Seasonal variation in nitrification and denitrification in estuarine sediment colonized by benthic microalgae and bioturbating infauna. *Marine Ecology Progress Series, 126*(1-3), 111-121.

Rysgaard, S., Risgaard-Petersen, N., Sloth, N. P., Jensen, K., & Nielsen, L. P. (1994). Oxygen regulation of nitrification and denitrification in sediments. *Limnology and Oceanography, 39*(7), 1643-1652.

Sabumon, P. C. (2009). Effect of potential electron acceptors on anoxic ammonia oxidation in the presence of organic carbon. *Journal of Hazardous Materials, 172*(1), 280-288.

Schelske, C. L. (1985). Biogeochemical silica mass balances in Lake Michigan and Lake Superior. *Biogeochemistry, 1*(3), 197-218.

Schelske, C. L. (1988). Historic trends in Lake Michigan silica concentrations. *Internationale Revue Der Gesamten Hydrobiologie, 73*(5), 559-591.

Schelske, C. L., Conley, D. J., Stoermer, E. F., Newberry, T. L., & Campbell, C. D. (1986). Biogenic silica and phosphorus accumulation in sediments as indices of eutrophication in the Laurentian great lakes. *Hydrobiologia, 143*(1), 79-86.

Schelske, C. L., Stoermer, E. F., & Kenney, W. F. (2006). Historic low-level phosphorus enrichment in the great lakes inferred from biogenic silica accumulation in sediments. *Limnology and Oceanography, 51*(1 II), 728-748.

Schindler, D. W., Hecky, R. E., Findlay, D. L., Stainton, M. P., Parker, B. R., Paterson, M. J., Beaty, K. G., Lyng, M., & Kasian, S. E. M. (2008). Eutrophication of lakes cannot be controlled by reducing nitrogen input: Results of a 37-year whole-ecosystem experiment. *Proceedings of the National Academy of Sciences of the United States of America, 105*(32), 11254-11258.

Schmidt, I., Sliekers, O., Schmid, M., Bock, E., Fuerst, J., Kuenen, J. G., Jetten, M. S. M., & Strous, M. (2003). New concepts of microbial treatment processes for the nitrogen removal in wastewater. *FEMS Microbiology Reviews, 27*(4), 481-492.

Scott, J. T., McCarthy, M. J., Gardner, W. S., & Doyle, R. D. (2008). Denitrification, dissimilatory nitrate reduction to ammonium, and nitrogen fixation along a nitrate concentration gradient in a created freshwater wetland. *Biogeochemistry, 87*(1), 99-111.

Seitzinger, S., Harrison, J. A., Böhlke, J. K., Bouwman, A. F., Lowrance, R., Peterson, B., Tobias, C., & Van Drecht, G. (2006). Denitrification across landscapes and waterscapes: A synthesis. *Ecological Applications, 16*(6), 2064-2090.

Seitzinger, S. P. (1988). Denitrification in freshwater and coastal marine ecosystems: Ecological and geochemical significance. *Limnology & Oceanography, 33*(4), 702-724.

Seitzinger, S. P., & Kroeze, C. (1998). Global distribution of nitrous oxide production and N inputs in freshwater and coastal marine ecosystems. *Global Biogeochemical Cycles, 12*(1), 93-113.

Seitzinger, S. P., Kroeze, C., & Styles, R. V. (2000). Global distribution of N_2O emissions from aquatic systems: Natural emissions and anthropogenic effects. *Chemosphere - Global Change Science, 2*(3-4), 267-279.

Seitzinger, S. P., Nielsen, L. P., Caffrey, J., & Christensen, P. B. (1993). Denitrification measurements in aquatic sediments: A comparison of three methods. *Biogeochemistry, 23*(3), 147-167.

Seitzinger, S. P., Pilson, M. E. Q., & Nixon, S. W. (1983). Nitrous oxide production in nearshore marine sediments. *Science, 222*(4629), 1244-1246.

Seitzinger, S. P., & Nixon, S. W. (1985). Eutrophication and the rate of denitrification and N_2O production in coastal marine sediments. *Limnology and Oceanography, 30*(6), 1332-1339.

Shimadzu Corporation (2001) Process & Environmental Instrumentation Division, Kyoto, Japan

Shigesada, N., & Okubo, A. (1981). Analysis of the self-shading effect on algal vertical distribution in natural waters. *Journal of Mathematical Biology, 12*(3), 311-326.

Silvennoinen, H., Liikanen, A., Torssonen, J., Stange, C. F., & Martikainen, P. J. (2008). Denitrification and N_2O effluxes in the Bothnian Bay (Northern Baltic Sea) river sediments as affected by temperature under different oxygen concentrations. *Biogeochemistry, 88*(1), 63-72.

Simons, J. (1994). Field ecology of freshwater macroalgae in pools and ditches, with special attention to eutrophication. *Netherlands Journal of Aquatic Ecology, 28*(1), 25-33.

Skadsen, J. (2002). Effectiveness of high pH in controlling nitrification. *Journal / American Water Works Association, 94*(7), 73-83.

Smayda, T. J. (1970). The suspension and sinking of phytoplankton in the sea. *Oceanography and Marine Biology Annual Review, 8*, 353-414.

Smil, V. (1997). Global population and the nitrogen cycle. *Scient. Am.*, 76-81.

Smith, R. E. H., Parrish, C. C., Depew, D. C., & Ghadouani, A. (2007). Spatial patterns of seston concentration and biochemical composition between nearshore and offshore waters of a great lake. *Freshwater Biology, 52*(11), 2196-2210.

Smith, V. H. (1985). Predictive Models for the Biomass of Blue-Green Algae in Lakes. *Water Resources Bulletin, 21*(3), 433-439.

Sommer, U., & Stabel, H. (1983). Silicon consumption and population density changes of dominant planktonic diatoms in Lake Constance. *Journal of Ecology, 71*(1), 119-130.

Spooner, D. R., & Maher, W. (2009). Benthic sediment composition and nutrient cycling in an intermittently closed and open lake lagoon. *Journal of Marine Systems, 75*(1-2), 33-45.

Stein, J. R. (1973). Culture methods and growth measurements. *Handbook of Phycological Methods,* 448.

Strohm, T. O., Griffin, B., Zumft, W. G., & Schink, B. (2007). Growth yields in bacterial denitrification and nitrate ammonification. *Applied and Environmental Microbiology, 73*(5), 1420-1424.

Sugimoto, R., Kasai, A., Miyajima, T., & Fujita, K. (2008). Nitrogen isotopic discrimination by water column nitrification in a shallow coastal environment. *Journal of Oceanography, 64*(1), 39-48.

Sutka, R. L., Ostrom, N. E., Ostrom, P. H., Breznak, J. A., Gandhi, H., Pitt, A. J., & Li, F. (2006). Distinguishing nitrous oxide production from nitrification and denitrification on the basis of isotopomer abundances. *Applied and Environmental Microbiology, 72*(1), 638-644.

Svensson, J. M. (1998). Emission of N2O, nitrification and denitrification in a eutrophic lake sediment bioturbated by chironomus plumosus. *Aquatic Microbial Ecology, 14*(3), 289-299.

Svensson, J. M., Enrich-Prast, A., & Leonardson, L. (2001). Nitrification and denitrification in a eutrophic lake sediment bioturbated by oligochaetes. *Aquatic Microbial Ecology, 23*(2), 177-186.

Tesoriero, A. J., Liebscher, H., & Cox, S. E. (2000). Mechanism and rate of denitrification in an agricultural watershed: Electron and mass balance along groundwater flow paths. *Water Resources Research, 36*(6), 1545-1559.

Thamatrakoln, K., & Hildebrand, M. (2008). Silicon uptake in diatoms revisited: A model for saturable and nonsaturable uptake kinetics and the role of silicon transporters. *Plant Physiology, 146*(3), 1397-1407.

Thomas, R. L. (1981). Sediments of the North American Great lakes. *Verb.Internat.Verein.Limnol., 21*, 1666-1680.

Tiedje, J. M. (1988). Ecology of denitrification and dissimilatory nitrate reduction to ammonium. In A. J. B. Zhender (Ed.), *In biology of anaerobic microorganisms* () Wiley-Liss.

Tiedje, J. M., Sexstone, A. J., Myrold, D. D., & Robinson, J. A. (1983). Denitrification: Ecological niches, competition and survival. *Antonie Van Leeuwenhoek, 48*(6), 569-583.

Tõnno, I., & Nõges, T. (2003). Nitrogen fixation in a large shallow lake: Rates and initiation conditions. *Hydrobiologia, 490*, 23-30.

Turner, R. E., & Rabalais, N. N. (1994). Coastal eutrophication near the Mississippi river delta. *Nature, 368*(6472), 619-621.

Twining, B. S., Mylon, S. E., & Benoit, G. (2007). Potential role of copper availability in nitrous oxide accumulation in a temperate lake. *Limnology and Oceanography, 52*(4), 1354-1366.

Umrath, K. (1941). Über die ausbreitung der durch verwundung bedingten viskositätsverminderung bei spirogyra. *Protoplasma, 36*(1), 410-413.

Van der Linden, M. J. H. A. (1989). Release of sedimentary nitrogen and phosphorus in polder ditches of a low-moor peat area. *Hydrobiological Bulletin, 23*(2), 125-134.

Van Donka, E., Hessen, D. O., Verschoor, A. M., & Gulati, R. D. (2008). Re-oligotrophication by phosphorus reduction and effects on seston quality in lakes. *Limnologica, 38*(3-4), 189-202.

Vrede, T., Ballantyne, A., Mille-Lindblom, C., Algesten, G., Gudasz, C., Lindahl, S., & Brunberg, A. K. (2009). Effects of N:P loading ratios on phytoplankton community composition, primary production and N fixation in a eutrophic lake. *Freshwater Biology, 54*(2), 331-344.

Wang, S., Liu, C., Yeager, K. M., Wan, G., Li, J., Tao, F., Lŭ, Y., Liu, F., & Fan, C. (2009). The spatial distribution and emission of nitrous oxide (N_2O) in a large eutrophic lake in eastern China: Anthropogenic effects. *Science of the Total Environment, 407*(10), 3330-3337.

Ward, B. B., Olson, R. J., & Perry, M. J. (1982). Microbial nitrification rates in the primary nitrite maximum off Southern California. *Deep Sea Research Part A, Oceanographic Research Papers, 29*(2), 247-255.

Weathers, P. J. (1984). N_2O evolution by green algae. *Applied and Environmental Microbiology, 48*(6), 1251-1253.

Welsh, D. T. (2003). It's a dirty job but someone has to do it: The role of marine benthic macrofauna in organic matter turnover and nutrient recycling to the water column. *Chemistry & Ecology, 19*(5), 321-342.

Wetzel, R. G. (1983). *Limnology* (2nd ed.). Philadelphia: Saunders College.

Wilhelm, C., Büchel, C., Fisahn, J., Goss, R., Jakob, T., LaRoche, J., Lavaud, J., Lohr, M., Riebesell, U., Stehfest, K., Valentin, K., & Kroth, P. G. (2006). The regulation of carbon and nutrient assimilation in diatoms is significantly different from green algae. *Protist, 157*(2), 91-124.

Woodruff, S. L., House, W. A., Callow, M. E., & Leadbeater, B. S. C. (1999). The effects of biofilms on chemical processes in surficial sediments. *Freshwater Biology, 41*(1), 73-89.

Xia, X., Li, S., & Shen, Z. (2008). Effect of nitrification on nitrogen flux across sediment-water interface. *Water Environment Research, 80*(11), 2175-2182.

Yoh, M., Terai, H., & Saijo, Y. (1983). Accumulation of nitrous oxide in the oxygen deficient layer of freshwater lakes. *Nature, 301*(5898), 327-329.

Zevenboom, W. (1982). N_2-fixing cyanobacteria: Why they do not become dominant in shallow hypertrophic lakes. *Hydrobiological Bulletin, 16*(2-3), 289-290.

Zevenboom, W., De Vaate, A. B., & Mur, L. R. (1982). Assessment of factors limiting growth rate of *Oscillatoria agardhii* in hypertrophic Lake Wolderwijd, 1978, by use of physiological indicators. *Limnol.Oceanogr., 27*, 39-52.

Zhou, S. (2007). Stoichiometry of biological nitrogen transformations in wetlands and other ecosystems. *Biotechnology Journal, 2*(4), 497-507.

Zumft, W. G. (1997). Cell biology and molecular basis of denitrification? *Microbiology and Molecular Biology Reviews, 61*(4), 533-616.

Appendix A. Microcosm/Mescosm Analysis

Part A: Nutrient Assay Analysis

1. Ammonium

1.1 Reagent Preparation

Reagent preparation involves making a phenol solution (diluting 11.1ml liquefied phenol (89%) with 95% v/v ethyl alcohol to 100ml), 0.5% w/v sodium nitroprusside solution (diluting 0.5g sodium nitroprusside in 100ml water), and oxidizing solution. The oxidizing solution is made by initially dissolving 200g trisodium citrate and 10g sodium hydroxide to 1L. A phenol/sodium nitroprusside combination was used instead. By taking 80ml of this mixture to 20ml sodium hypochlorite (commercial bleach), the final oxidizing reagent was formed. Sample standards were made by dissolving 3.189g anhydrous NH_4Cl (1.22mg/ml) in 1L water (Greenberg *et. al.*, 1999; Solarzano, 1969). There were 4 standards (i.e. 0.25ml, 0.75ml, 1.25ml, 2.50ml stock dissolved with 25ml water) made including a water blank. In cases where samples or standards were too concentrated, the highest standard concentration was diluted before incrementing the standard curve concentrations. For example, all the samples from the mesocosm were too concentrated. A second dilution series was made from the most concentrated standard of the first dilution series.

1.2 Sample Analysis

Frozen water samples were thawed and 5ml water samples measured in screw capped test tubes. For each sample, 0.4ml phenol/sodium nitroprusside solution and then 1ml oxidizing solution were immediately added. Samples were allowed an hour up to 24 hours to develop under low light conditions at room temperature (22 °C to 27°C). UV-Vis spectrometer analysis at 640nm was carried out on all samples (Greenberg *et. al.*, 1999).

2. Nitrate

2.1 Cadmium Column Construction

The cadmium column was constructed from a steel cylinder with dimensions length 18.5 cm and a 3.5mm diameter. Both cylinder bolt ends were fitted with steel wool to prevent Cu-Cd granule leak and plastic aquarium tube adapters to connect to external setup. Preliminary washing of stock Cu-Cd granule was conducted by rinsing 20g of granules with 6N HCl followed by Millipore water. The secondary wash involved a rinse with 50ml 2% $CuSO_4$ (5g $CuSO_45H_2O$ diluted to 250ml water) for at least 5 minutes or until blue colour partially fades. Successive 50ml 2% $CuSO_4$ washings were repeated until a brown colloidal precipitate was formed. A gentle water wash was followed afterwards to remove all precipitated Cu. Granule packing was set up by placing the column setup (column end with bolt fitting down and the open cylinder end up) in a plastic tube filled with buffer (13g NH_4Cl and 1.7g disodium ethylenediamine tetraacetate dissolved in 1L with 8.5 pH adjustment with concentrated NH_4OH before dilution) (Methods for chemical analysis of water and wastes.1979; Greenberg *et. al.*, 1999; Wood *et. al.*, 1967).

About 5-10 granules intervals were placed in the column opening and pushed down using a metal rod. Due to the granule varying sizes and rigid form, numerous granules at one time may prematurely clog the column. It is essential that the column be immersed in the buffer at all times ensuring that there is a buffer head space a few millimetres above the opening for an easy granule decent and to allow air bubbles to escape. The column is capped tight with the bolt ending when the granules are level with the column mouth ensuring that the buffer level will also immerse the bolt ending. Column is stored in the same tube with dilute buffer (300ml buffer mixed with 500ml water) and positioned standing up in the fridge.

In the circumstance of column leaks, sample collection is based on a final 6.5ml total second sample collection as it is the volume of two cuvette volumes (i.e. first volume for rinse, second volume for sample reading). With this column, 13ml total sample was collected where 6.5ml taken as for analysis. Due to the constant transfer of the peristaltic pump tube from sample to sample, minute air bubbles may gather internally. This is rectified by shaking the tube to gather all the air bubbles and reverse flow the column into a beaker of buffer making sure that the column is immersed in buffer within the plastic storage container.

2.2 Sample Preparation/Column Operation

Upon column use, it was hooked to a peristaltic pump with buffer filled tubes. Air bubbles were prevented from entering the initial column/pump hook-up by connecting the pump tubes while the column is still stored in its buffer. The storage tube can be removed when there are no air bubbles coming from column as the pump reverse pumps

buffer from the column to an empty vessel. The empty vessel is replaced with a 200ml diluted buffer solution where it is forward pumped into the column. The column becomes activated for experimentation when a 100ml mixture volume of 25% 1.0mg/L nitrate standard and 75% buffer solution ran through the column. Nitrate standards were prepared by drying KNO_3 in an oven at 105°C for at least 24 hours before use. Nitrate standards were made daily by weighing out 0.18045g dry KNO_3 (100ug/ml) and diluting to 250ml with water. By collecting 25ml from this stock, and then diluting it to 250ml with water would produce a 10.0ug/ml. From this stock, 5 standards were produced (i.e. 0.05 mg/L, 0.1 mg/L, 0.2 mg/L, 0.5 mg/L, 1.0 mg/L) including a blank which was Millipore water. Samples were prepared using 25ml screw cap test tubes, 2 test tubes (i.e. sample test tube and collection test tube) for every one sample. The sample test tube consisted of 15ml buffer and 5ml sample. Whereas, the collection test tubes remained empty (Methods for chemical analysis of water and wastes, 1979; Greenberg *et. al.*, 1999; Wood *et. al.*, 1967).

Samples were processed through the Cd column at a rate of 0.043ml/s. After column activation, sample collection was performed by discarding the first 10ml and then collecting the second 10ml. The second collection is subjected to a colour reagent at a ratio of 0.260ml for every 6.5ml sample immediately after collection. This colour reagent is made by dissolving 1.0g sulphanilamide with 80ml water and 10ml 85% phosphoric acid. Once the solid has been dissolved, 0.1g N-(1-naphthyl)-ethylenediamine dihydrochloride is added where the whole solution is diluted with water to 100ml. considering that this solution is light sensitive, the container was wrapped with aluminium foil and kept in a dark compartment when in use. A pink colour development

will mature after 10 minutes and will over develop if the samples are not analyzed before 2 hours. A UV-Vis spectrometer is used to identify the colour development at 543nm (Methods for chemical analysis of water and wastes, 1979; Greenberg *et. al.*, 1999; Wood *et. al.*, 1967).

3. Phosphorus

3.1 Reagent Preparation

The volume reagent combination was determined by the number of samples being analyzed. This combination was made as a series of additions in this order: 50ml 5N H_2SO_4, 5ml potassium antimonyl tartrate solution (1.3715g $K(SbO)C_4H_4O6$ $_{1/2}H_2O$ dissolved in 400ml and diluted to 500ml with water), 15ml ammonium molybdate solution (4g $(NH_4)6Mo_7O_{24}$ $4H_2O$ dissolved in 100ml water), and 30ml ascorbic acid solution (1.76g ascorbic acid dissolved in 100ml water, stored in the fridge) (Edwards *et. al.*, 1965; Greenberg *et. al.*, 1999; Murphy & Riley, 1962).

3.2 Sample Preparation

Frozen samples were thawed and measured at 5ml into each screw capped test tube. Phosphorus standards were created by dissolving 219.5mg anhydrous KH_2PO_4 (50.0 µg/ml PO_4^{-3}) in 1L water and taking 1.25ml to dilute to 25ml, a 2.50µg/ml stock phosphate solution was created. A standard series of 4 concentrations and a water blank was used. A 0.8ml reagent combination was added to each sample and mixed thoroughly. This was analyzed under the UV-Vis spectrometer at 880nm ensuring that samples were read between 10min and 30min.(Edwards *et. al.*, 1965; Greenberg *et. al.*, 1999; Murphy

& Riley, 1962). In cases where samples or standards were too concentrated, the highest standard concentration was diluted before incrementing the standard curve concentrations. For example, all the samples from the mesocosm were too concentrated. A second dilution series was made from the most concentrated standard of the first dilution series.

4. Silica

Silica standards were made fresh from the dilution of stock solution (4.73g Na_2SiO_3 $9H_2O$ dissolved in 1L water). There were 4 standards made with a water blank. Frozen samples were prepared by placing 5ml of each sample in individual screw cap test tubes when they were uniformly thawed. Upon analysis, 0.1ml diluted HCl (2:1) and 0.2ml ammonium molybdate were added rapidly and in succession. After mixing and a 5 to 10 minute resting time, 0.2ml oxalic acid was added and mixed thoroughly. From 2 to 15 minutes, the samples turned shades of yellow and were measured under the UV-Vis spectrometer at 410nm (Eaton *et. al.*, 1995; Greenberg *et. al.*, 1999).

Part B: Gas Analysis

1. N_2O GC/MS

Gas chromatography mass spectrometry (GC/MS) initially ran a $^{15}N_2$ gas blank (100µl $^{15}N_2$ purged in a vial) at set parameters. The blank along with subsequent samples were manually injected into the GC/MS via a glass 100µl glass gastight syringe. Injection preparation for each sample injection consisted of drawing ambient air and emptying the syringe. Then the syringe is inserted into the rubber septum of the sample vial where 100µl is drawn in and emptied into the room. Re-insertion of the syringe into the vial

follows with a drawn in 90µl gas which is pumped back into the vial twice (2 pumps). While still in the inserted in the vial, the syringe will draw in 80µl and then down to 50µl. At this time, the syringe should be placed vertically over the injector port once the pre-run program on the GCMS is at the 0.1 seconds countdown, in order to prevent gas sample loss. With a swift controlled manner the syringe should be directed into the injector port once the LCD monitor indicates "READY", and injection proceeds immediately by pushing the syringe barrel downwards. With the same swift motion, the whole syringe apparatus should be lifted vertically up to prevent the syringe from bending, and where the "RUN" button is pushed immediately after to active the sample sequence. After the sample run, the chromatogram is selected by selecting "mass" and 30 <Enter> (Holt, 2007).

Part C: Phytopigment Analysis (Denmark)

According to Schluter, *et. al.* (2000) water samples would be initially stored in liquid nitrogen after being filtered onto GF/F filters. Upon analysis, filters were thawed and placed in 3ml 100% acetone (resultant 90% acetone estimation), sonication on ice for 10 minutes, and extracted at 4 °C for 24 hours. The contents (cells and filter) were filtered using 0.2 µm Teflon syringe filters and disposable syringes. HPLC vials were filled with 1 ml of the resultant sample and 0.3ml HPLC grade water. These samples were injected into a Shimadzu LC-10A HPLC system according to methodology described by Wright *et. al.*, (1991). This HPLC system would be calibrated using pigment standards provided from The International Agency for ^{14}C Determination, VKI, Horsholm, Denmark (Schlüter & Havskum, 1997; Schlüter *et. al.*, 2000).

Part D: Algal Nutrient Stock Solution (CHU-10)

1. CHU-10 Reagent Preparation

Sterile technique is involved with reagent use. Pipets, reagent bottles, and glassware were autoclaved before use. The following reagents were prepared first before CHU-10 formula was made.

1.1. Reagent Preparation

1.1.1 Fe-EDTA

A 1L volume of distilled water was boiled to remove carbon dioxide and dissolve Fe-substrate. This warm water (about 90% volume) initially dissolved 5.2g EDTA in a 1L volumetric flask. After EDTA had been dissolved, 5.4g $KHCO_3$ and 5.0g $FeSO_4 \cdot 7H_2O$ were added. Venting periodically once every few minutes must be performed as pressure may build inside. Adding 1ml/L into the CHU-10 stock will give a final Fe concentration of 1mg/ml. May need to shake before use as Fe may precipitate out of solution. Other substitutes may be used and were defined in the original recipe.

1.1.2. Trace Metals

Metals should be mixed and completely dissolved individually in order of the list below as precipitation may occur. Reagents are dissolved in a 1L volumetric flask.

Reagents

Na_2 EDTA	1.00g
H_3BO_3	2.86g
$MnCl_2 \cdot 4H_2O$	1.81g
$ZnSO_4 \cdot 7H_2O$	0.222g
Na MoO4$\cdot 5H_2O$	0.390g
$CuSO_4 \cdot 5H_2O$	0.079g
$Co(NO_3)_2 \cdot 6H_2O$	0.0494g

1.1.3. F/2 Vitamin

Requires a small reagent volume to manufacture. The reagents were measured and diluted with a smallest available volumetric flask. For every 1ml stock F/2 vitamin made, the reagents were measured as follows:

Vitamin B_{12} (pharmaceutical vitamin used, may be filtered before use)	1mg/ml
Biotin	0.1mg/ml
Thiamin HCl	200mg/L

2. CHU-10 Stock Solution

Stock Solution was mixed in following order:

Reagents	Conc.	ml/L
$Na_2SiO_3 \cdot 9H_2O$	5.8 g/L	10ml
$Ca(NO_3)_2\ 4H_2O$	57.56 g/L	1ml
K_2HPO_4	10 g/L	1ml
$MgSO_4\ 7H_2O$	25 g/L	1ml
Fe-EDTA		0.8ml
Na_2CO_3	20 g/L	1ml
F/2 Vitamins		1ml
Trace Metal Mix		1ml

Generally, CHU-10 was initially acidic. The pH was adjusted according to the microbes involved. NaOH and HCl were used for pH adjustment. Stock diatoms and green algae require 6.4 pH, and cyanobacteria stock used 8.5 pH. For a general community, a neutral pH was ideal. Solutions were stored in the fridge (Stein, 1973).

Appendix B – Mesocosm Nutrient Concentration Data

Markham (µmol/L)	High Si:N	Low Si:N	High N:P	Low N:P	Hamilton (µmol/L)	High Si:N	Low Si:N	High N:P	Low N:P
NH_4^+ Mesocosm 1	2.971	2.236	2.971	4.070	NH_4^+ Mesocosm 1	0.000	0.179	0.000	0.000
Mesocosm 2	2.404	2.416	2.404	1.512	Mesocosm 2	0.004	1.248	0.004	0.760
Mesocosm 3	1.162	3.839	1.162	3.081	Mesocosm 3	0.829	1.242	0.829	0.425
Mesocosm 4	4.070	1.319	2.236	1.319	Mesocosm 4	0.000	0.442	0.179	0.442
Mesocosm 5	1.512	2.018	2.416	2.018	Mesocosm 5	0.760	1.594	1.248	1.594
Mesocosm 6	3.081	3.292	3.839	3.292	Mesocosm 6	0.425	0.107	1.242	0.107
Average	2.533 +/- 1.077	2.520 +/- 0.908	2.505 +/- 0.882	2.549 +/- 1.097	Average	0.336 +/- 0.392	0.802 +/- 0.636	0.584 +/- 0.596	0.555 +/- 0.576
NO_3^- Mesocosm 1	7.458	17.784	7.458	11.577	NO_3^- Mesocosm 1	35.122	10.548	35.122	10.736
Mesocosm 2	12.344	7.311	12.344	9.133	Mesocosm 2	12.673	11.005	12.673	20.389
Mesocosm 3	7.750	15.642	7.750	8.822	Mesocosm 3	26.624	12.999	26.624	8.638
Mesocosm 4	11.577	10.948	17.784	10.948	Mesocosm 4	10.736	9.364	10.548	9.364
Mesocosm 5	9.133	9.866	7.311	9.866	Mesocosm 5	20.389	27.513	11.005	27.513
Mesocosm 6	8.822	7.482	15.642	7.482	Mesocosm 6	8.638	22.184	12.999	22.184
Average (+/- std)	9.514 +/- 2.011	11.505 +/- 4.320	11.381 +/- 4.588	9.638 +/- 1.490	Average	19.030 +/- 10.350	15.602 +/- 7.451	18.162 +/- 10.249	16.471 +/- 7.933

Markham	High Si:N	Low Si:N	High N:P	Low N:P	Hamilton	High Si:N	Low Si:N	High N:P	Low N:P
% N_2 Saturation Mesocosm 1	101.88	99.288	101.9	99.516	% N_2 Saturation Mesocosm 1	100.08	100.08	100.08	100.08
Mesocosm 2	99.228	99.253	99.23	99.463	Mesocosm 2	100.26	100.20	100.26	100.15
Mesocosm 3	99.386	99.140	99.39	99.263	Mesocosm 3	100.06	99.891	100.06	102.78
Mesocosm 4	99.516	99.297	99.29	99.297	Mesocosm 4	100.08	100.08	100.08	100.08
Mesocosm 5	99.463	99.246	99.25	99.246	Mesocosm 5	100.38	100.15	100.20	100.38
Mesocosm 6	99.263	99.151	99.14	99.151	Mesocosm 6	101.04	102.78	99.891	101.04
Average	99.696 +/- 1.032	99.229 +/- 0.068	99.7 +/- 1.075	99.323 +/- 0.139	Average	100.317 +/- 0.377	100.532 +/- 1.108	100.096 +/- 0.127	100.753 +/- 1.059
% O_2 Mesocosm 1	102.76	101.56	102.8	101.56	% O_2 Mesocosm 1	99.315	94.527	99.315	85.227
Mesocosm 2	100.73	98.547	100.7	98.547	Mesocosm 2	88.279	71.512	88.279	79.448
Mesocosm 3	99.926	97.528	99.93	97.528	Mesocosm 3	82.657	89.930	82.657	93.080
Mesocosm 4	101.42	97.2	101.6	97.200	Mesocosm 4	95.294	85.227	94.527	95.294
Mesocosm 5	105.37	97.346	98.55	97.346	Mesocosm 5	79.262	79.448	71.512	79.262
Mesocosm 6	104.79	100.87	97.53	100.87	Mesocosm 6	104.53	93.080	89.930	104.53
Average	102.5 +/- 2.213	98.840 +/- 1.908	100.2 +/- 1.929	98.840 +/- 1.908	Average	91.556 +/- 9.834	85.621 +/- 8.841	87.703 +/- 9.740	89.473 +/- 9.964

Markham (mg/L)	High Si:N	Low Si:N	High N:P	Low N:P	Hamilton (mg/L)	High Si:N	Low Si:N	High N:P	Low N:P
TOC Mesocosm 1	3.981	5.274	3.981	4.996	TOC Mesocosm 1	7.321	8.048	7.321	8.060
Mesocosm 2	6.473	6.589	6.473	6.244	Mesocosm 2	8.062	7.344	8.062	6.827
Mesocosm 3	3.329	3.834	3.329	3.517	Mesocosm 3	6.229	6.327	6.229	7.663
Mesocosm 4	4.996	4.718	5.274	4.718	Mesocosm 4	8.060	5.707	5.707	8.048
Mesocosm 5	6.244	3.360	6.589	3.360	Mesocosm 5	6.827	6.844	6.844	7.344
Mesocosm 6	3.517	3.924	3.834	3.924	Mesocosm 6	7.663	8.238	8.238	6.327
Average	4.757 +/- 1.371	4.460 +/- 1.088	4.913 +/- 1.408	4.617 +/- 1.184	Average	7.361 +/- 0.726	7.085 +/- 0.986	7.067 +/- 1.003	7.378 +/- 0.694
N_2O (µmol/L) Mesocosm 1	0.0333	0.0131	0.0333	0.0106	N_2O (µmol/L) Mesocosm 1	0.0139	0.0118	0.0139	0.0171
Mesocosm 2	0.1391	0.0528	0.1391	0.0420	Mesocosm 2	0.0584	0.0493	0.0584	0.0695
Mesocosm 3	0.2577	0.0679	0.2577	0.0554	Mesocosm 3	0.1029	0.0864	0.1029	0.1081
Mesocosm 4	0.0106	0.0155	0.0131	0.0155	Mesocosm 4	0.0123	0.0171	0.0118	0.0123
Mesocosm 5	0.0420	0.0637	0.0528	0.0637	Mesocosm 5	0.0504	0.0695	0.0493	0.0504
Mesocosm 6	0.0554	0.0817	0.0679	0.0817	Mesocosm 6	0.0735	0.1081	0.0864	0.0735
Average	0.0897 +/- 0.0934	0.0491 +/- 0.0285	0.0940 +/- 0.0963	0.0448 +/- 0.0278	Average	0.0519 +/- 0.0350	0.0570 +/- 0.0383	0.0538 +/- 0.0371	0.0551 +/- 0.0365

Markham (µmol/L)	High Si:N	Low Si:N	High N:P	Low N:P	Hamilton (µmol/L)	High Si:N	Low Si:N	High N:P	Low N:P
SiO_2 Mesocosm 1	0.312	0.356	0.312	0.422	SiO_2 Mesocosm 1	0.584	0.534	0.584	0.699
Mesocosm 2	0.367	0.349	0.367	0.498	Mesocosm 2	0.656	0.520	0.656	0.894
Mesocosm 3	0.437	0.461	0.437	0.413	Mesocosm 3	1.080	0.522	1.080	0.703
Mesocosm 4	0.422	0.373	0.356	0.373	Mesocosm 4	0.699	0.512	0.534	0.512
Mesocosm 5	0.498	0.260	0.349	0.260	Mesocosm 5	0.894	0.624	0.520	0.624
Mesocosm 6	0.413	0.359	0.461	0.359	Mesocosm 6	0.703	0.422	0.522	0.422
Average	0.408 +/- 0.0635	0.360 +/- 0.064	0.380 +/- 0.057	0.387 +/- 0.0791	Average	0.769 +/- 0.184	0.522 +/- 0.522	0.649 +/- 0.217	0.642 +/- 0.165
PO_4^{-2} Mesocosm 1	0.012	0.021	0.012	0.010	PO_4^{-2} Mesocosm 1	0.013	0.018	0.013	0.026
Mesocosm 2	0.015	0.020	0.015	0.016	Mesocosm 2	0.025	0.033	0.025	0.046
Mesocosm 3	0.016	0.012	0.016	0.017	Mesocosm 3	0.025	0.017	0.025	0.026
Mesocosm 4	0.013	0.010	0.021	0.013	Mesocosm 4	0.026	0.018	0.018	0.018
Mesocosm 5	0.023	0.016	0.020	0.023	Mesocosm 5	0.046	0.038	0.033	0.038
Mesocosm 6	0.011	0.017	0.012	0.011	Mesocosm 6	0.026	0.010	0.017	0.010
Average	0.015 +/- 0.004	0.016 +/- 0.004	0.016 +/- 0.004	0.015 +/- 0.005	Average	0.027 +/- 0.011	0.022 +/- 0.011	0.022 +/- 0.007	0.028 +/- 0.011